Effects of H_2O_2 at rat myenteric neurones in culture

Inaugural Dissertation

submitted to the

Faculty of Veterinary Medicine

in partial fulfilment of the requirements

for the PhD Degree

of the Faculties of Veterinary Medicine and Medicine

of the Justus Liebig University Giessen

Germany

by

Pouokam Kamgne Ervice Vidal

from

Douala, Cameroon

Giessen 2009

From the Institute For Veterinary Physiology

of the Justus Liebig University Giessen

First Supervisor and Committee Member : Prof. Dr. Martin Diener

Second Supervisor and Committee Member : Prof. Dr. Winfried Neuhuber

Chairman of the oral panel : Prof. Dr. Norbert Weissmann

Examiner : Prof. Dr. Stefan Arnhold

Date of the Doctoral Defense : March 1st, 2010.

Dedication

This thesis is dedicated to my parents Kamgne Jacques and Metchuiam Elise, my brothers and sisters Kamche Pelagie, Kamsu Sylvain, Feutseu Yves, Kouam Alliance, and Tameu Jacques, my nephew Mouam Gilles and the entire Taguieguem family.

Table of contents

List of Figures

List of Tables

List of abbreviations

- °C degree centigrade
- µg microgram
- µg/ml microgram per milliliter
- µl microliter
- µM micromolar
- µmol micromol
- 2-APB 2-Aminoethoxydiphenylborate
- AnkG Ankyrin G
- ATP Adenosine 5'-triphosphate
- ACh Acetylcholine
- CCh Carbachol
- cGMP Cyclic guanosine monophosphate
- CGRP Calcitonin gene-related peptide
- CPA Cyclopiazonic acid
- CRAC Calcium release activated current channels
- Cys Cysteine
- DMEM Dulbecco's modified Eagle's Medium
- DMSO Dimethylsulphoxide
- DNA Deoxyribonucleic acid
- dV/dt Potential difference per time difference
- EGTA Ethylene glycol bis-(ß-aminoethylether) N,N,N';N'-tetraacetic acid
- ENS Enteric nervous system
- EPAN Enteric primary afferent neurone
- EPSP Excitatory postsynaptic potential
- FCS Fetal calf serum
- Fura-2AM Fura-2 acetoxymethylester
- g gram
- g/l gram per liter

- GSH Glutathione (reduced form)
- GΩ GigaOhm
- GTP Guanosine 5'-triphosphate
- h hour
- 5-HT Serotonin
- H_2O_2 Hydrogen peroxide
- HEPES N-(2-hydroxyethyl)piperazine-N'-(2-ethansulphonic acid)
- HVA High voltage-activated
- Hz Hertz
- IPAN Intrinsic primary afferent neurone
- IP_3R Inositol-1,4,5-trisphosphate receptor
- IPSP Inhibitory postsynaptic potential
- K_D Dissociation constant
- kDa kiloDalton
- KGluc Potassium gluconate
- kHz kiloHertz
- LVA Low voltage-activated
- MCU Mitochondrial calcium uniporter
- mg milligram
- mg/ml milligram per milliliter
- min minute
- ml milliliter
- ml/min milliliter per minute
- mm millimeter
- mmol/l millimol per liter (millimolar)
- mol/l mol per liter
- MPG N-(2-Mercaptopropionyl)glycine
- MPO Myeloperoxidase
- ms millisecond
- mV milliVolt

- MΩ MegaOhm
- nA nanoAmpere
- NADPH Nicotinamide adenine dinucleotide phosphate (reduced)
- nm nanometer
- nM nanomolar
- NMDG N-Methyl-D-glucamine
- nmol nanomol
- NO Nitric oxide
- NPY Neuropeptide Y
- pA picoAmpere
- PKC Protein kinase C
- PMN Polymorphonuclear
- PP1 Serine/threonine protein phosphatase type 1
- PP2A Serine/threonine protein phosphatase type 2A
- PTP Permeability transition pore
- ROC Receptor-operated channel
- ROS Reactive oxygen species
- rpm revolutions per minute
- RuR Ruthenium red
- RyR Ryanodine receptor
- s second (time)
- SERCA Sarcoplasmic-endoplasmic reticulum ATPases
- SOC Store-operated calcium channel
- SOM Somatostatin
- TEA Tetraethylammonium
- TPA Tetrapentylammonium
- Tris Tris(hydroxymethyl)aminomethane
- TRP Transient receptor potential
- Trx Thioredoxin
- TTX Tetrodotoxin

- U Unit
- U/mg Unit per milligram protein
- U/ml Unit per milliliter
- V/s Volt per second
- VOC Voltage-operated channel
- VIP Vasoactive Intestinal Peptide
- vol/vol Volume per total volume
- Weight/vol Weight per total volume

1 Introduction

1.1 Short description of the enteric nervous system

The autonomous nervous system comprises three divisions: the enteric nervous system (ENS), the parasympathetic system and the sympathetic system (Langley 1921). The ENS represents the intrinsic nervous system of the gastrointestinal tract. It was first mentioned by Bayliss and Starling (1899), who described the "law of the intestine": application of a pressure to the luminal surface of the bowel is followed by a stereotyped wave of descending propulsive activity, which consists of oral contraction and anal relaxation. They further established that "the local nervous mechanism" of the gut was responsible for their law as they realized that this motoric pattern was still observed in loops of bowel to which they had severed all extrinsic nerves. Their observations were confirmed *in vitro* later by Trendelenburg (1917), who raised the intraluminal pressure within isolated segments of guinea pig intestine mounted on a J-shaped tube. This "law of the intestine" was renamed by Trendelenburg into the term "peristaltic reflex".

The ENS mediates reflex behavior independently of input from the brain or the spinal cord (Bayliss and Starling 1899, Trendelenburg 1917, Gershon 1981). Therefore, it is referred to as a "second brain". Moreover, it communicates with the main brain via the parasympathetic and the sympathetic systems (Gershon and Erde 1981, Gershon 1999, Figure 1.1B).

The ENS is organized in two types of ganglionated plexuses, the myenteric (Auerbach's) plexus and the submucosal (Meissner) plexus, which are interconnected by nerve fiber bundles (Meissner 1857, Auerbach 1862, 1864). It includes ganglia within the intestinal wall, consisting of neurones, their axons, and enteric glia cell, controlling many functions of the gastrointestinal tract (Furness 2006). The myenteric plexus is a network of nerve strands and small ganglia that lie between the outer longitudinal and the inner circular muscle layers of the external muscle coat

(muscularis externa) of the intestine (Figure 1.1A, Furness 2006). This network regulates the intestinal motility (Gershon 1981). It is continuously expressed around the circumference and along the gut wall. The myenteric plexus is connected with the submucosal plexus, which controls the transport of water and electrolytes across the intestinal epithelium (Furness and Costa 1987) and also the microcirculation (Surprenant 1994). The myenteric plexus is the larger of the two. Its interganglionic connectives are thicker and its ganglia include more neurones (about five fold) than those of the submucosal plexus (Furness and Costa 1987). The enteric ganglia are small clusters of neurones and glial cells, which are interconnected by nerve fiber bundles and, unlike other autonomic ganglia, do not contain blood vessels, connective tissue cells, or collagen fibers (Furness and Costa 1987, Furness 2006). The absence of connective tissue and the close packing of neurones and glia give an appearance similar to the central nervous system (Furness 2006). The ganglia are discontinuously covered by fibroblasts and are not encapsulated, but lie in the connective tissue between the muscle layers (Furness and Costa 1987, Furness 2006). They are so numerous that the enteric nervous system appears to be made up of about the same number of neurones as found in the spinal cord (Furness and Costa 1980).

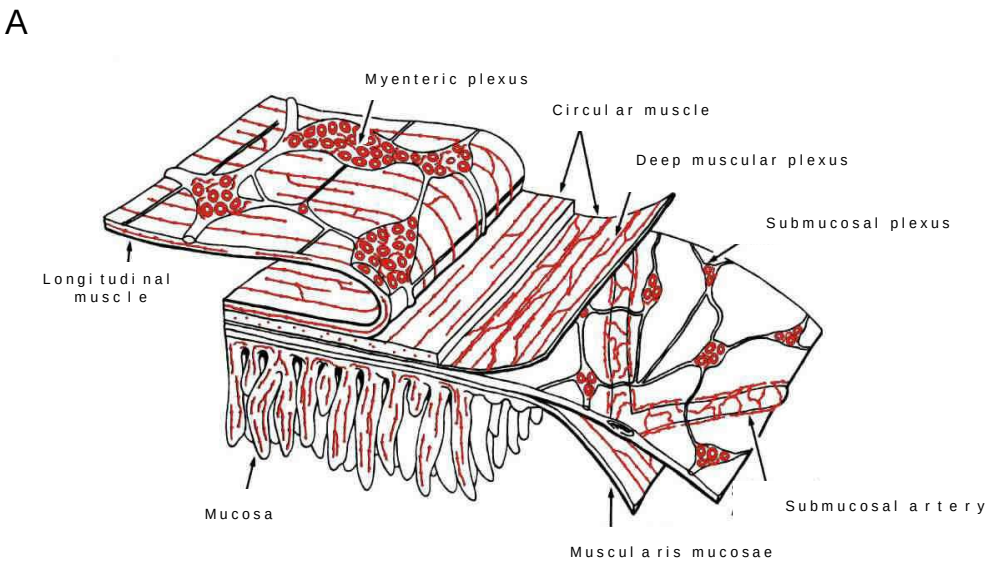

Figure 1.1A: Schematic drawing of the enteric nervous system showing the muscle layers and the plexuses. Modied from Furness and Costa (1987). B: Drawing depicting the communication between the ENS and the parasympathetic and the sympathetic systems. Modied from Gershon and Erde (1981).

1.2 Types and functions of enteric neurones

Enteric neurones have been classified according to their shape, location, specific histochemical and immunohistochemical staining, projections, connections, neurotransmitter expression, physiological properties, and function. Three morphological types of enteric neurones had been described by the neuroanatomist Dogiel. They are known as Dogiel types I, II and III, each of them is present in both plexuses (Wood 1994). According to Dogiel (1899), the type I neurones are flattened, have cell bodies with many short dendrites and a long axon. The soma of the Dogiel type II is relatively smooth with long and short dendrites, which can reach the mucosa. This type II includes an adendritic and a dendritic subtype (Brehmer et al. 1999). The type III is similar to type II. The only difference is that the type III has much more dendrites which are also shorter in length.

The Dogiel classification of neurones has been associated with electrical activities. Based on intracellular recordings, two classes of neurones have been described: the AH/type 2 and the S/type 1. This denomination derives from a combination of the alphabetical terms of Hirst, Holman and Spence (1972, 1974) and the numerical designations of Nishi and North (Nishi and North 1973, Hirst et al. 1974). These latter authors and Wood (1994) described both types of neurones as below: generally, S-neurones are those having a low resting membrane potential relative to other cell types, a higher input resistance relative to other cell types, and they respond to a suprathreshold stimulus by a burst of action potentials (Figure 1.2 B). In contrary, AH-neurones are characterized by a higher resting membrane potential, a lower input resistance than S/type 1 neurones, and an unability of prolonged spike discharging during depolarizing current injection, or when possible, only by one or two spikes at the onset of intracellular injection of the long-duration depolarizing current pulses (Figure 1.2.A). In addition, the action potentials of AH-neurones are followed by a long lasting afterhyperpolarization. Furthermore, action potentials in S-neurones can be evoked by stimuli originating from adjacent neurones, meaning that they possess synaptic inputs (therefore the designation as “S”- neurones). Those action potentials

in S/Type I are generated by fast Na^+ inward currents through voltage-gated sodium channels. These channels can be blocked by the neurotoxin, tetrodotoxin, preventing by this way the generation of action potentials, i.e. these cells fire tetrodotoxin-sensitive action potentials (Figure 1.3). On the other hand, AH/Type II neurones have tetrodotoxin-insensitive action potentials (Figure 1.3, Surprenant 1984,Wood 1994) which are generated by calcium inward currents. The long lasting (up to 30 s) afterhyperpolarization (AHP; see Figure 1.2.D) following action potentials observed in these neurones is caused by an outward Ca^{2+}-dependent K^+ current (Nishi and North 1973, Hirst et al. 1974); the influx of Ca^{2+} gives a characteristic "shoulder" shape to the repolarizing phase of AH-neurones action potentials (Figure 1.2 C). However, there are other neurones in the myenteric plexus, whose shape and electrophysiological behavior do not fit to this general classification (Wood 1994).

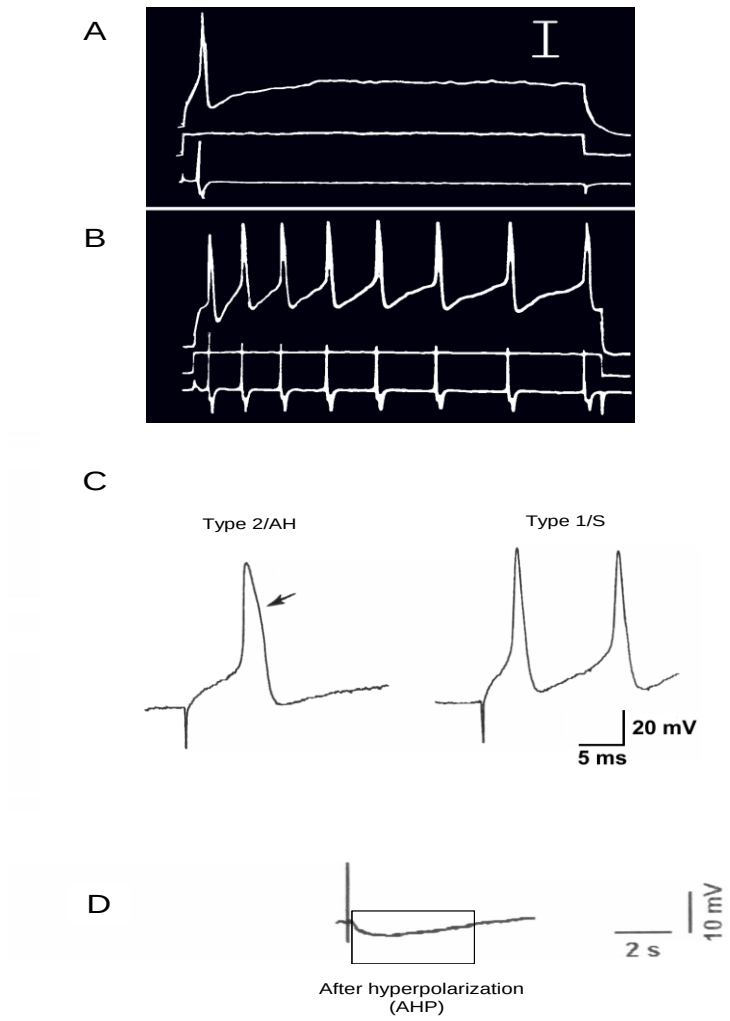

Figure 1.2: Electrophysiological properties and classification of enteric neurones. A: Single spike evoked by injection of a depolarizing current pulse in AH-neurones. B: Volley of spikes during the depolarizing current pulse in S-neurones. In A, B the current injected has a 200 ms-duration, upper trace is transmembrane voltage, middle trace is injected current, lower trace is dV/dt of membrane voltage, vertical calibration: 20 mV, 1 nA, or 60 V/s (Wood 1994). C: AH-neurones unlike S-neurones present a Ca^{2+}-evoked "hump" (see arrow) at the repolarization phase (for references, see Gershon et al. 1994). D: AH-neurones unlike S-type display a characteristic afterhyperpolarization (Surprenant 1984).

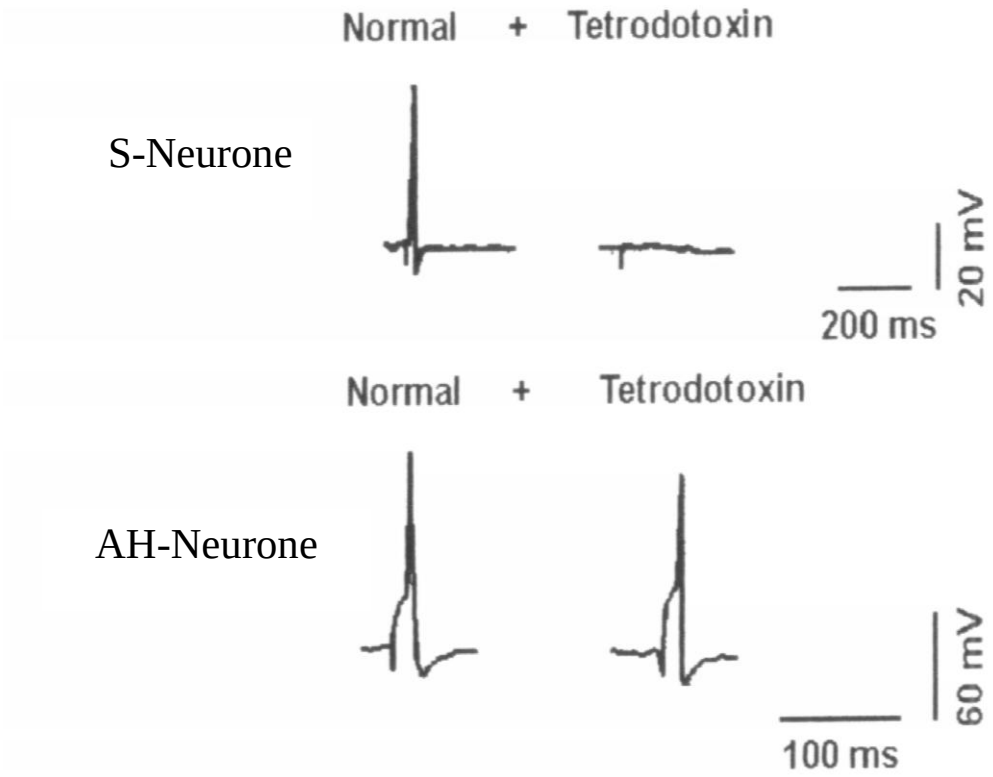

Figure 1.3: Pharmacological properties and classification of myenteric neurones. The action potentials of S-neurones unlike those of AH/type 2 is tetrodotoxin-sensitive (according to Surprenant 1984).

Intense research from several laboratories over the past two decades introduced a functional classification of enteric neurones. This new classification system used different strategies based on methods combining immunohistochemistry, eletrophysiology, retrograde tracing, neuronal labelling, lesion techniques and pharmacological analysis (Costa et al. 2000).

Following those researches, the established functional classes of myenteric neurones are the primary afferent neurones (also termed enteric primary afferent neurones; EPANs), intrinsic primary afferent neurones (IPANs), interneurones and motorneurones (Wood 1994, Costa et al. 2000). A functional overview is given in the Table 1.1.

The IPANs are present in both myenteric and submucous ganglia and present an AH/type 2 phenotype (Costa et al. 2000). They respond to luminal chemical stimuli, to mechanical deformation of the mucosa and to radial stretch and muscle tension. This suggests the presence of their processes into the mucosa (Costa et al. 2000).

Interneurones exhibit both S/type 1 and AH/type 2 morphology (Wood 1994) and are subdivided into two functional groups: the ascending and the descending interneurones. The ascending interneurones have a S/type I phenotype, drive ascending excitation interconnecting primary afferent neurones and motorneurones, and participate in the synthesis of acetylcholine, tachykinins and opioid peptides (Brookes et al. 1997). The descending interneurones are organized in subclasses according to their neurochemistry, participate in the synthesis of neurotransmitters, and drive descending excitations.

The motorneurones are S/type I and include different groups. There are excitatory circular muscle motorneurones and inhibitory circular muscle motorneurones, responsible for activation or inhibition of the contractile activity of the intestinal muscle, respectively (Wood 1994, Costa 2000). The longitudinal muscle layer is under control of the longitudinal muscle motorneurones. Secretomotor and vasomotor neurones, projecting to the mucosa, complete the motorneurones scheme.

Neurones type	**Main transmitters**	**Actions**
IPANs	Substance P, calcitonin gene-related peptide (CGRP), acetylcholine	Activation of enteric neurones (increased perfusion, secretion, motility)
Interneurones	Acetylcholine, somatostatin (SOM), serotonin (5-HT), substance P	Activation of inhibitory and excitatory neurones via nicotinic (and also partially muscarinic) receptors
Excitatory motor neurones	Acetylcholine, substance P	Activation of myocytes via muscarinic receptors
Inhibitory motor neurones	Nitric oxide (NO), vasoactive intestinal peptid (VIP), ATP	NO-evoked increase in cGMP concentration in myocytes leads to relaxation
Excitatory secretomotor neurones	Acetylcholine, VIP	Activation of secretory cells of the mucosa via muscarinic and VIP receptors
Inhibitory secretomotor neurones	Neuropeptid Y (NPY), somatostatin (SOM)	Inhibition of secretory cells of the mucosa via NPY and SOM receptors
Vasomotor neurones	VIP, acetylcholine, NO	Relaxation of blood vessels via VIP and muscarinic receptors

Table 1.1: Overview of the main neurotransmitters in the gastrointestinal tract and their main effects (Modified from Schemann 2000).

1.3 Synaptic behavior of myenteric neurones

The principal electrophysiological events found in the myenteric neurones are fast excitatory postsynaptic potentials (fast EPSPs), slow excitatory postsynaptic potentials (slow EPSPs), slow inhibitory postsynaptic potentials (slow IPSPs), and the presynaptic inhibition of neurotransmission from excitatory synapses (Wood 1994).

1.3.1 Fast excitatory postsynaptic potentials

Fast EPSPs are membrane depolarizations that last less than 50 ms. They are found in both AH and S type neurones. The putative neurotransmitters involved in fast EPSPs are reported to be acetylcholine (ACh) and serotonin (5-HT), which act via nicotinic and 5-HT_3 receptors, respectively, which function as nonselective cation channels (Derkach et al. 1989).

1.3.2 Slow excitatory postsynaptic potentials

These potentials, lasting from several seconds to minutes after termination of the release of the neurotransmitter from the presynaptic terminal, are found in both S- and AH-neurones, but are much more pronounced in AH/type 2, where they cause a conversion from hypoexcitability to hyperexcitability (Wood 1994). The slow EPSPs are associated with a reduction of the membrane permeability for potassium ions (Wood and Mayer 1979) due to a blockade of Ca^{2+} channels by a neurotransmitter, a reduction of intracellular Ca^{2+} concentration and/or a closure of Ca^{2+}-activated K^+ channels (Wood 1994). In addition, experimental evidence demonstrates that the second messenger cyclic AMP is involved in EPSPs of AH/type 2 neurones (Nemeth et al. 1984). The neurotransmitters responsible for the generation of slow EPSPs are listed in Table 1.2.

Slow excitatory post-synaptic potentials	Slow inhibitory post-synaptic potentials	Presynatic inhibition
Acetylcholine	Acetylcholine	Dopamine
Serotonin (5-HT)	Serotonin (5-HT)	Norepinephrine
Substance P	Enkephalines	Histamine
Histamin	Neurotensin	Serotonin (5-HT)
Vasoactive Intestinal Peptide (VIP)	Cholecystokinin	Opioid peptides
Cholecystokinin	Somatostatin	Acetylcholine
Gastrin-releasing peptide	Purines	Peptide YY
Bombesin	Galanine	Adenosine
Caerulein	Neuropeptide Y	Neuropeptide Y

Table 1.2: Myenteric synapses and transmitters.

1.3.3 Slow inhibitory postsynaptic potentials

Slow IPSPs are hyperpolarizing synaptic potentials lasting for 2 - 40 s and associated with an increase in potassium conductance (Johnson and North 1980). Surprenant and North (1988) provided evidence suggesting that GTP-binding proteins are involved in direct coupling of the receptors to the potassium channels. The putative neurotransmitter responsible for IPSPs is norepinephrine (Johnson and North 1980). It is believed that the functional significance of slow IPSPs is the termination of the excitatory state of slow synaptic excitation and reestablishement of the low excitability state in the ganglion cell soma (Wood 1994).

1.3.4 Presynaptic inhibition

Also called autoinhibition, the presynaptic inhibition is a mechanism that suppresses the release of neurotransmitters from axons. This occurs by the action of chemical messengers at receptors on the axon terminal. It is found at both fast and slow excitatory and inhibitory synapses and also at neuroeffector junctions (Schemann and Wood 1989). The function of presynaptic inhibition is the regulation of the neurotransmitter concentration within the synaptic or junctional space (Wood 1994).

1.4 Ionic channels and excitability in neurones

The equipment of neurones with ion channels mainly determines their electrophysiological properties. Neurones express different categories of channels, namely: voltage-gated channels, ligand-gated channels, ion-gated channels, TRP (transient receptor potential) channels, and gap-junction channels.

The voltage-gated channels are the object of interest in this thesis. Therefore, voltage–gated-sodium, potassium and calcium channels will be described in more detail. They represent a gene-superfamily of transmembrane proteins, which in the case of Na^+ or Ca^{2+} channels are made up of four repeated domains (labelled I through IV) or of a tetramer in the case of most K^+ channels.

1.4.1 Voltage-gated sodium channels

Voltage-gated sodium channels include an α-subunit consisting of four homologous domains, and an auxiliary β-subunit (Scheuer and Catterall 2006). The α-subunit forms the core of the channel and can be functional on its own. When the α-subunit is expressed in the absence of the β-subunit, it can form a channel conducting Na^+, which still exhibits voltage-dependent gating. Specific amino acid sequences of the α-subunit form the voltage sensor, the wall of the ion channel pore, the inactivation gate, the sites of binding for local anesthetics as well as toxins, and also modulatory

phosphorylation sites for numerous kinases (Figure 1.4). The β-subunit (Figure 1.4) acts as modulator of the channel gating, inactivation, cellular localization, translocation and clustering in different regions of the neurones.

Every domain includes six transmembrane segments or membrane-spanning regions labeled S1 through S6. The highly conserved S4 segment of each domain contains positively charged amino acid residues and forms part of the voltage sensor. In case of a suprathreshold depolarization of the membrane, this S4 segment moves towards the extracellular side of the cell membrane, allowing by this way the channel to be permeable to ions. The inflow of ions is operated at a pore which is functionally divided into two regions: the more external region formed by the "P-loops", representing the linker that connects S5 and S6 and which appears as the most narrow part of the pore constituting then the selectivity filter (Figure 1.4); the cytoplasmic region, linking the domains III and IV and containing a critical hydrophobic motif that functions as a "hinged lid" (h) and is responsible for fast inactivation. Ankyrin G (Ank) binds to a conserved amino acid sequence at the intercellular loop that links the domains II and III, and helps for the targeting of channels to specific regions of the cells. The large intracellular loop between the domains I and III contains numerous modulatory phosphorylation sites (P) for the protein kinases A and C (Figure 1.4).

The β-subunit and cytoskeletal proteins associate with the carboxy-terminus domain. The typical voltage-gated sodium channel opens (activates) on membrane depolarization and then inactivates either rapidly on repolarization or more slowly on sustained depolarization. The kinetics includes a fast inactivation which is the primary mechanism for the repolarization of the membrane after an action potential and secondly, a slow inactivation that regulates excitability and modulates burst discharges of neurones and axons.

Specific toxins can be used as pharmacological tools because they change these kinetic parameters. Sodium influx through voltage-gated Na^+ channels triggers the membrane depolarization that is responsible for the generation and the conduction of action potential in the axon and activation of presynaptic Ca^{2+} channels for

exocytosis. Voltage-gated Na^+ channels also modulate the excitability by modulating the subthreshold oscillations of the membrane potential. They are diverse according to the subtypes of α-subunits, which determine the threshold for activation, the kinetics of activation and inactivation, recovery from inactivation, as well as sensitivity to blockade by TTX. The proteins of the channels are named $Na_v1.1$ through $Na_v1.9$ (Catterall et al. 2005).

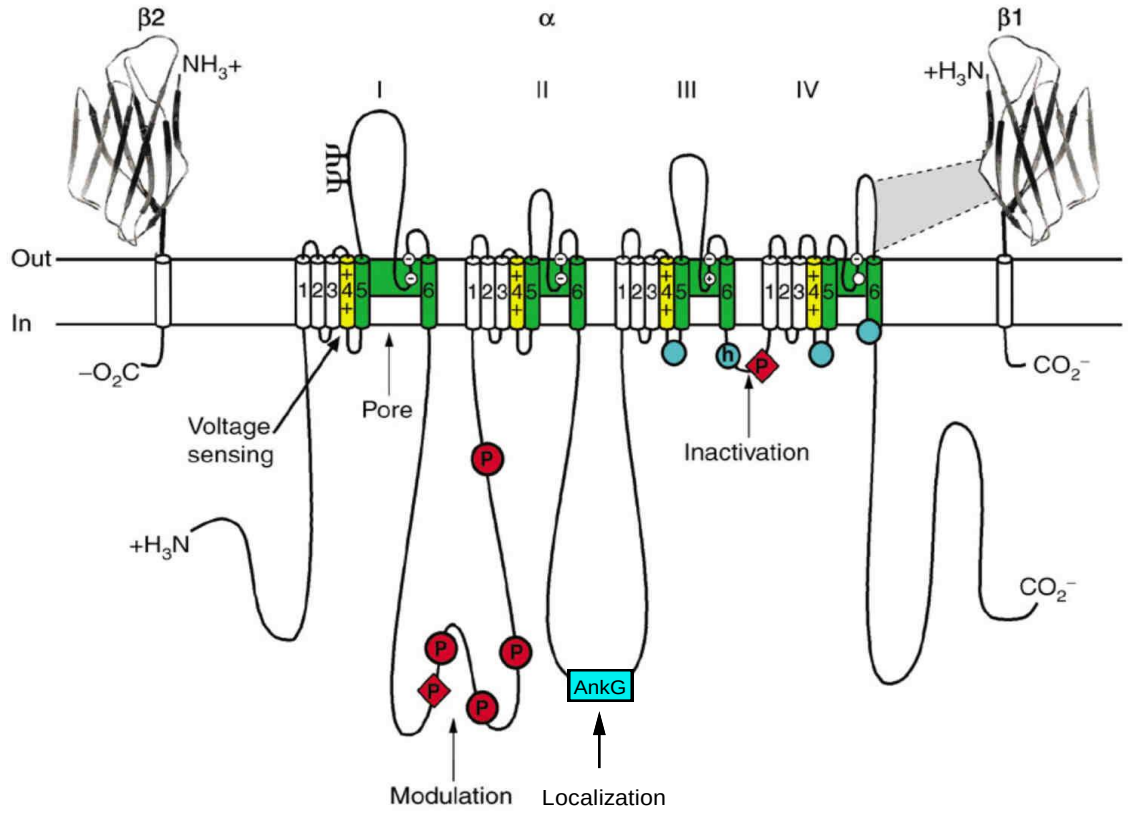

Figure 1.4: Molecular structure of voltage-gated sodium channels. The α-subunit is associated with two β-subunits β1/3 and β2/4 and comprises four domains (I-IV), each domain containing six segments (S1-S6). The ion-conducting pore is formed by the transmembrane segments 5 and 6 of each homologous domain. The segment S4 contains positive charges at each third amino acid, which functions as a transmembrane voltage sensor. The intracellular surface of the α-subunit presents many sites for inactivation with the intracellular segment connecting domains III and IV, h, forming the inactivation gate. Phosphorylation sites are indicated by the symbol "P" as circles for protein kinase A and as diamonds for protein kinase C. The localization region is indicated by Ankyrin G (AnkG) (modified from Scheuer and Catterall 2006).

1.4.2 Potassium channels

Potassium channels are structurally and functionally organized into voltage-gated channels (K_v), Ca^{2+}-activated channels (K_{Ca}), inward rectifiers (K_{ir}), ATP-sensitive channels (K_{ATP}), G protein-coupled channels, and others (such as e.g. K_{2P} formed by subunits/pore tandems) (International Union of Pharmacology 2002).

The Ca^{2+}-activated K^+ channels fall in three categories: the maxi-K or BK (big or large conductance) that are mostly activated by an increase in the cytoplasmic Ca^{2+} concentration (Jiang et al. 2001) resulting in hyperpolarization and reduction of the cell excitability, the SK channels (small conductance) whose activation via increase in intracellular Ca^{2+} concentration limits the firing frequency of action potentials and also determines the afterhyperpolarization (Faber and Sah 2007), and the IK channels (intermediate conductance) found mainly in epithelial and blood cells where they sense intracellular Ca^{2+} independently from voltage.

1.4.3 Calcium channels

Calcium channels are responsible for the transduction of membrane electrical signals into intracellular chemical signals when the cytosolic Ca^{2+} concentration rises. By this way, they participate in and regulate Ca^{2+}-dependent intracellular mechanisms. For instance, they participate in muscle contraction stimulation, neurotransmitter secretion, gene regulation, activation of other ion channels, or the control of the shape and the duration of action potentials. There are three main types of Ca^{2+} channels: the voltage-gated Ca^{2+} channels, the Ca^{2+} release channels (such as ryanodine receptors and the inositol-1,4,5-trisphosphate (IP_3) receptors), and the mitochondrial and nuclear ion channels (Hool and Corry 2007).

1.4.3.1 The voltage-gated calcium channels

In the plasma membrane, several subtypes of voltage-dependent calcium channels are found, which - according to their pharmacological properties and their current kinetics - were initially classified into two groups. The first group contains the T-Ca^{2+}-channels. They are activated by a small depolarization and are termed "transient calcium channels" or "low voltage-activated" (LVA). They are insensitive to dihydropyridines. The second group was named "high voltage-activated" (HVA) Ca^{2+} channels, which are activated by a large depolarization. They mediate long-lasting Ca^{2+} currents due to their slow inactivation. These currents are sensitive to 1,4 – dihydropyridines such as nifedipine.

The nomenclature of calcium channels has evolved over decades. Tsien et al. (1988) introduced a nomenclature based on single letters which continues to be in use today. In addition to the T-Ca^{2+} channels (transient currents) and the L-Ca^{2+} channels, other channels have been identified with different single channels conductances and resistance to dihydropyridines. These channels are predominantly found in neurones and are sensitive to ω-conotoxin GVIA from cone snails. They have been named N-type (Nowycky et al. 1985). Later on, P-type (Llinas et al. 1989), Q-type (Randall and Tsien 1995) and R-type calcium channels have been identified and characterized (Randall and Tsien 1997).

1.4.3.2 Ca^{2+} release channels: ryanodine receptors and IP_3 receptors

Ryanodine receptors (RyR) and IP_3Rs are the calcium channels that release Ca^{2+} from internal stores (sarcoplasmic and/or endoplasmic reticulum). They induce increases in the cytoplasmic Ca^{2+} concentration (Figure 1.5A, B). The resulting reduction in the Ca^{2+} content of the intracellular Ca^{2+} stores ("store depletion") is followed by an influx of extracellular Ca^{2+}. In nonexcitable cells such as lymphocytes, this store-operated Ca^{2+} entry (SOC) is predominantly mediated by calcium release activated current (CRAC) channels. Most agonists affect the cytosolic Ca^{2+} concentration in a

biphasic way: an initial increase due to a release of stored Ca^{2+} is followed by an influx of extracellular Ca^{2+} (Hool and Corry 2007).

1.4.3.3 Mitochondrial and nuclear ion channels

The mitochondria can accumulate Ca^{2+} through the mitochondrial calcium uniporter (MCU), which is located in the inner mitochondrial membrane and can be inhibited by ruthenium red (Kirichok et al. 2004). Mitochondria can release Ca^{2+} via the permeability transition pore (PTP) or via a Na^{+}/Ca^{2+} exchanger extruding one Ca^{2+} in exchange for three Na^{+}. Calcium can be stored in the luminal space of the nuclear membrane, which also contains calcium transport proteins such as sarcoplasmic-endoplasmic Ca^{2+}-ATPases (SERCA), IP_3Rs and RyRs (Gerasimenko et al. 1996).

1.4.3.4 Regulation of Ca^{2+} fluxes

Under physiological conditions, the cytosolic Ca^{2+} concentration amounts to about 100 nmol/l. In case of activation, this concentration can rise up to the micromolar range. According to Berridge et al. (2000), the Ca^{2+} signaling network can be organized in four functional units (Figure 1.5A): The signaling is triggered by a stimulus that generates various Ca^{2+}-mobilizing signals, the latter activate the "ON" mechanism that feeds Ca^{2+} into the cytoplasm. Ca^{2+} functions as a messenger in order to stimulate numerous Ca^{2+}-sensitive processes, and an "OFF" mechanism including pumps (the SERCAs pumping back calcium into internal stores) and exchangers. They remove Ca^{2+} from the cytoplasm restoring by this way the resting state (Figure 1.5A, B).

The entry of external Ca^{2+} is carried by channels that are differently activated (Figure 1.5A, B). Some are voltage-activated and are therefore termed voltage-operated channels (VOCs), while others open in response to receptor activation by external stimuli such as glutamate, ATP or acetylcholine (ACh), and are termed receptor-

operated channels (ROC). Emptying of internal stores induces entry of calcium from the external milieu via activation of store-operated channels (SOC), this process is referred to as capacitative Ca^{2+} entry (Putney 1986, 2003). A detailed view of these processes is presented in the Figure 1.5A. In neurones, N- and P/Q-type VOCs at synaptic endings trigger the release of neurotransmitters.

A

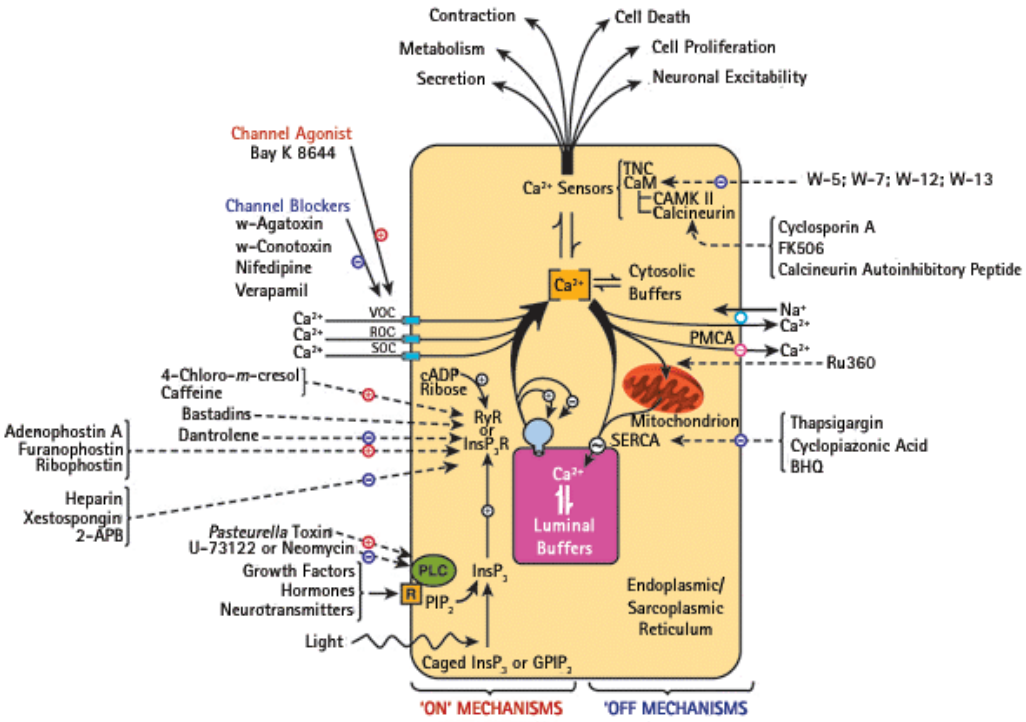

B

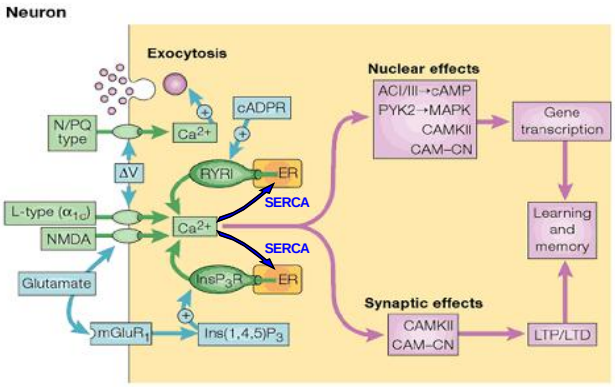

Figure 1.5A: Overview of regulation of calcium fluxes in cells. B: Regulation of calcium fluxes in neurones. The signs + and - mean activation and inhibition, respectively. ΔV: potential difference at the membrane. Modied from Berridge et al. 2000.

1.5 Enteric nervous system and gastrointestinal motility

The regulation of gut motility involves hormones and neurotransmitters which act directly or indirectly on muscle cells. Hormones released locally from endocrine cells in the mucosa activate receptors on sensory fibers, the extrinsic (vagal) and the intrinsic primary afferent neurones (IPANs). These neurones exhibit a feed-back on the endocrine cells resulting in an autoregulation mechanism, which modulates gastrointestinal motility. Extrinsic neurones of the parasympathetic and sympathetic systems influence smooth muscle cells indirectly by acting on neurones of the myenteric plexus.

The smooth muscle cells constitute an electrical syncytium innervated by excitatory and inhibitory neurones. Excitatory stimuli (from excitatory motorneurones) are exerted by ACh, 5-HT, or tachykinins, while inhibitory ones (from inhibitory motorneurones) imply VIP or NO. Additively, local interactions like reflex activation of myenteric neurones by stimuli (stretch or mucosal stimulation) contribute to modulatory muscle relaxation via VIP release or NO production (Olsson and Holmgren 2001). The longitudinal muscle layer is innervated mainly by excitatory motorneurones, while the circular layer is innervated by both excitatory and inhibitory nerves. The predominant neural influence under basal conditions is an inhibitory one (Hansen 2003).

The intestinal rhythmicity is associated with slow waves that oscillate at different frequencies, amplitudes and durations in different regions of the gut. Pacemaker regions, in which the slow waves are generated, have been identified. They are located at the myenteric and submucous borders of circular muscles (Hansen 2003). They contain a network of cells referred to as intestinal cells of Cajal (ICC) which are distinctive populations of muscle-like, stellate cells. These cells are present in both circular and longitudinal muscle layers, make contact with each other and with muscle cells as well as with nerve terminals and function as pacemakers in gastrointestinal muscles initiating rhythmic electrical activity (Vanderwinden 1999).

1.6 Aim of the study

Reactive oxygen species are derivatives of oxygen such as superoxide anion (O^{2-}), hydroxyl radical (•OH), hydrogen peroxide (H_2O_2), or hypochlorous acid (HOCl). Reactions of these compounds with amines can lead to the generation of monochloramine (NH_2Cl; Tamai et al. 1991) or of the peroxynitrite anion ($ONOO^-$; Broillet 1999). Reactive oxygen species can be continuously produced in small amounts under physiological conditions within cells (see e.g. Yu 1994, Bae et al. 1997), e.g. by the enzymes NADPH oxidase or the so-called dual oxidase (Lambeth 2004).

A natural protection against these oxidants is maintained by endogenous enzymes from peroxisomes and other cells compartments, notably superoxide dismutase, catalase, and glutathione peroxidase, which prevent oxidative damage (Yu 1994). Peroxisomes participate in cell metabolisms that lead to oxidant production or degradation. Catalase is the principal enzyme that degrades H_2O_2 so that its expression gives a hint at H_2O_2 clearance within the cell.

However, during bacterial infections as well as leucocyte activation, these oxidants are produced in amounts overwhelming the physiological defence mechanisms, leading to diarrhoea and tissue destruction within the gut (Sugi et al. 2001, Pavlick et al. 2002, Cao et al. 2004) mediated in part by damage to all classes of biologically important macromolecules such as e.g. DNA or proteins (Halliwell and Whiteman 2004). On the other hand, there is evidence that oxidants might act as signaling molecules at subtoxic concentrations (Suzuki et al. 1997, Bogeski et al. 2006). Most gastrointestinal functions such as motility of the muscle layers, electrolyte transport across the epithelium, permeability of the epithelial tight junctions, or intestinal perfusion are autonomously regulated by enteric neurones located in the myenteric and the submucosal plexus (Wood 1994).

Although the ability of oxidants to induce diarrhoea is well known (Sugi et al. 2001), and several action sites on the intestinal epithelium have been characterized (Sugi et

al. 2001, Schultheiss et al. 2005), only a few studies deal with their effects on enteric neurones. In guinea pig small intestine, H_2O_2 induces a hyperpolarization of the membrane concomitant with a reduction of excitability and the amplitude of action potentials (Wada-Takahashi and Tamura 2000, Vogalis and Harvey 2003). In rat colon, oxidants such as monochloramine and H_2O_2 activate colonic anion secretion, a response which is partially mediated by cholinergic enteric neurones as shown by its sensitivity to the neuronal blocker, tetrodotoxin, and the muscarinic antagonist, atropine (Tamai et al. 1991).

As there is no information about direct effects of H_2O_2 on enteric neurones from this species, the aim of the present study was to characterize the actions of this oxidant on cultured rat myenteric neurones using electrophysiological and imaging methods.

2 Materials and Methods

2.1 Materials

2.1.1 Chemicals

The chemicals used (Table 2.1) were of the highest available purity and were obtained from Alfa Aesar (Karlsruhe, Germany), Axxora (Lörrach, Germany), Biochrom (Berlin, Germany), Biomol (Hamburg, Germany), B. Braun AG (Melsungen, Germany), Calbiochem (Bad Soden, Germany), Globus Apotheke (Giessen, Germany), Invitrogen (Karlsruhe, Germany), Life Technologies (Eggenstein, Germany), Merck (Darmstadt, Germany), Merz + co (Frankfurt, Germany), Molecular Probes (Eugene, USA), neoLab Migge (Heidelberg, Germany), PAA Laboratories (Cölbe, Germany), Germany), and Sigma-Aldrich (Steinheim, Germany).

Chemical	Source
Agar	Merck, Darmstadt
2-APB (2-Aminoethoxy-diphenylborate)	Calbiochem, Bad Soden
ATP (Adenosine 5'-triphosphate disodium salt)	Sigma, Steinheim
$BaCl_2 \cdot 2\ H_2O$	Sigma, Steinheim
$CaCl_2 \cdot 2\ H_2O$	Sigma, Steinheim
Calyculin A	Calbiochem, Bad Soden
Carbachol (Carbamoylcholine chloride)	Sigma, Steinheim
Citric acid	Sigma, Steinheim
CsCl	Sigma, Steinheim
Cyclopiazonic acid	Axxora, Lörrach
DMSO (Dimethylsulphoxide)	Merck, Darmstadt
EGTA (ethylene glycol bis-(ß-aminoethylether) N,N,N',N'-tetraacetic acid)	Sigma, Steinheim
Endothall	Calbiochem, Bad Soden
$FeSO_4 \cdot 7\ H_2O$	neoLab Migge, Heidelberg

Fura-2AM (fura-2 acetoxymethylester)	Invitrogen, Karlsruhe
$GdCl_3 \cdot 6\ H_2O$	Sigma, Steinheim
Genistein	Calbiochem, Bad Soden
D-Glucose	Sigma, Steinheim
L-Glutamine	Sigma, Steinheim
Glutathione (reduced form)	Sigma, Steinheim
HCl	Sigma, Steinheim
HEPES (N-(2-hydroxyethyl)piperazine-N'-(2-ethansulphonic acid)	Sigma, Steinheim
H_2O_2 (Hydrogen peroxide)	Biomol, Hamburg
Isopropyl alcohol	Globus Apotheke, Giessen
KCl	Sigma, Steinheim
KGluconate	Sigma, Steinheim
$MgCl_2$	Sigma, Steinheim
MPG (N-(2-Mercaptopropionyl)-glycine)	Sigma, Steinheim
NaCl	Sigma, Steinheim
NaOH	Paraformaldehyde
NMDG (N-Methyl-D-glucamine) chloride	Sigma, Steinheim
Paxilline	Axxora, Lörrach
Pluronic acid	Invitrogen, Karlsruhe
Poly-L-lysine	Biochrom, Berlin
Sodium orthovanadate	Sigma, Steinheim
Staurosporine	Axxora, Lörrach
Tautomycin	Axxora , Lörrach
Tetrapentylammonium chloride	Sigma, Steinheim
Tetrodotoxin	Calbiochem , Bad Soden
Tris (Tris(hydroxymethyl)aminomethane)	Sigma, Steinheim
Trolox	Sigma, Steinheim

Table 2.1: List of chemicals used.

Hydrogen peroxide was purchased as a 30 % (weight/vol) solution and further diluted in the Tyrode solution. 2-Aminoethoxydiphenylborate (2-APB), calyculin A, cyclopiazonic acid, fura-2AM, genistein, paxilline, staurosporine, tautomycin, and trolox were dissolved in dimethylsulphoxide (DMSO). Tetrodotoxin was dissolved in $2 \cdot 10^{-2}$ mol/l citrate buffer. $BaCl_2$, endothall, $FeSO_4$, $GdCl_3$, glutathione (GSH), N-(2-mercaptopropionyl)glycine (MPG), ruthenium red, sodium orthovanadate and tetrapentylammonium chloride (TPA) were dissolved in aqueous stock solutions.

2.1.2 Antibiotics

Antibiotics	Stock solution	Working concentration	Source
Gentamycin	10 mg/ml	20 µg/ml	PAA Laboratories, Cölbe, Germany
Metronidazol	500 mg/100 ml	5 µg/ml	B. Braun AG, Melsungen, Germany
Penicillin	10000 U/ml	100 U/ml	Life Technologies, Eggenstein, Germany
Streptomycin	10000 µg/ml	100 µg/ml	Life Technologies, Eggenstein, Germany

Table 2.2: List of antibiotics used in the cell culture.

2.1.3 Enzymes

Enzymes	Stock solution	Working concentration	Source
Collagenase type II	290 U/mg	1 mg/ml	Biochrom, Berlin, Germany
DNase type I from bovine pancreas	2000 U/mg	1 mg/ml	Sigma, Steinheim, Germany

Table 2.3: List of enzymes used.

2.1.4 Biological Material

The myenteric plexuses were isolated from Wistar rats (see 3.1).

2.1.5 Buffers and Solutions

2.1.5.1 Myenteric Plexus Culturing Solutions

Medium	Purpose	Source	Supplements (for 500 ml)
DMEM (Dulbecco's modified Eagle's Medium)	Isolation of myenteric plexuses	Sigma, Steinheim, Germany	+ 10 ml L-glutamate (200 mmol/l) + 1 ml gentamycin+ 500 µl metronidazol
Start-V®	Incubation and growth of neurones	Biochrom, Berlin, Germany	+ 5 ml of the mixture Streptomycin/Penicillin

Table 2.4: List of buffer solutions for plexus isolation and cell culture.

2.1.5.2 Solutions for Patch-Clamping and Imaging

Solution	Technique	Function
Standard pipette solution : In mmol/l: K gluconate (KGluc) 100, KCl 30, NaCl 10, ethylene glycol bis (ß-aminoethylether) N,N,N',N'-tetraacetic acid (EGTA) 0.1, Tris 10, adenosine 5'-triphosphate disodium salt (ATP) 5, and $MgCl_2$ 2, pH was adjusted to 7.2 with Tris/HCl.	Patch-clamping	Intracellular-like medium and intracellular application of specific drugs.
K^+-free pipette solution: CsCl 140, EGTA 0.1, Tris 10, ATP 5, and $MgCl_2$ 2, pH was adjusted to 7.2 with Tris/HCl	Patch-clamping	Isolation of Na^+ currents.
HEPES-buffered Tyrode solution: In mmol/l: NaCl 135, KCl 5.4, HEPES 10, $CaCl_2$ 1.25, $MgCl_2$ 1, and glucose 12.2, pH was adjusted to 7.4 with NaOH/HCl.	Patch-clamping and imaging	Superfusing cells and extracellular application of specific drugs.
Na^+-reduced Tyrode solution: In mmol/l: NaCl 70, NMDG chloride 50, KCl 5.4, $MgCl_2$ 5, TEA chloride 20, CsCl 2, glucose 12.2, HEPES 10, and $CaCl_2$ 0.1. The pH was adjusted to 7.4 with Tris/HCl	Patch-clamping	Isolation of Na^+ currents.

Table 2.5: List of buffer solutions used for patch-clamp and imaging experiments.

2.2 Methods

2.2.1 Isolation and culture of the myenteric neurones

Myenteric ganglia were isolated from the complete small intestine of 5 to 10 days old rats as described previously (Schäfer et al. 1997, Haschke et al. 2002, Rehn et al. 2004). Animals were killed by decapitation followed by exsanguination (approved by Regierungspräsidium Gießen, Gießen, Germany). The serosa was stripped away under optical control (microscope Olympus SZX9, Japan) and the entire intestine was removed from the caudal end (Figure 2.1). The small intestine was cut off and transfered into a 35 mm Petri dish filled with DMEM. The muscle layer was separated from the mucosa using fine forceps (Dumont 5 Biologie Titan T5013; Plano, Wetzlar, Germany), then transfered to a vial of DMEM containing 1 mg/ml Collagenase type II (Biochrom, Berlin, Germany) which was afterwards placed at 37°C in an incubator (CO_2 Incubator MCO-17AI Sanyo electrics Co, Japan).

After one hour incubation, the vial was vortexed for about 15 s, the content was divided into small samples, which were transfered into 35 mm Petri dishes and washed with ice-cold DMEM. The ganglia, forming net-like structures, were collected with a 20 µl micropipette and washed with DMEM on ice. The residual pieces of muscle layer were collected with a 1 ml pipette and transfered to a vial of DMEM containing 1 mg/ml collagenase type II for further incubation. This enzymatic digestion was repeated 3 times. Then the ganglia were spun down for 10 min (600 rpm, Centrifuge K2S, Hettich, Tuttlingen, Germany), transfered (under a class II cell culture hood Laminair, Heraeus Instruments, Hanau, Germany) into Start-V® medium supplemented with penicillin (100 U/ml), streptomycin (100 µg/ml) and 10 % (vol/vol) fetal calf serum (PAA Laboratories, Cölbe, Germany).

Next, ganglia were placed on 13 mm glass coverslips coated with poly-L-lysine (molecular weight > 300 kDa; Biochrom, Berlin, Germany) in conventional four well-dishes. A 45 min incubation allowed the ganglia to settle down. Afterwards each well

was filled up with Start-V® to a final volume of 500 µl for overnight incubation at 37°C under continuous supply of carbogen (95 % O_2, 5 % CO_2, vol/vol, CO_2 Incubator MCO-17AI Sanyo electrics Co, Japan). The ganglionic cells growing on the coverslips could be used from the next day up to the seventh day; culture medium was changed every two days. Some experiments were performed with isolated myenteric neurones instead of intact ganglia. For this purpose, the net-forming ganglia were triturated 3 to 5 times through a 0.4 mm needle and then cultured as described above for about 12 h.

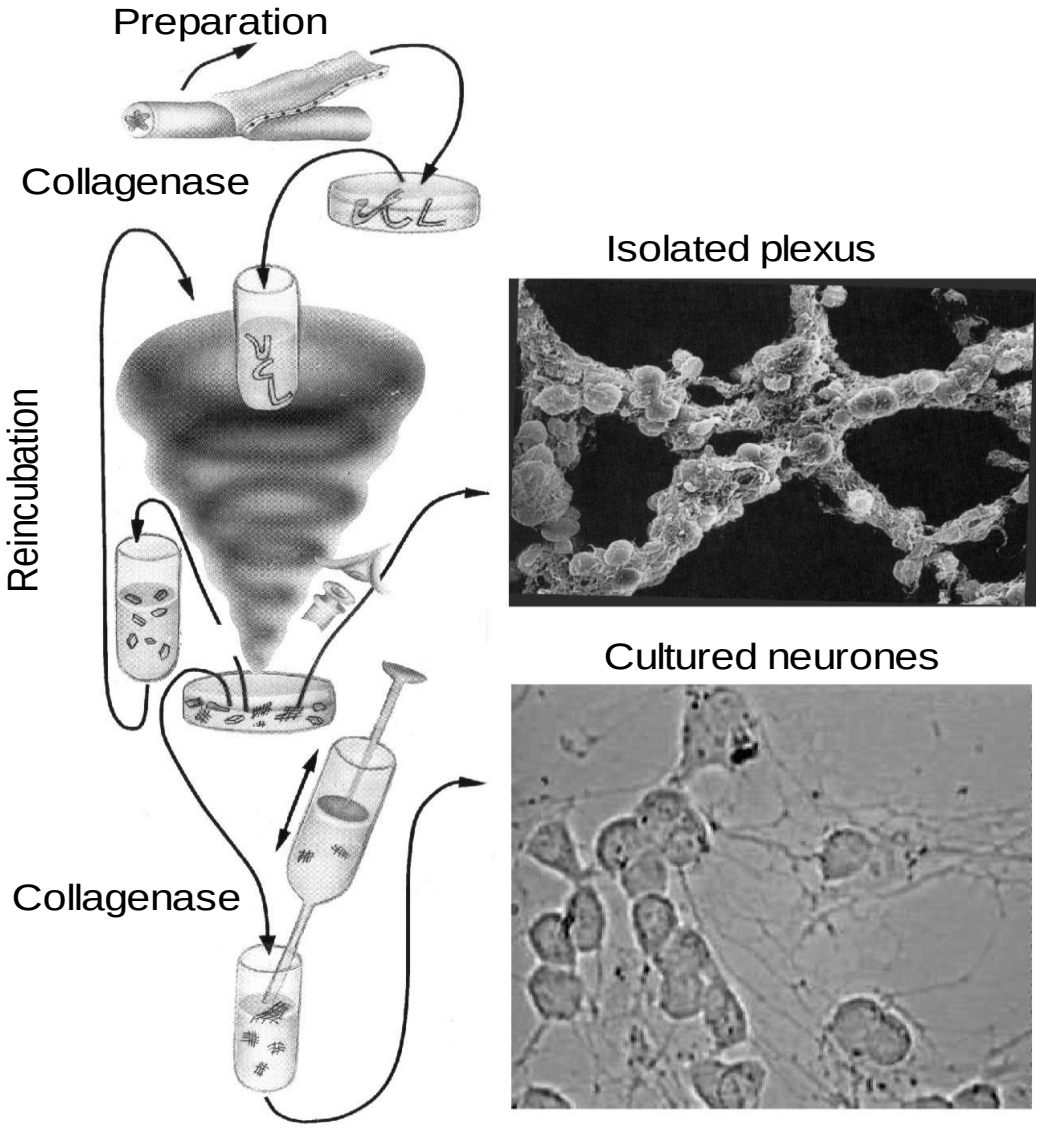

Figure 2.1: Isolation of myenteric plexus, modified from Schäfer et al. 1997.

2.2.2 Patch-clamp experiments

2.2.2.1 Technique

The Figure 2.2 illustrates the principle of the technique. The experiments were performed as described previously (Hamodeh et al. 2004, Rehn et al. 2004). Briefly, the myenteric ganglia grown on glass coverslips were transferred into the experimental chamber (volume of the chamber 0.5 ml). The chamber was mounted on an inverted microscope (Olympus IX-70; Olympus Optical, Hamburg, Germany) which was mounted on a vibration-free table (Vibration-protected table Micro.g, Technical manufacturing corporation, USA). The patch pipettes pulled from borosilicate glass capillaries (Patch-Pipettes Jencons borosilicate (100H15/10/137; BioMedical Instruments, Zöllnitz, Germany) on a two-stages puller (H. Ochotzki, Homburg/Saar, Germany) had a resistance of 5 - 10 MΩ when filled with the standard pipette solution. The bath electrode (reference electrode) was connected with the bathing solution via an agar bridge made of 3 mol/l KCl in 3 % (weight/vol) agar. A micromanipulator (MHW-103; Narishige, London Japan) was used to position the pipette on cells.

For whole-cell recordings, the membrane was broken by a suction pulse at the patch under the tip of the pipette after a seal with a resistance of 5 - 10 GΩ had formed. Membrane capacitance was corrected for by cancellation of the capacitance transient (subtraction) using a 10 mV pulse. In order to differentiate neurones from glial cells or fibroblasts, a pulse of 50 mV amplitude and 30 ms duration was used as described previously (Haschke et al. 2002, Rehn et al. 2004). In this voltage range only neurones exhibit a voltage-dependent fast sodium inward current in the ganglionic preparation (Figure 2.3). The membrane potential as well as the currents were recorded before (control) and after oxidant administration.

Based on the “Ohm’s law”, current-voltage (I-V) curves were obtained by clamping the cell to a holding potential of -80 mV and stepwise depolarization for 30 ms. After

each depolarization, the cell was clamped again to the holding potential for 1 s before the following voltage step (incremented by 10 mV up to +80 mV) was applied. The latter mode is the so-called "voltage-clamp" (Figure 2.4**)** In contrast, in the current-clamp mode either the basal membrane potential (zero-current potential) was measured or by injection of an inward current actions potentials were evoked. For statistical comparison of membrane currents, inward (Na^+) currents were measured for each potential at the time point when it had reached a maximum.

The signals from cells being tiny, so an amplification had to be conducted. For this purpose, a main amplifier (model RK 400, Biologics, Meylan, France) was used. Its preamplifier (headstage) mounted on the micromanipulator and electrically connected to the pipette via a silver/silver chloride wire, measured the current flowing across the membrane patch and converted it into a voltage, then amplified this voltage and transduced it to the main amplifier. For data collection and analysis, the amplifier was connected to several peripheral electronic devices:

- a computer for the generation of command/pulses and storage using the software pClamp 8 (Axon Instruments, Foster City, CA, USA) and for analyses with Origin 5.0 (OriginLab Corporation, Northampton, MA, USA),

- a digitizer that digitized signals at 50 kHz (Digidata 1322 A, Axon instruments, Foster City CA, USA),

- a chart recorder (Phywe type L250 E; Linseis, Selb, Germany),

- a magnetic tape (DAT) recorder for further storage (DAT recorder Sony PCM-R300; Bio-logic, Claix, France).

All experiments were carried out at room temperature. The inverted microcope was mounted on an antivibration table in a Faraday cage.

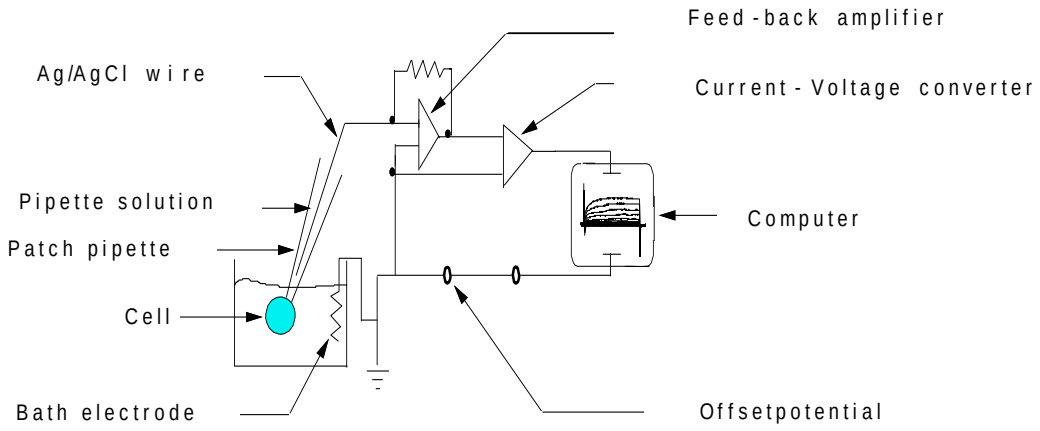

Figure 2.2: Schematic representation of the patch-clamp technique.

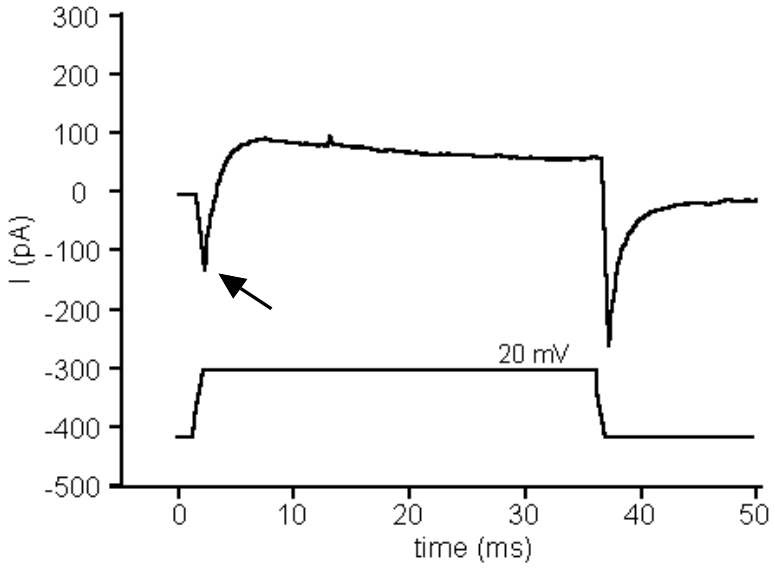

Figure 2.3: Fast sodium inward current in neurones. The arrow shows the fast sodium inward current in neurones in the beginning of a depolarizing pulse (30 ms depolarizatzion from –80 mV to +20 mV).

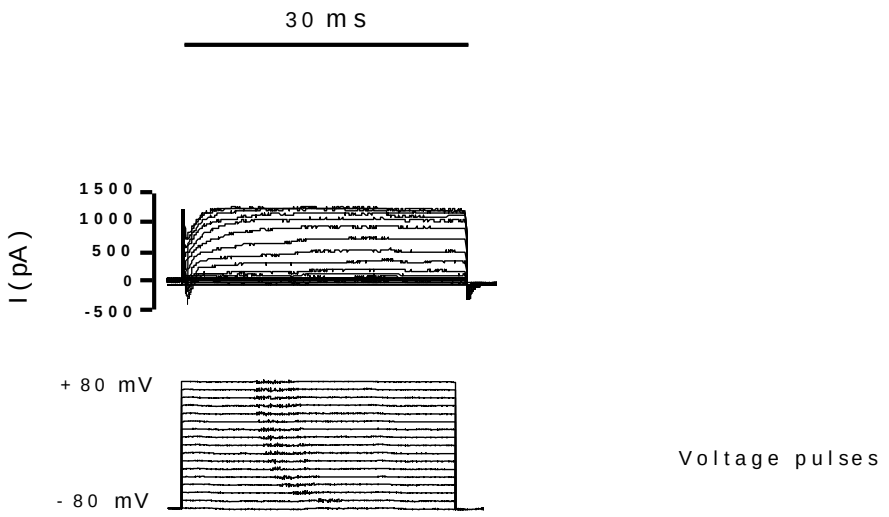

Figure 2.4: Voltage-clamp on a myenteric neurone by 30 ms pulses.

2.2.2.2 Isolation of sodium currents and effects of H_2O_2

The standard solution for superfusion of the cells during the patch-clamp experiments was a HEPES-buffered Tyrode solution. In order to study selectively the contribution of Na^+ currents, a Na^+-reduced Tyrode solution was used (see Table 2.5). In addition, the standard pipette solution (used throughout the patch-clamping) was replaced by a K^+-free pipette solution (see Table 2.5).

2.2.3 Calcium imaging

Changes in the intracellular Ca^{2+} concentration were measured using the Ca^{2+}-sensitive fluorescent dye fura-2 as described previously (Haschke et al. 2002). The neurones grown on coverslips were loaded for 60 min with 2.5 µmol/l fura-2 acetoxymethylester (fura-2AM) in the presence of 0.05 g/l pluronic acid. Then fura-2 was washed away twice. Next, the cells were transfered into the experimental

chamber with a volume of about 0.5 ml and superfused hydrostatically (Hydrostatic pump OLE DICH Type 110 SC G18.CH5B, Instrumentmakers ApS, Hvidovre, Denmark) at about 1 ml/min. The experiments were performed at room temperature on an inverted microscope (IX-50; Olympus, Hamburg, Germany) equipped with an epifluorescence set-up and an image analysis system (Till Photonics, Gräfelfing, Germany). Several regions of interest (Figure 2.5.), each with the size of about one cell, were selected.

Fura-2, being a "wavelength shifting dye", changes the wavelength at which it shows maximal excitation after binding of Ca^{2+}. This property permits ratio measurements, which are obtained by dividing emission values from the ion-bound part of fura-2 by the emission values from the free part of fura-2. The wavelength, at which fura-2 is maximally excited, shifts depending on the cytosolic Ca^{2+} concentration (Figure 2.6.). The dissociation constant (K_D) of fura-2 for Ca^{2+} is 224 nmol/l, making this dye an excellent indicator for Ca^{2+} concentration changes in the concentration range typically found in the cytosol (about 100 nmol/l under resting conditions). The cells were excited alternatively at 340 nm and 380 nm (Figure 2.6.) for 20 ms and the ratio of the emission signal (above 470 nm) at both excitation wavelengths was calculated. Data were sampled at 0.2 Hz (one pair of pictures every 5 s).

The baseline in the fluorescence ratio of fura-2 was measured during at least 5 min, superfusing with a standard or a Ca^{2+} free Tyrode solution (depending on the experiment), before any drug was administered. Carbachol (CCh, 50 µmol/l) was used for vitality test of cells and identifying neurones.

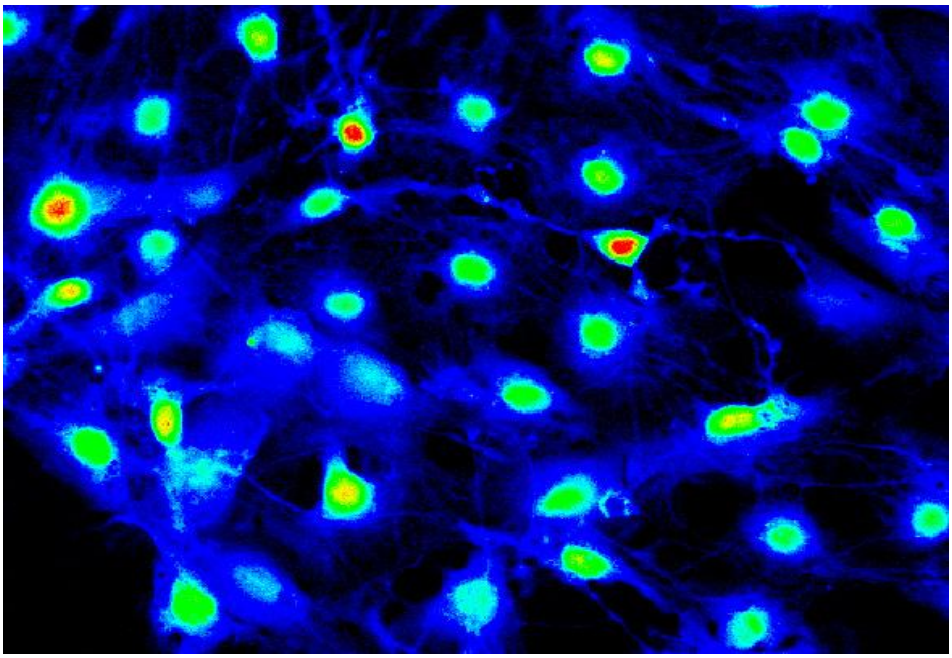

Figure 2.5: Picture of myenteric neurones loaded with fura-2. The red color represents the highest loading rate.

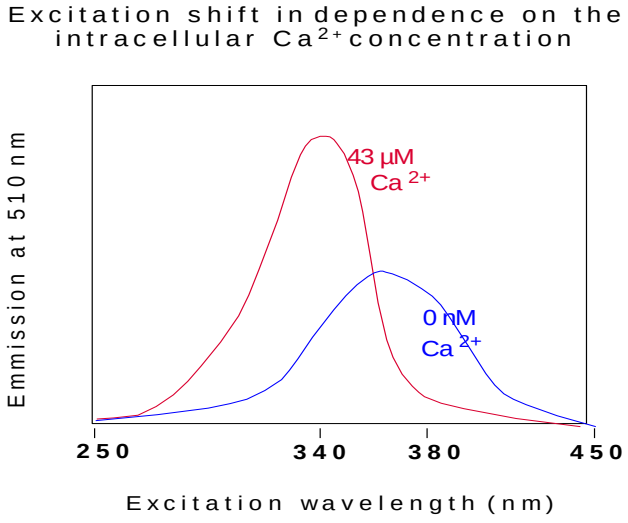

Figure 2.6: Excitation spectra of fura-2 at a high Ca^{2+} concentration (red line) and at low Ca^{2+} concentration (blue line).

2.2.4 Statistics

Results are given as mean ± standard error of the mean (S.E.M.) with the number (n) of investigated neurones. For the comparison of two groups, either a Student's t-test or a Mann Whitney U-test was applied. The Wilcoxon test for matched pairs was used for comparing changes in the same group before and after administration of the oxidant. An F-test decided which test method had to be used. Both paired and unpaired two-tailed Student's t-tests were applied as appropriate. When the mean values of more than two groups had to be compared, a one-way ANOVA test was performed followed by analysis of linear contrasts with the Tukey's test.

3 Results

The major results of the thesis have been published in the journal „European Journal of Pharmacology“ by Pouokam et al. (2009).

3.1 Effect of H_2O_2 on the membrane potential and the cytosolic Ca^{2+} concentration

Hydrogen peroxide (5 mmol/l) hyperpolarized the membrane of the myenteric neurones, when the oxidant was administered under current-clamp conditions during whole-cell patch-clamp recordings (Figure. 3.1). Prior administration of H_2O_2, basal membrane potential amounted to -41.2 ± 0.8 mV. The membrane hyperpolarized to -52.5 ± 0.8 mV in the presence of the oxidant. In average, the hyperpolarization amounted to 11.3 ± 0.8 mV ($n = 30$, $P < 0.05$). A further effect was a strong inhibition of the fast Na^+ inward current under voltage-clamp conditions (see e.g. Figure. 3.4). The effect of H_2O_2 on membrane potential, also that of lower concentrations, was not reversible upon wash out suggesting a covalent modification of ion channels or their respective regulator proteins.

The concentration of H_2O_2 was chosen according to concentration-response experiments (Figure. 3.1 inset), which revealed a maximal hyperpolarization at a concentration of 5 mmol/l

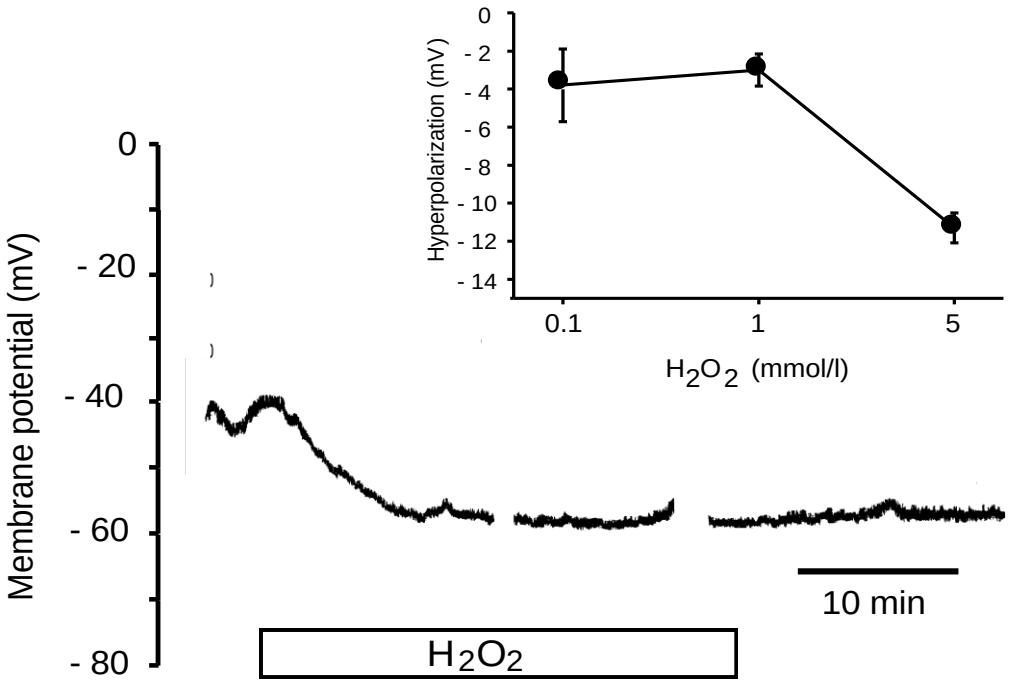

Figure 3.1: Hydrogen peroxide (5 mmol/l; white bar) hyperpolarizes the membrane. Original tracing representative for 30 recordings. In average, H_2O_2 hyperpolarized the membrane by 11.3 ± 0.8 mV (n = 30, P < 0.05). Line interruptions are caused by measurements of I-V curves in the voltage-clamp mode. The effect of H_2O_2 on membrane potential was not reversible upon wash out. Inset: Concentration-dependent hyperpolarization induced by H_2O_2. Tested concentrations were 0.1, 1 and 5 mmol/l. Values are means (symbols) ± S.E.M. (vertical bars), n > 5 for each concentration.

Rat myenteric neurones have functionally been shown to express Ca^{2+}-dependent K^+ channels (Hamodeh et al. 2004) and oxidants are known to induce an increase in the cytosolic Ca^{2+} concentration in other cells (see e.g. Schultheiss et al. 2005, Bogeski et al. 2006, Ishii et al. 2006). Therefore, I investigated whether H_2O_2 induced an increase in the cytosolic Ca^{2+} concentration at fura-2 loaded myenteric ganglia. In deed, the oxidant evoked an increase in the fura-2 ratio signal (Figure 3.2A), which in average increased by 0.35 ± 0.08 above baseline (measured 30 min after administration of H_2O_2; Table 3.1). The action of the oxidant on the cytosolic Ca^{2+} concentration was concentration-dependent (Figure 3.2B) and was not reversible upon washout of H_2O_2.

Both an influx of extracellular Ca^{2+} as well as a release of stored Ca^{2+} seem to contribute to this effect, because superfusion with a Ca^{2+}-free buffer as well as store depletion with the inhibitor of sarcoplasmic-endoplasmic reticulum ATPases (SERCA; for references to this and the following inhibitors used, see e.g. Schultheiss et al. 2005), cyclopiazionic acid (40 μmol/l), both reduced the effect of the oxidant (Figure 3.3A and B; Table 3.1).

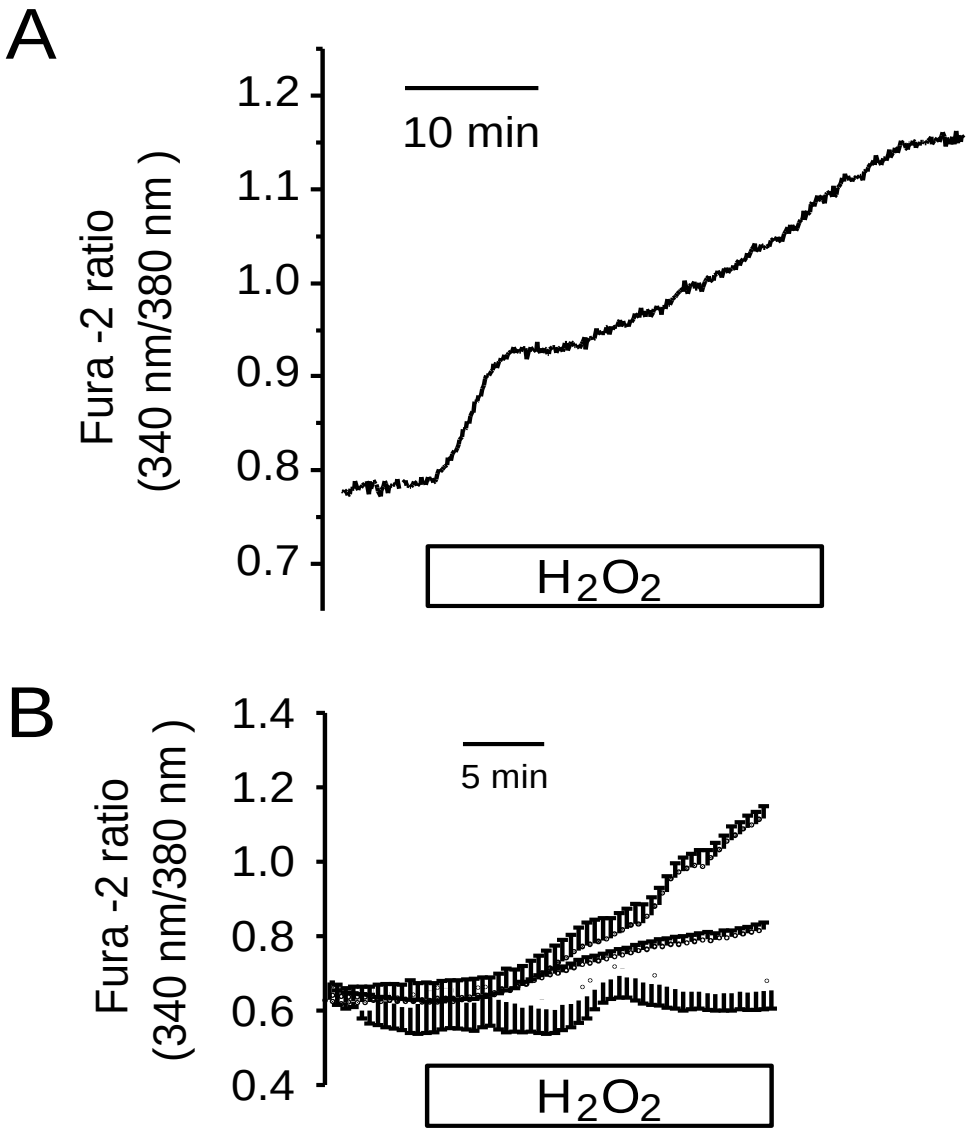

Figure 3.2A: Hydrogen peroxide (5 mmol/l; white bar) caused an increase in the fura-2 ratio signal at rat myenteric neurones. Typical tracing; for statistics, see Table 3.1. The effect of H_2O_2 on the cytosolic Ca^{2+} concentration was not reversible upon wash out. B: Effect of different concentrations of H_2O_2 (filled squares: 0.1 mmol/l ; open circles: 0.5 mmol/l ; filled circles: 5 mmol/l) on the fura-2 ratio signal. Values are means (symbols) ± S.E.M. (vertical bars), n > 6 for each concentration.

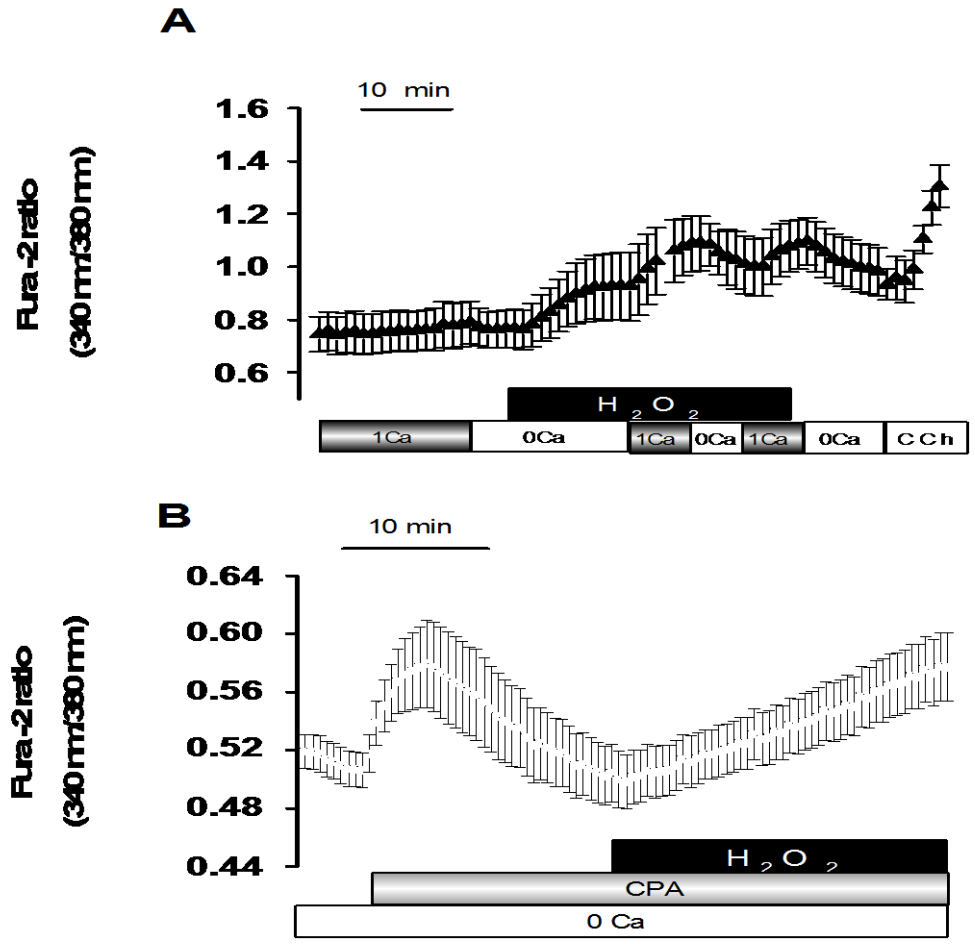

Figure 3.3A: Hydrogen peroxide induces the release of Ca^{2+} from internal stores and an influx of extracellular Ca^{2+}. The response to H_2O_2 (5 mmol/l; black bar) was reduced under Ca^{2+}-free conditions (0 Ca; white bar) and reversibly enhanced upon readministration of Ca^{2+} (1 Ca; grey bar). At the end of this experiment, carbachol (CCh, 50 µmol/l) was administered as viability control. B: Depletion of internal stores by cyclopiazonic acid (CPA, 40 µmol/l; grey bar) also reduced the effect of H_2O_2 (5 mmol/l; black bar). The experiment was performed under Ca^{2+}-free conditions (0 Ca). Values are means (symbols) ± S.E.M. (vertical bars), n = 5 –9. For statistics, see Table 3.1.

Experimental condition	**Δ Fura-2 ratio (340/380 nm)**	**n**
1.25 mmol/l Ca^{2+} + H_2O_2 (control)	0.35 ± 0.08^a	11
0 Ca^{2+} + H_2O_2	0.11 ± 0.02^b	17
0 Ca^{2+} + CPA + H_2O_2	0.07 ± 0.00^b	9
1.25 mmol/l Ca^{2+} + CPA + H_2O_2	0.25 ± 0.04^a	10
1.25 mmol/l Ca^{2+} + CPA + Gd^{3+} + H_2O_2	0.04 ± 0.01^b	31
0 Ca^{2+} + RuR + H_2O_2	0.06 ± 0.01^b	18
0 Ca^{2+} + 2-APB + H_2O_2	0.05 ± 0.00^b	12

Table 3.1: Changes in the fura-2 ratio evoked by H_2O_2

Increase in the fura-2 ratio signal evoked by H_2O_2 (5 mmol/l) in the presence of Ca^{2+} (control conditions) or the absence of extracellular Ca^{2+} combined with the SERCA-blocker cyclopiazonic acid (CPA; 40 µmol/l), the inhibitor of the capacitative Ca^{2+} influx Gd^{3+} (1 mmol/l), the IP_3-receptor blocker 2-APB (100 µmol/l), or the ryanodine receptor blocker ruthenium red (RuR; 30 µmol/l). Data are given as difference in the fura-2 ratio to the baseline just prior administration of the oxidant (Δ ratio). Statistically homogeneous groups are indicated by the same letter (a, b; analysis of variances followed by Tukey's test).

The response to H_2O_2 was nearly suppressed, when - in addition to cyclopiazonic acid - Gd^{3+} (1 mmol/l), a known blocker of capacitative Ca^{2+} influx (see e.g. Kerst et al. 1995), was present.

These data suggest that H_2O_2 may induce a release of Ca^{2+} from intracellular stores, which evokes a capacitative Ca^{2+} influx. Both IP_3 receptors as well as ryanodine receptors seem to be involved as 2-APB (100 µmol/l) or ruthenium red (30 µmol/l), two typical inhibitors of these intracellular Ca^{2+} channels, also strongly inhibited the effect of the oxidant (Figure 3.4, Table 3.1). Both inhibitors were administered in the absence of extracellular Ca^{2+} in order to prevent unspecific effects on Ca^{2+} transporters in the plasma membrane (see Discussion).

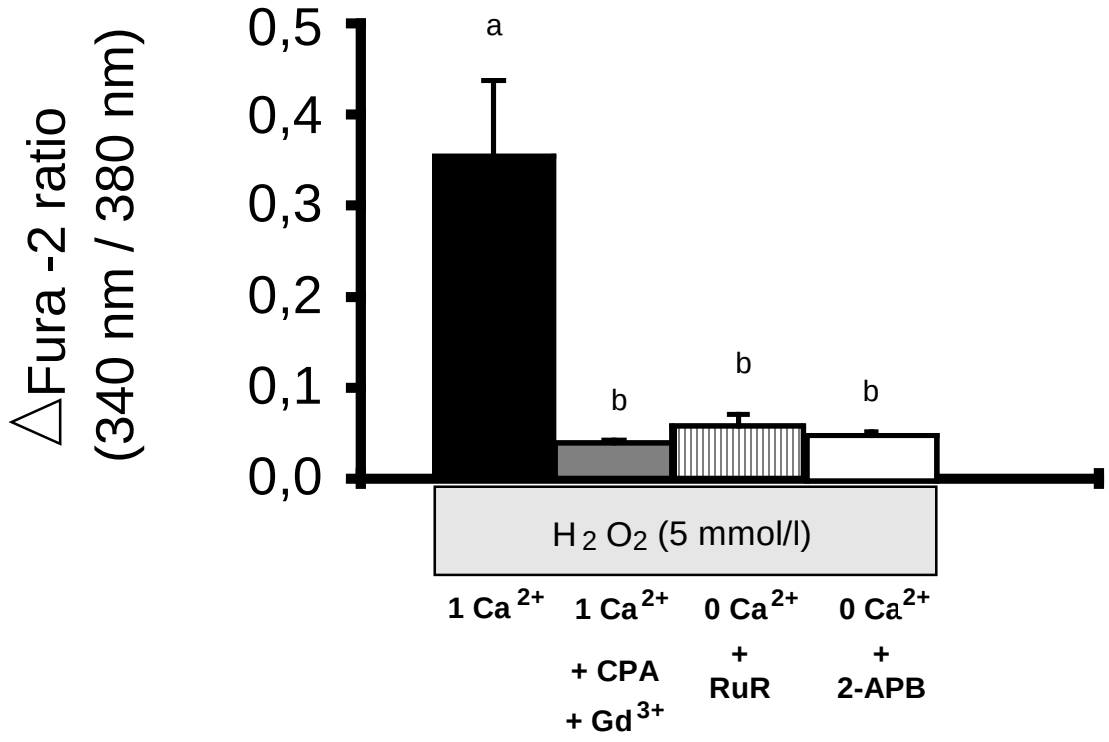

Figure 3.4: Effect of H_2O_2 (5 mmol/l) on the fura-2 ratio in the absence of any inhibitors (black bar), or in the combined presence of cyclopiazonic acid (CPA; 40 µmol/l) and Gd^{3+} (measured in the presence of Ca^{2+}; grey bar; n = 20), in the presence of ruthenium red (RuR; 30 µmol/l; measured in the absence of Ca^{2+}; vertically shaded bar; n = 18), or in the presence of 2-APB (100 µmol/l; measured in the absence of Ca^{2+}; white bar; n = 12). Data are given as means (symbols) ± S.E.M. (vertical bars) corresponding to differences in the fura-2 ratio to the baseline just prior administration of the oxidant (Δ ratio). Statistically homogeneous groups are indicated by the same letter (a, b; analysis of variances followed by Tukey's test).

In order to find out, whether an activation of Ca^{2+}-dependent K^+ channels couple the two phenomena, i.e. the increase in the cytosolic Ca^{2+} concentration (Figure 3.2) and the observed hyperpolarization (Figure 3.1), two strategies were followed. First, a combination of inhibitors, i.e cyclopiazonic acid (40 µmol/l, applied via the patch pipette solution) and Gd^{3+} (1 mmol/l, added to the bathing solution), which in the fura-2 experiments nearly suppressed the H_2O_2 response, was administered during the patch-clamp recordings.

Administration of Gd^{3+} (1 mmol/l) alone induced a depolarization of the membrane from –46.5 ± 4.5 mV to –30.0 ± 9.0 mV (n = 7). Under these conditions, H_2O_2 did no more evoke a hyperpolarization of the membrane, i.e. membrane potential amounted to –27.5 ± 3.9 mV in the combined presence of the oxidant and Gd^{3+} ($P < 0.05$ versus the change in the membrane potential of 11.3 ± 0.8 mV under control conditions as shown in the Figure 3.1).

Furthermore, the sensitivity of H_2O_2 response to tetrapentylammonium (100 µmol/l), a K^+ channel blocker with a high affinity for Ca^{2+}-dependent K^+ channels (see e.g. Maguire et al. 1999), was tested (Figure 3.5A). The K^+ channel blocker depolarized the membrane from –44.5 ± 4.3 mV to –37.5 ± 4.6 mV and subsequent administration of H_2O_2 shifted the membrane potential to –35.6 ± 5.1 mV (n = 10); i.e. the response to the oxidant was completely suppressed. A similar inhibition was observed with paxilline (1 µmol/l; Figure 3.5B; n = 6), another inhibitor of Ca^{2+}-dependent K^+ channels (see Strobaeck et al. 1996, Sanchez and Mc Manus 1996, Wei et al. 2005 for references to this inhibitor). This latter inhibitor slightly depolarized the neuronal membrane from –37.8 ± 5.5 mV to –40.3 ± 5.4 mV (n = 6) and suppressed the H_2O_2-induced hyperpolarization as the potential in the presence of both paxilline and the oxidant amounted only to –38.1 ± 6.6 mV.

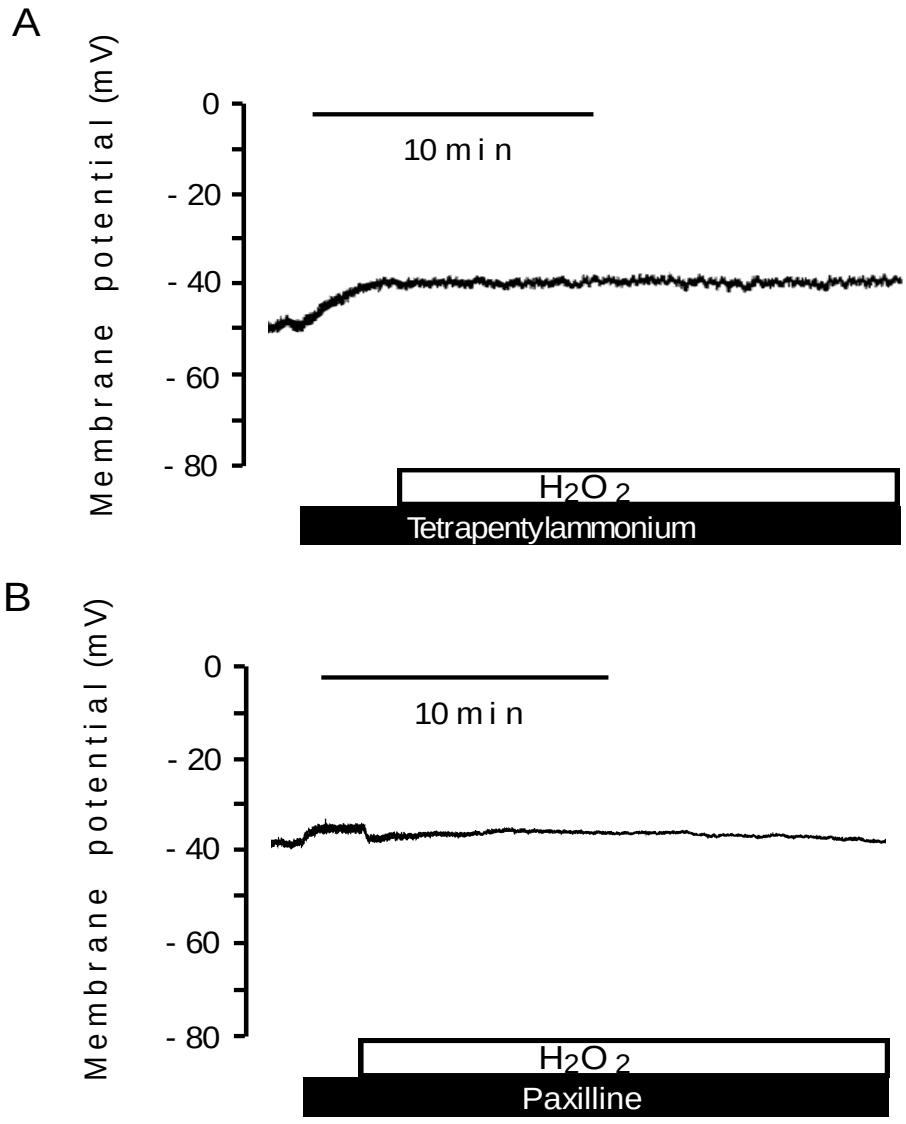

Figure 3.5A: The hyperpolarization evoked by H_2O_2 (5 mmol/l; white bar) was suppressed in the presence of the broad inhibitor of Ca^{2+}-dependent K^+ channels tetrapentylammonium (100 µmol/l; black bar, A). B: Inhibition of Ca^{2+}-dependent K^+ channels by paxilline (1 µmol/l ; black bar) prevented the hyperpolarization observed in Figure 3.1. Typical recordings. For statistics, see text.

3.2 Inhibition of the Na^+ currents

As already mentioned, inward currents, evoked by depolarizing steps during voltage-clamp experiments, were inhibited by H_2O_2 in a concentration-dependent manner (Figure 3.6). Under control conditions, the myenteric neurones developed an inward current (measured at its maximum) of 487 ± 106 pA (n = 7). The inward current was strongly inhibited to a value of 136 ± 106 pA in the presence of H_2O_2 (5 mmol/l; n = 7, $P < 0.05$ versus inward current before administration of the oxidant; Table 3.2). These changes were not reversible upon wash out (data not shown).

The inhibition of the inward current was concomitant with a shift (of 10 to 20 mV) of the maximum of the inward current to more negative potentials (Figure 3.6 and 3.9B). The reversal potential was also shifted (about 20 mV) to more negative values while the activation as well as the inactivation slopes appeared to be less steep compared to control (Figures 3.6, 3.8 and 3.9). In difference to the ability of the oxidant to induce a hyperpolarization, it did not change the activation threshold of the sodium channels as currents inflow started at the same potential prior or after administration of H_2O_2 (Figure 3.6, 3.8 and 3.9). Therefore, the shifts to more negative potentials and the changes in the activation/inactivation slopes may reflect changes in the gating properties of the channels.

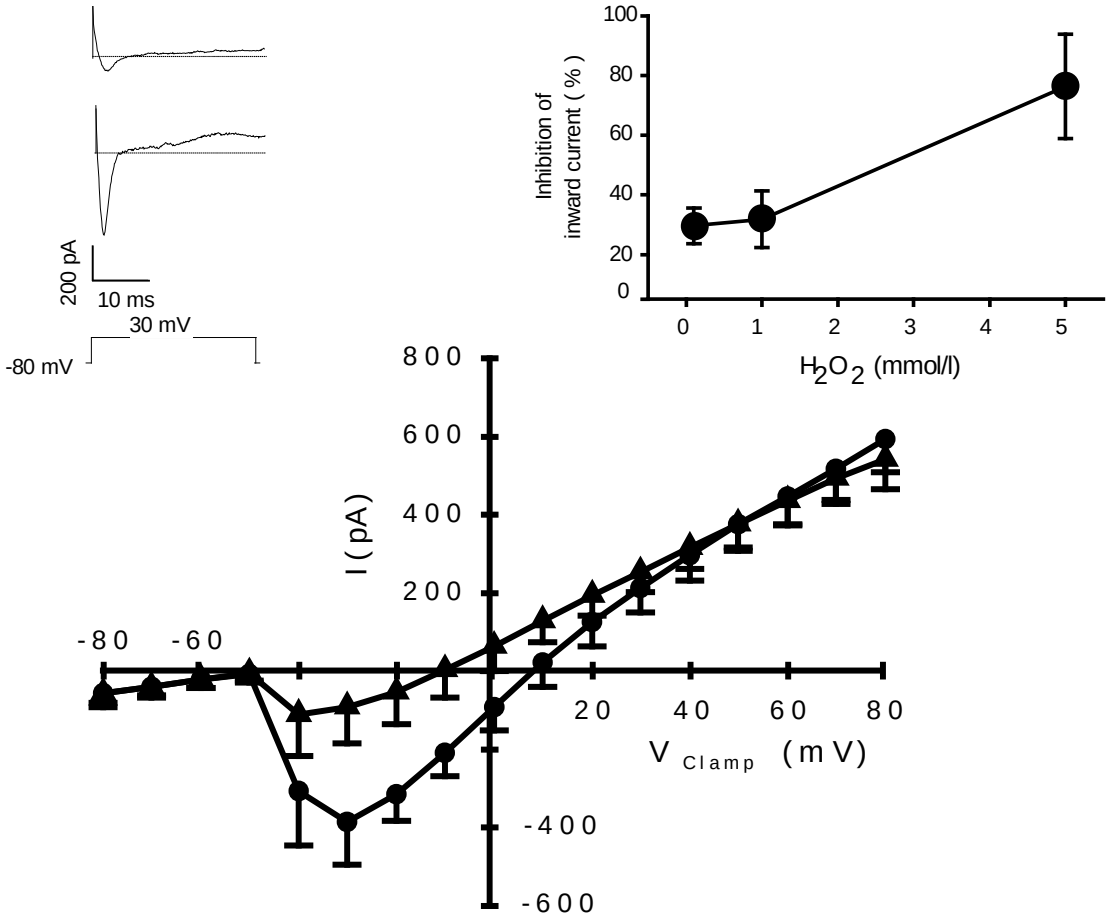

Figure 3.6: Fast sodium inward currents measured in the voltage-clamp mode under control conditions (filled circles, n = 7), and in the presence of 5 mmol/l H_2O_2 (filled triangles, n = 7). Values are means (symbols) ± S.E.M. (vertical bars). The inset at the upper left shows an original tracing of the inward current of one neurone evoked by a 30 ms depolarizing pulse in the presence (upper tracing) or absence (lower tracing) of H_2O_2. The inset at the upper right shows the concentration-dependence of the inhibition of the sodium inward current by H_2O_2. Tested concentrations were 0.1, 1 and 5 mmol/l. Values are means (symbols) ± S.E.M. (vertical bars), n = 4 - 5 for each concentration.

The inward current at cultured rat myenteric neurones from newborn rats has been demonstrated to be mediated by a tetrodotoxin-sensitive inflow of Na^+ (Haschke et al. 2002). Tetrodotoxin (TTX) is a neurotoxin, which inhibits voltage-dependent Na^+ currents in many neurones (Catterall 1980), although tetrodotoxin-resistant Na^+ channels are known, too (see e.g. Browning and Lees 1996, Padilla et al. 2007).

This was confirmed in the present experiments. In 5 out of 6 neurones tested, tetrodotoxin (100 nmol/l) completely suppressed the inward current (Figure 3.7). When the neurotoxin was washed out and H_2O_2 (5 mmol/l) was administered, the oxidant inhibited the current, too (Figure 3.7). The remaining inward current, which still could be evoked in the presence of H_2O_2, was suppressed when in addition to H_2O_2 TTX was administered. Only in 1 out of 6 neurones tested, the inward current proved to be partially resistant against TTX. From the 627 pA recorded as control inward current in this cell, a residual current of 206 pA was insensitive to the neurotoxin. Also in this neurone, H_2O_2 inhibited the inward current (data not shown).

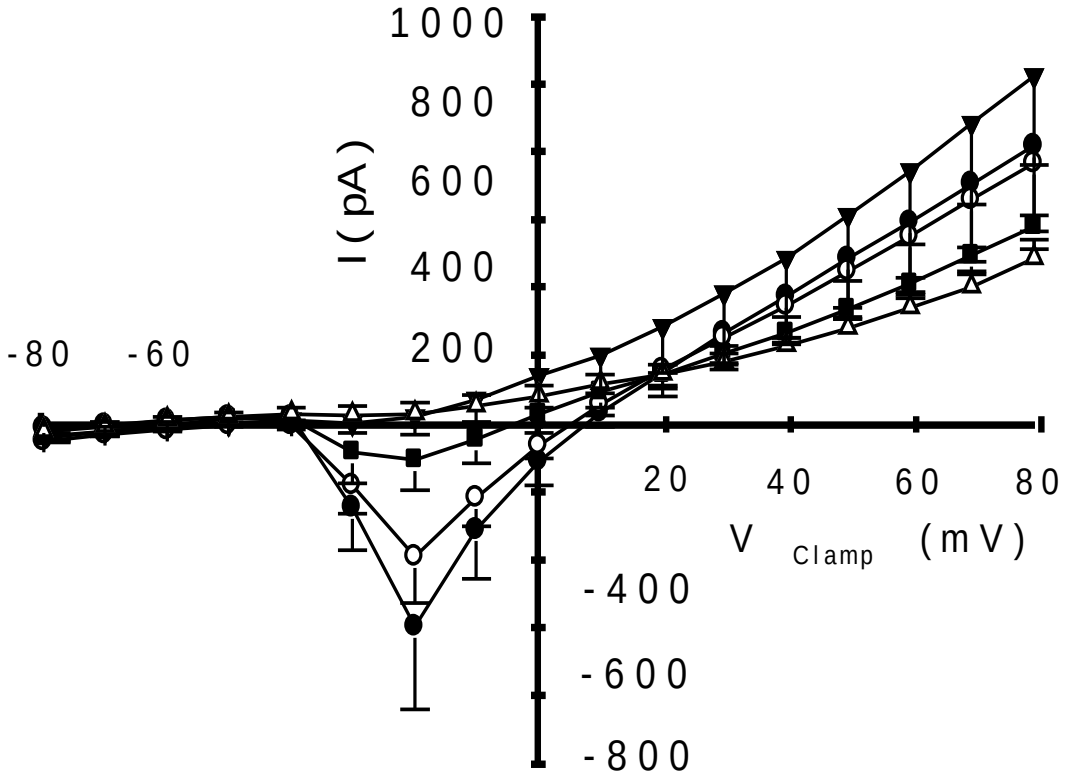

Figure 3.7: Hydrogen peroxide (5 mmol/l) inhibits the tetrodotoxin-sensitive sodium currents. The inward currents were measured under standard conditions, i.e. during superfusion with a 135 mmol/l NaCl-Tyrode (filled circles). Then the superfusion was changed to a 135 mmol/l NaCl-Tyrode solution containing tetrodotoxin at the concentration 100 nmol/l (filled triangles). Next, the sodium currents were recorded after washing out tetrodotoxin (open circles); the oxidant H_2O_2 (5 mmol/l) was then applied (filled squares). Finally, tetrodotoxin (100 nmol/l; open triangles) suppressed the remaining sodium currents. Values are means (symbols) ± S.E.M. (vertical bars), n = 5.

In order to check the selectivity of the oxidant-inhibited inward current for Na^+, K^+ currents were inhibited by the use of K^+ channel blockers, i.e. tetraethylammonium (TEA) in the superfusion medium and CsCl in the pipette solution, which replaces the cytoplasm during conventional whole-cell recordings (for K^+ channel blocking actions of these compounds, see Cook and Quast 1990). Ca^{2+} currents were inhibited by reducing the extracellular Ca^{2+} concentration and increasing in parallel the Mg^{2+} concentration (see Methods). When the extracellular Na^+ concentration was reduced from 135 mmol/l to 70 mmol/l, the inward current decreased from 835 ± 208 pA to 573 ± 82 pA (n = 6; Figure 3.8) as one should expect for a Na^+ conductance when reducing the concentration of the permeant ion. Under these conditions, H_2O_2 still strongly inhibited the inward currents from 573 ± 82 to 150 ± 46 pA ($P < 0.05$; Figure 3.8).

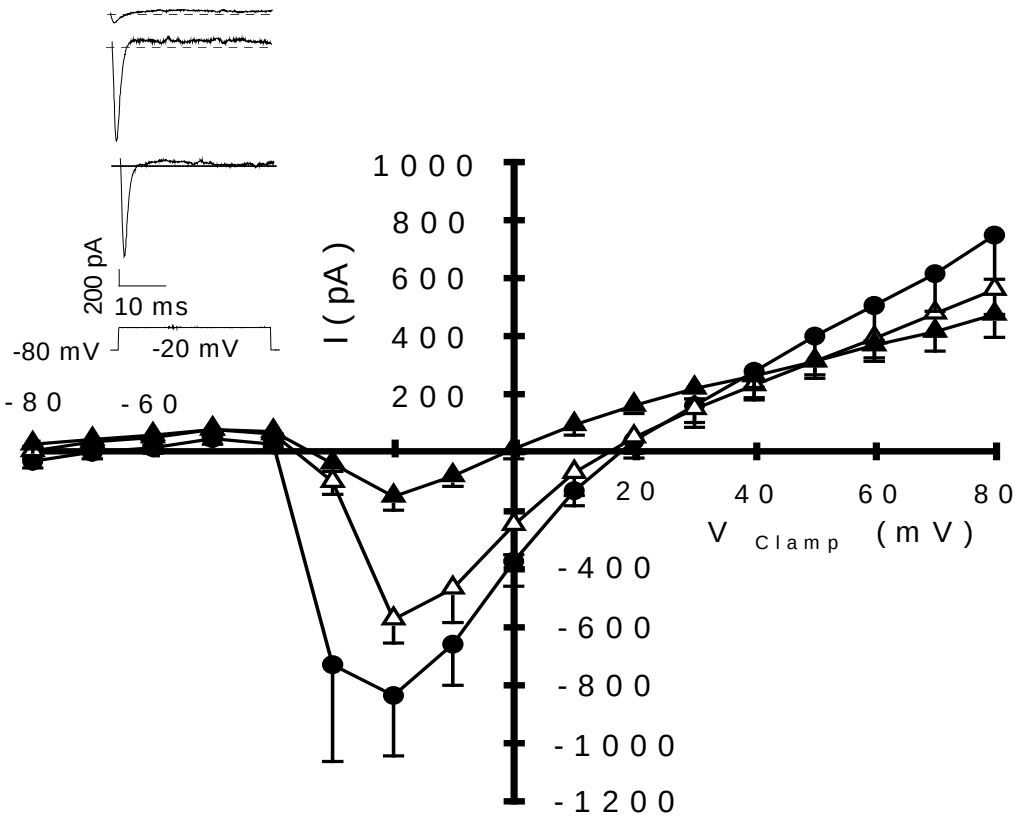

Figure 3.8: Specificity of the H_2O_2–inhibited current for Na^+. The inward current was first measured under standard conditions, i.e. during superfusion with a 135 m mol/l NaCl-Tyrode (filled circles). Then the superfusion was changed to a solution with a reduced Na^+ concentration (70 mmol/l) and a mixture of K^+ channel blockers (see Methods; open triangles). Finally, H_2O_2 (5 mmol/l) was added (filled triangles). The pipette solution used for this set of whole-cell recordings contained CsCl (140 mmol/l) in order to further suppress K^+ currents. Values are means (symbols) ± S.E.M. (vertical bars), n = 6. The inset shows an original tracing of the inward current of one neurone evoked by a 30 ms depolarizing pulse in the presence of 70 mmol/l NaCl-Tyrode + H_2O_2 (upper tracing), 70 mmol/l NaCl-Tyrode (middle tracing), or 135 mmol/l NaCl-Tyrode (lower tracing).

The obvious discrepancy between the reversal potential of the Na^+ current (about +20 mV; Figure 3.8) and the theoretical Na^+ equilibrium of about +65 mV under the conditions used (10 mmol/l Na^+ in the pipette, 135 mmol/l in the superfusion medium, and room temperature) might indicate an incomplete voltage control during the voltage-clamp experiments, e.g. by space clamp problems due to the complex geometry of the neurones (Bar-Yehuda and Korngreen 2008). As described above, in the current-clamp mode, the zero-current potential hyperpolarized in the presence of H_2O_2 (Figure 3.1), presumably by the opening of Ca^{2+}-dependent K^+ channels. Consequently, it might be thought that the hyperpolarization of poorly clamped membrane areas could apparently shift the clamped voltage during the depolarizing pulses to more negative values and thereby simulate an inhibition of the Na^+ current simply by preventing the membrane potential to reach the necessary threshold for its activation. In order to exclude an interference of space-clamping problems with the response to H_2O_2, two sets of experiments were performed. First, Na^+ inward currents were measured at isolated neurones, which upon isolation have a spherical form without pronounced dendrites and axons, which improves the conditions for voltage-clamping. At these cells, the reversal pontential of the Na^+ amounted to +40 mV (Figure 3.9A) compared to only about +10 mV as measured in intact ganglionic preparations (see e.g. Figure 3.1). Also under these conditions of improved voltage-control, H_2O_2 (5 mmol/l) strongly inhibited the Na^+ current from 422 ± 57 pA to 120 ± 52 pA ($n = 6$, $P < 0.05$, Figure 3.9A).

In a second set of experiments, intact ganglia were patched, at which the K^+ conductance, i.e. the dominant membrane conductance of these neurones (Rehn and Diener 2006), was inhibited by extracellular Ba^{2+} (10 mmol/l), a blocker of many types of K^+ channels (Cook and Quast 1990). Also under these conditions, the reversal potential of the Na^+ current was shifted to more positive values (about +45 mV) and H_2O_2 (5 mmol/l) strongly inhibited this current (from 388 pA ± 29 to 86 pA ± 26, $n = 6$, Figure 3.9B), suggesting that the hyperpolarization induced by the oxidant (Figure 3.1) together with an incomplete voltage-control can not be the reason for the inhibition of the Na^+ current. However, under both conditions, i.e. at the

isolated cells as well as in the presence of Ba^{2+}, the reversal potential of the Na^+ current was shifted by H_2O_2 to less positive values (Figure 3.9), which might indicate that the oxidant also induces alterations at the selectivity filter of the voltage-dependent Na^+ channel.

A **B**

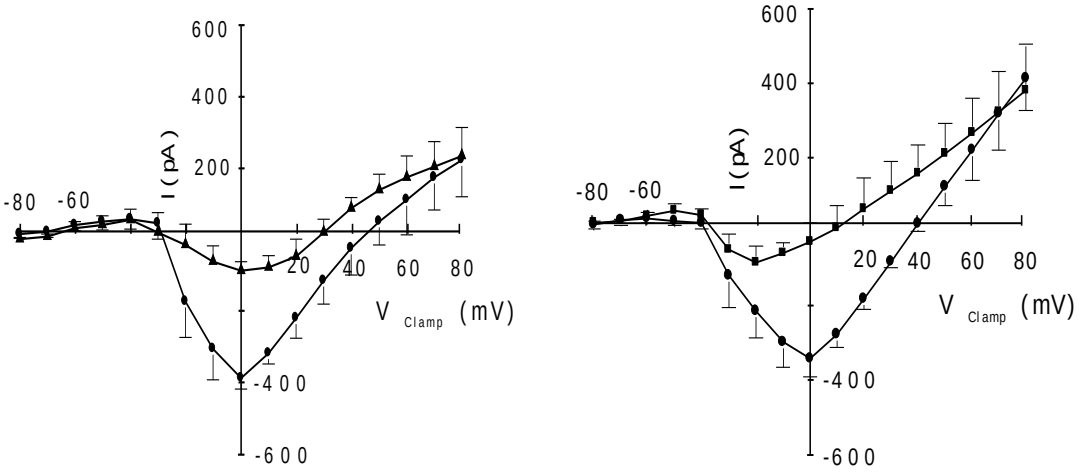

Figure 3.9A: Effect of H_2O_2 on Na^+ currents at spherical, isolated myenteric neurones. Fast sodium inward currents were measured in the voltage-clamp mode under control conditions (filled circles, n = 6), and then in the presence of 5 mmol/l H_2O_2 (filled squares, n = 6). B: Effect of H_2O_2 on Na^+ currents on intact ganglionic cells after blockade of K^+ currents with Ba^{2+}. Fast sodium inward currents were measured in the voltage-clamp mode in the presence of 10 mmol/l Ba^{2+} (filled circles, n = 6), and then in the additional presence of 5 mmol/l H_2O_2 (filled triangles, n = 6). Values are means (symbols) ± S.E.M. (vertical bars).

3.3 Alteration of the excitability

The inhibition of sodium currents should impair the generation of action potentials of the myenteric neurones. To confirm this hypothesis, action potentials were evoked by injection of an inward current under current-clamp conditions in the absence or presence of H_2O_2. This inward current evoked action potentials in all (22 out of 22) neurones tested (Figure 3.10A, C, E). As already reported by Browning and Lees (1990), in rat myenteric neurones a long (150 ms) depolarizing current evokes either a single (or a pair) of action potentials in "single firing neurones" (Figure. 3.10E), or a train of action potentials during the whole stimulation period in "multiple firing neurones" (Figure 3.10A, C).

The oxidant induced three types of responses in dependence on the firing properties of the neurones. The multiple firing neurones (Figure 3.10A, C) responded in two ways (indicating a probable subgrouping) to H_2O_2. Fifteen out of 22 neurones presented only a single action potential in the beginning of the depolarizing pulse after administration of the oxidant (Figure 3.10B), while 3 out of 22 showed one action potential of normal amplitude followed by a low amplitude oscillation of the membrane potential (Figure 3.10D). In the three single firing neurones tested (Figure 3.10E), the single action potential was suppressed by the oxidant (Figure 3.10F).

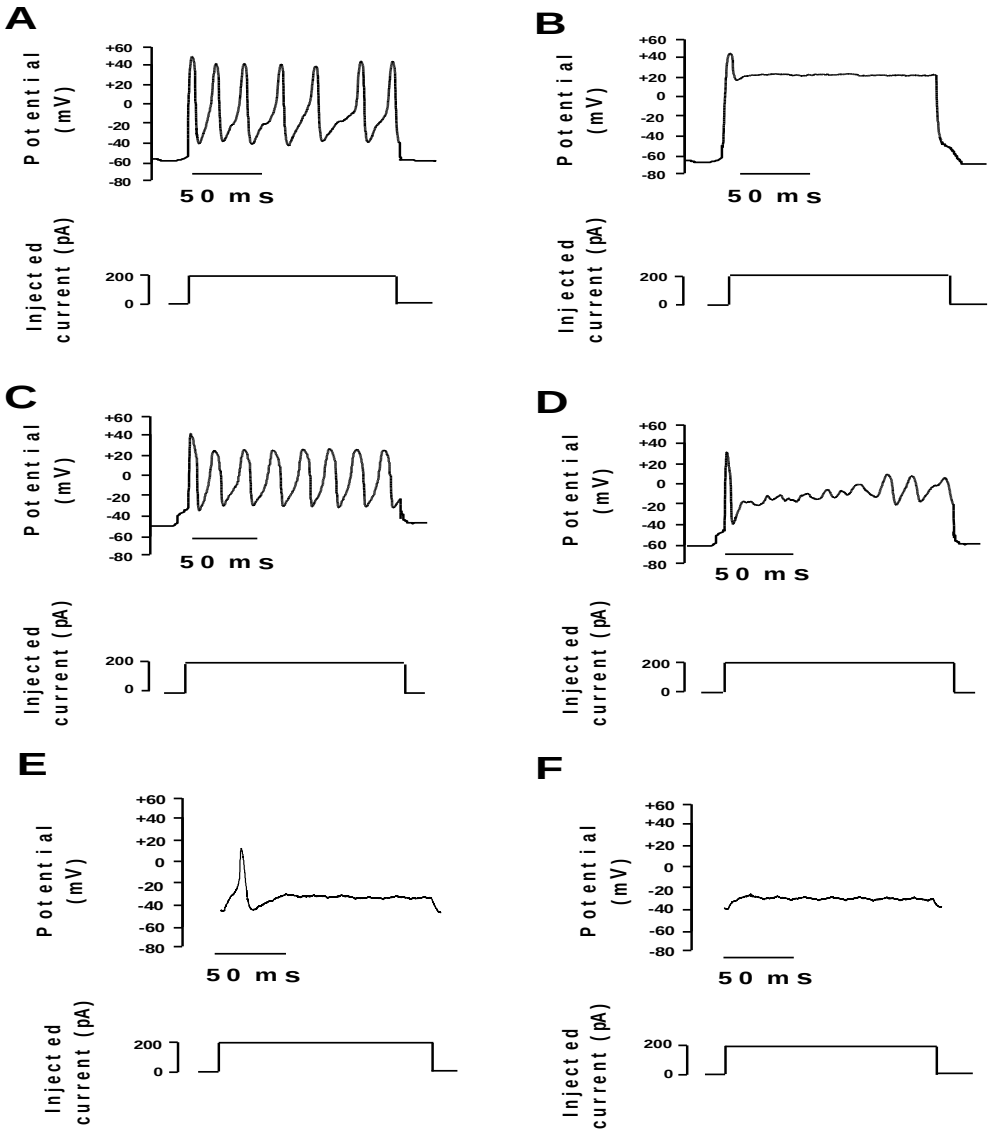

Figure 3.10: Change in action potential generation induced by H_2O_2 measured in the current-clamp mode. Repetitive action potentials were evoked by injection of an inward current (200 pA during 150 ms) under control conditions (A, C and E), or in the presence of H_2O_2 (5 mmol/l ; B, D, F). Three types of responses to the oxidant were observed. In multiple firing neurones (A, C), depolarization in the presence of H_2O_2 evoked either only a single action potential in the beginning of the depolarizing pulse (observed in 15 out 22 neurones; B), or it induced one action potential of normal amplitude followed by a low amplitude oscillation of the membrane potential (observed in 3 out 22 neurones; D). In single firing neurones (E), the oxidant suppressed the action potential (observed in 3 out 22 neurones). The figure pairs A/B, C/D, and E/F show the same neurone in the absence (A, C, E) or presence (B, D, F) of H_2O_2.

3.4 Mediation of the H_2O_2 effects on Na^+ currents

The inhibition of the Na^+ inward current was also observed under conditions, where the changes in the cytosolic Ca^{2+} concentration evoked by the oxidant should be suppressed, i.e. in the presence of cyclopiazonic acid combined with Gd^{3+} (data not shown), a blocker combination, which prevents the hyperpolarization induced by H_2O_2. Therefore, mechanisms other than the increase in the cytosolic Ca^{2+} level must be responsible for this phenomenon. Hydrogen peroxide easily crosses the cell membrane and can release •OH, a derivative with potent oxidative properties (Grisham et al. 1990, Ishi et al. 2006, Hool and Corry 2007).

In order to find out, whether this radical might mediate the inhibition of the fast Na^+ inward current, two sets of experiments were performed. In a first attempt, N-(2-mercaptoproprionyl)-glycine (MPG, 1 mmol/l), which acts as a radical scavenger (Ishii et al. 2006), was included in the patch pipette. In the presence of MPG, the inhibition of Na^+ inward current by H_2O_2 (5 mmol/l) was smaller (inhibition of 52.3 % compared to 73.5 % in the absence of the scavenger, Table 3.2), although this reduction did not reach statistical significance. It was not possible to use a higher concentration (5 mmol/l) of MPG, because the scavenger obviously reduced the viability of the cells during the whole-cell recording at this concentration (data not shown).

However, when another scavenger, trolox (10 µmol/l; for references to this drug see e.g. Angelova and Müller 2006), was included in the patch pipette solution, the inhibition of the sodium inward current by H_2O_2 was significantly ($p < 0.05$) attenuated (Table 3.2).

Condition	**I_{in}^{max} (pA) under control conditions**	**I_{in}^{max} (pA) in the presence of H_2O_2**	**Inhibition of I_{in}^{max} by H_2O_2 (%)**	**n**
Control	487.1 ± 106.5	135.9 ± 106.2	73.5 ± 14.1[a]	7
MPG	437.1 ± 68.6	208.2 ± 35.5	52.3 ± 4.6[a]	5
Trolox	529.8 ± 83.7	393.7 ± 115.6	28.8 ± 0.12[b]	5
GSH	377.6 ± 40.9	313.2 ± 42.7	17.7 ± 5.4[b]	7
Calyculin A	434.5 ± 57.3	313.1 ± 47.9	27.4 ± 7.0[b]	6
Endothall	528.6 ± 51.7	376.0 ± 62.1	28.4 ± 10.7[b]	7
Tautomycin	526.2 ± 64.2	286.7 ± 48.0	46.1 ± 8.0[a]	8
Staurosporine	277.5 ± 22.4	197.1 ± 33.7	29.9 ± 8.6[b]	6

Table 3.2: Changes in sodium currents observed with different drugs.

Values are means ± S.E.M. of inward sodium peaks recorded from individual neurones. In the first column, the maximal inward currents (I_{in}^{max}) prior oxidant administration are given. The second column shows the inward current after administration of H_2O_2 (5 mmol/l). Inhibitor concentrations were MPG (1 mmol/l), trolox (10 µmol/l), GSH (3 mmol/l), staurosporine (1 µmol/l), calyculin A (100 nmol/l), endothall (100 nmol/l), and tautomycin (3 nmol/l). In the third column, the relative inhibition (% of control current) is given. Values are means ± S.E.M.. Statistically homogeneous groups are indicated by the same letter (a, b; analysis of variances followed by Tukey's test). Basal inward current (I_{in}^{max}) in the 7 groups were not significantly different from each other (analysis of variances followed by Tukey's test). The apparent discrepancy between the maximal inward current (487 pA) in the control group as presented in Table 3.2 and in Figure 3.6 (only about 400 pA) is due to the fact that for quantification in Table 3.2 the maximal inward current of each cell was taken independently from the clamp-voltage, at which it developped, whereas the data in Figure 3.6 are averaged data, so that cells, which developped I_{in}^{max} at voltages different from –30 mV (where most of the cells had the maximum), dampen the current curve.

In order to clarify the potential role of •OH more further, a low concentration of H_2O_2 (100 µmol/l) was used, which, when administered alone, did not inhibit Na^+ inward current (Figure 3.11A). However, when $FeSO_4$ (100 µmol/l) was included in the patch pipette, this concentration of the oxidant induced a strong inhibition of Na^+ inward current (Figure 3.11B).

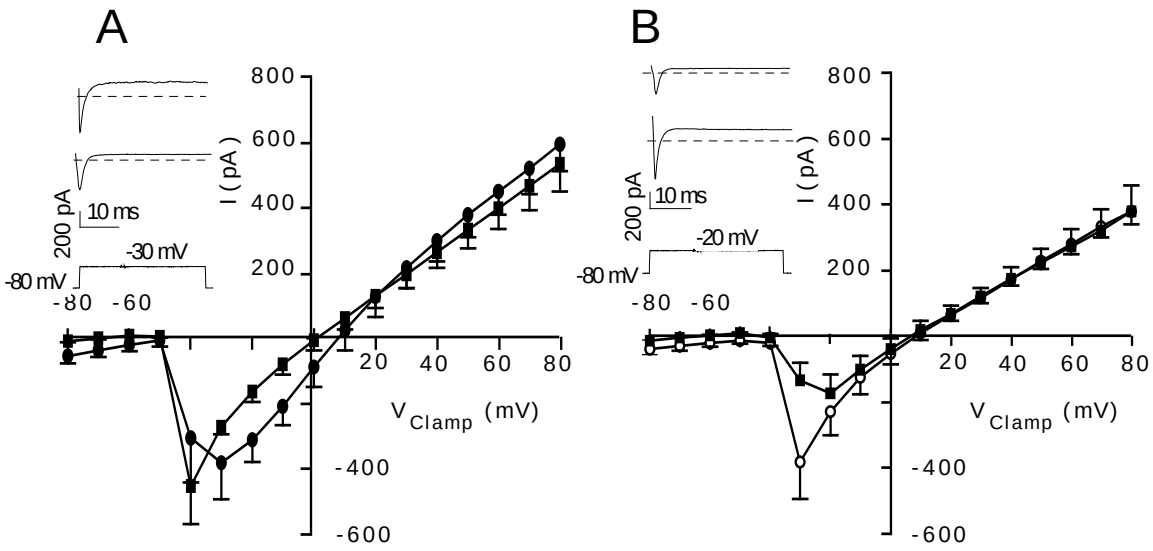

Figure 3.11A: A low concentration of H_2O_2 (100 µmol/l) failed to inhibit the inward sodium currents (filled squares, n = 7) compared to control (filled circles, n = 7). B : Enhancing the production of hydroxyl radical from H_2O_2 by Fe^{2+} (100 µmol/l, filled squares, n = 5) potentiated the action of this low concentration of H_2O_2 compared to the control without Fe^{2+} (open circles, n = 5). Values are means (symbols) ± S.E.M. (vertical bars). The insets show original tracings of the inward current of two neurones evoked by a 30 ms depolarizing pulse in the presence (upper tracings) and absence (lower tracings) of H_2O_2.

The maximal inward current (measured at a potential of –30 mV) in the presence of Fe^{2+} alone amounted to 383 ± 112 pA (n = 5), whereas in the combined presence of Fe^{2+} and H_2O_2 (100 µmol/l) the maximal inward current (measured at a potential of –20 mV) only amounted to 174 ± 60 pA (n = 5, Figure 3.11B). Ferrous iron is known to catalyze the production of •OH via the Fenton reaction ($Fe^{2+} + H_2O_2 \rightarrow Fe^{3+} + \bullet OH + OH^-$; Cohen 1985, Ishii et al. 2006), suggesting a role of the hydroxyl radical in the mediation of the H_2O_2 response at rat myenteric neurones.

H_2O_2 is a potent oxidant. Therefore, it was tested whether an antioxidant, i.e. the reduced form of glutathione (GSH), was able to interfere with the response to H_2O_2. In the presence of GSH (3 mmol/l), H_2O_2 caused only a weak inhibition of Na^+ inward current of 17.7 ± 5.4 % (n = 7), which was significantly smaller than the inhibition of 73.5 ± 14.1 % in the absence of GSH ($P < 0.05$ versus response in the presence of GSH; Table 3.2). Consequently, it seems to be likely that the oxidant interacts with key thiol groups of ion channels or regulatory proteins at the myenteric neurones.

Neuronal Na^+ currents are regulated by phosphorylation (Scheuer and Catterall 2006), and in the human colonic tumour cell line, Caco-2, oxidants have been shown to interact with a protein phosphatase, the serine/threonine protein phosphatase 2A (PP2A), which is normally responsible for the dephosphorylation of proteins (Rao and Clayton 2002). In order to find out, whether a similar phenomenon might underlie the effect of H_2O_2 at the myenteric neurones, different protein phosphatase inhibitors were used. Inhibition of protein phosphatases with calyculin A, an unselective serine/threonine protein phosphatase blocker (Cohen and Cohen 1989, Barford et al. 1998), reduced the inhibition of Na^+ inward current by H_2O_2. In the presence of this inhibitor, the oxidant inhibited only 27.4 ± 7.0 % of the inward current ($P < 0.05$ versus inhibition in the absence of any inhibitor, Table 3.2). Calyculin A inhibits serine/threonine protein phosphatases such as PP1 or PP2A, which are the major cytosolic (PP2A) or membrane bound (PP1) protein phosphatases (Cohen and Cohen 1989, Barford et al. 1998). In order to differentiate between both forms of the enzyme, more selective blockers were used. Endothall (100 nmol/l), a specific blocker of PP2A

(Thièry et al. 1999), completely mimicked the action of calyculin A (Table 3.2), whereas tautomycin (3 nmol/l), a specific blocker of PP1 (MacKintosh and Klumpp 1990, Gupta et al. 1997), was ineffective (Table 3.2).

Beside serine/threonine phosphatases, also tyrosine phosphatases are known (Barford et al. 1998). Therefore, it was relevant to check whether the oxidant also interfered with this type of phosphatases. For this purpose, inward sodium currents were measured after pretreating the neurones with vanadate (100 µmol/l), a tyrosine protein phosphatases inhibitor (Gordon 1991) Vanadate alone did not influence the control level of inward sodium currents. Addition of H_2O_2 in the presence of vanadate changed the inward sodium currents from the control value 460 ± 124 pA (n = 6) to 240 ± 80 pA. This means a 47.9 % inhibition of sodium currents by the oxidant, i.e. the inhibition tended to be smaller compared to the 73.5 % inhibition measured in the absence of any inhibitors (Table 3.2). However, this tendency did not reach statistical significance (Wilcoxon test for matched pairs).

Consequently, protein phosphatases, predominantly of the type PP2A, might be involved in the regulation of the fast Na^+ inward current by oxidants suggesting that a shift in the equilibrium between phosphorylation and dephosphorylation of the voltage-dependent Na^+ channel (or of regulator proteins of the channel) towards a stronger phosphorylation causes an inhibition of Na^+ inward current. The presumed mechanism of action, i.e. inhibition of a phosphatase by H_2O_2, will not itself induce phosphorylation, but depends on the ongoing activity of protein kinase. Therefore, in a final set of experiments, neurones were pretreated with protein kinase inhibitors.

In a first set of experiment, staurosporine (1 µmol/l) was used, which inhibits a broad range of protein kinases (Tamaoki et al. 1986). When the oxidant was administered in the presence of staurosporine, the Na^+ current was only reduced by 29.9 ± 8.6 % ($P < 0.05$ versus an inhibition of 73.5 ± 14.1 % under control conditions; Table 3.2), indicating that an intact protein phosphorylation is a prerequisite for the inhibitory action of H_2O_2. A similar effect was observed after pretreatment of the neurones with the protein tyrosine kinase inhibitor, genistein (50 µmol/l). In the presence of

genistein, H_2O_2 was unable to inhibit sodium inward currents as the current recorded was 556 ± 115 pA i.e not significantly different from control that amounted to 468 ± 127 pA (n = 6; Wilcoxon test for matched pairs).

4 Discussion

4.1 Mechanism of the hyperpolarization evoked by H_2O_2

Hydrogen peroxide, along with the inhibition of the fast inward sodium current, hyperpolarized the neuronal membrane of rat myenteric neurones (Figure 3.1) concomitant with an increase in the cytosolic Ca^{2+} concentration (Figure 3.2) leading to the subsequent activation of a Ca^{2+}-dependent, tetrapentylammonium- and paxilline-sensitive K^+ conductance (Figure 3.5). A hyperpolarization of similar amplitude induced by H_2O_2 has already been observed at myenteric neurones from guinea-pig small intestine (Vogalis and Harvey 2003) suggesting that it might represent a more or less general feature of myenteric neurones.

4.1.1 Ca^{2+} fluxes affected by H_2O_2

The primary mechanism underlying this increase in the cytosolic Ca^{2+} concentration is probably a release of Ca^{2+} from intracellular cyclopiazonic acid-sensitive stores. A release of stored Ca^{2+} is in general mediated by IP_3 receptors and by ryanodine receptors, which both are expressed by neurones and which both are influenced by oxidants. Indeed the sulfhydryl oxidizing reagent, thimerosal, has been found to be acting at a critical thiol group of the purified IP_3R protein reconstituted in vesicles, an action, which depended on the redox state of the receptor. Thimerosal according to the same report (Kaplin et al. 1994) enhanced the affinity of the IP_3R for IP_3 and stimulated the activity of the receptor acting at a location remote from the IP_3 binding domain. Administered along with β-mercaptoethanol used as a reducing agent that prevented the oxidation of the IP_3R at thiol groups, thimerosal evoked a 8-fold increase in the cytosolic calcium concentration (Kaplin et al. 1994). In cardiac cells, Zima et al. (2004) showed that O_2^- generated by the ROS generator system xanthine /xanthine oxidase increased calcium spark frequency and stimulated RyR channel activity in lipid bilayer experiments.

Both types of intracellular Ca^{2+} channels seem to be involved in the effect of H_2O_2 at rat myenteric ganglia, as 2-APB, which blocks IP_3 receptors (Maruyama et al. 1997), as well as ruthenium red, which inhibits ryanodine receptors (Xu et al. 1999), reduced the effect of the oxidant (Table 3.1).

Both blockers are known to exert additional effects on Ca^{2+} permeable ion channels in the plasma membrane, especially of the transient receptor potential (TRP) superfamily such as e.g. transient receptor potential ankyrin 1 (TRPA1), which is inhibited by ruthenium red (Fajardo et al. 2008), or transient receptor potential melastatin 2 (TRPM2), which is inhibited by 2-APB (Togashi et al. 2008). Furthermore, it has to be taken into account that H_2O_2 can activate channels of the TRP family such as TRPA1 (Sawada et al. 2008). TRP channels are good candidates for components of the cation channels responsible for capacitative calcium entry (Birnbaumer et al. 1996). Therefore, it was important in the present study, where the mechanism of intracellular release of Ca^{2+} evoked by H_2O_2 should be investigated, to exclude effects of the oxidant on Ca^{2+} fluxes across the plasma membrane. Otherwise, H_2O_2 via activation of TRP channels would evoke a Ca^{2+} influx from the external milieu and thereby mask any release from internal stores. On the other hand, the simultaneous inhibition of TRPs channels by 2-APB or RuR would lead to an inhibition of Ca^{2+} influx across the membrane since H_2O_2 and the two inhibitors might exert opposite actions on TRP channels.

The easiest way to overcome this possible interference of the agonists and antagonists used with plasma membrane Ca^{2+} channels was to carry out the experiments under Ca^{2+}-free conditions, so that any potential inhibition of plasma membrane Ca^{2+} channels should be without consequence on the fura-2 signal. In deed, both the IP_3 receptor blocker, 2-APB, as well as the ryanodine receptor blocker, ruthenium red, strongly inhibited the action of H_2O_2 on the fura-2 signal ratio under Ca^{2+}-free conditions (Table 3.1). Consequently, it seems likely to conclude that the oxidant evokes a release of stored Ca^{2+} from internal stores via IP_3 receptors and via ryanodine receptors.

A similar, nearly complete inhibition of the rise in the fura-2 ratio was observed, when intracellular Ca^{2+} stores were depleted by cyclopiazonic acid. This toxin inhibits the Ca^{2+}-dependent phosphorylation of the reticulum vesicles by ATP (Goeger and Riley 1989), decreases the affinity of sarco(endo)plasmic reticulum Ca^{2+}-ATPase (SERCA) for Ca^{2+} and reduces the maximum specific activity of the enzyme (Martinez-Azorin 2004). Thus, the toxin is an efficient blocker of SERCAs, which are 110-kDa membrane proteins that catalyze the ATP-dependent transport of Ca^{2+} from the cytosol to the lumen of the sarco(endo)plasmic reticulum. The SERCAs, in the presence of CPA, fail to pump back Ca^{2+} from the cytosol to the lumen.

The inhibition by cyclopiazonic acid was strongly enhanced, when in addition Ca^{2+} influx from the extracellular space was prevented by superfusion with a Ca^{2+}-free solution or in the presence of Gd^{3+}, a blocker of capacitative Ca^{2+} influx (Table 3.1). Although the relevance of capacitative Ca^{2+} influx for neurones has been debated for some time (Friel and Tsien 1992, Lupu-Meiri et al. 1994, Usachev and Thayer 1999, Emptage et al. 2001), the activation of Ca^{2+} influx after store depletion, e.g. after administration of the SERCA blocker cyclopiazonic acid, has been demonstrated in cultured cortical (Yoo et al. 2000) or in other types of neurones (for review, see Putney 2003). Consequently, the fact that superfusion of the enteric ganglia with a Ca^{2+}-free buffer reduced the long-lasting increase in the fura-2 ratio signal by more than two thirds (Table 3.1) underlines the importance of capacitative Ca^{2+} influx for the sustained response to the oxidant. Interestingly, it has been found recently (reviewed by Wang et al. 2008) that the emptying of intracellular stores (such as endoplasmic reticulum) mediated by IP_3R triggers the translocation of a protein "sensor" of the endoplasmic Ca^{2+}. This protein has been termed *st*omal-*i*nteracting *m*olecule (STIM) 1. The sensing function is operated by the EF-Hand Ca^{2+}-binding domain on the N-terminal endoplasmic reticulum luminal portion of the STIM1. The Ca^{2+} binding induces a conformational change of the N-terminus and the dissociation of the cation leads to multimerization of the molecule that translocates into defined endoplasmic reticulum-plasma membrane junctional areas in which coupling occurs to Orai proteins. Orai proteins being themselves store-operated moieties (reviewed by

Wang et al. 2008), whose activation is a key event to mediate long-term cytosolic Ca^{2+} signals and also the refilling of internal stores (Parekh and Putney 2005). Thus, they are capacitative calcium channels moieties and serve as plasma membrane Ca^{2+} entry channels with a high Ca^{2+} selectivity and a low single channel conductance.

Considering that H_2O_2 obviously activates IP_3R and RyR, the increase in Ca^{2+} concentration should be a short-time process. Otherwise a desensitization of the receptors would soon end the mobilization of Ca^{2+} from the Ca^{2+} storing organelles. This, however, was not the case, as the oxidant evoked a long-lasting biphasic increase in the cytosolic Ca^{2+} concentration (Figure 3.2A). An initial rising phase ending with a plateau was followed by a second rise. The first phase likely corresponds to the release of calcium from internal stores via IP_3R and RyR, which reached a maximum at the plateau. The second phase probably corresponds to the influx of calcium from the external milieu (capacitative entry). This phase is quite long-lasting (and was indeed not reversible after washout of the agonists), probably because of the establishment of a permanent "depleted state" of the internal stores. Interestingly, reactive oxygen species are known to inactivate SERCAs (Pereira et al. 1996), which means ROS prevent the replenishing of internal stores and elicit a feed-back, i.e hold/activate a continuous "call" of Ca^{2+} from the external milieu in order to refill the "depleted stores" as shown in the present study (Figure 3.2A). This may further contribute to the long lasting activation of capacitative Ca^{2+} influx. However, how the signal for refilling internal stores is transmitted from the SERCAs to the plasma membrane calcium channels is still not known, but a possible mechanism could be a conformational change of the RyR or IP_3R as suggested by Berridge et al. (2000) or a similar conformational change of the STIM1 that approaches as close as 10 - 20 nm to the plasma membrane likely interacting with the plasma membrane proteins such as Orai1 in a reversible process.

4.1.2 The role of Ca^{2+} in the hyperpolarization

A common mechanism, by which an increase in the cytosolic Ca^{2+} concentration can lead to a hyperpolarization is the activation of Ca^{2+}-dependent K^+ channels. This is, for example, the dominant mechanism which evokes the long-lasting afterhyperpolarization in AH-neurones (Wood 1994, Vogalis et al. 2001). In rat myenteric neurones, these channels mediate e.g. the hyperpolarization following the release of stored Ca^{2+} after exposure of the cells to short-chain fatty acids (Hamodeh et al. 2004).

Three classes of calcium-activated potassium channels are known (see Introduction), the small conductance (SK), the intermediate conductance (IK) and the large conductance (BK or maxi-K) K^+ channels. The maxi K^+ channels can be activated by increases in the cytosolic Ca^{2+} concentration and/or depolarizing voltage steps (for review, see Schreiber and Salkoff 1997, Jiang et al. 2001). They are specifically inhibited by charybdotoxin, paxilline or TEA. In the present study, paxilline prevented the hyperpolarization evoked by H_2O_2 (Figure 3.5B), suggesting that maxi K^+ channels might be the channels linking the increase in the cytosolic Ca^{2+} concentration evoked by the oxidant to a change of the membrane potential.

In fact, afterhyperpolarization (AHP), a characteristic of AH-neurones, has been shown to be a consequence of Ca^{2+} entry through ω-conotoxin GVIA-sensitive Ca^{2+} channels during action potentials, Ca^{2+}-triggered Ca^{2+} release from caffeine-sensitive stores, and interestingly the opening of Ca^{2+}-sensitive small conductance K^+ channels (SK) (Vogalis et al. 2001). Furthermore, the activation of IK channels has been shown to be the origin of the hyperpolarizing effects of H_2O_2 in AH-neurones from the guinea pig small intestine (Vogalis and Harvey 2003). These authors used clotrimazole (a selective IK channel blocker, see Shah et al. 2001, Wei et al. 2005) to restore the resting membrane potential after a hyperpolarization induced by H_2O_2. Taken together, SK and IK are determining the hyperpolarization in AH-cells from guinea pig myenteric neurones. In contrast, the present results obtained at rat myenteric neurones show a sensitivity of the H_2O_2-response against paxilline and

therefore suggest the involvement of maxi K^+ channels in the Ca^{2+}-induced hyperpolarization in S-neurones.

4.2 Alteration of the excitability

In addition to the change in basal membrane potential, the present data demonstrate that the oxidant, H_2O_2, inhibits the tetrodotoxin-sensitive inward sodium current at rat myenteric neurones (Figures 3.6 – 3.7). This leads to a reduction in excitability as shown by the impaired ability of the neurones to generate action potentials upon injection of a depolarizing inward current (Figure 3.10).

Again, these findings are consistent with previous studies performed at guinea pig myenteric neurones, where hydrogen peroxide reduced the amplitude of action potentials at AH/Dogiel type 2 neurones, so that stronger current pulses were necessary to trigger action potentials upon oxidant superfusion (Vogalis and Harvey 2003). A similar phenomenon was observed in the present study, i.e. in two (out of 22) cells action potentials could only be induced in the presence of H_2O_2, when stronger current pulses were applied (data not shown). The action of the oxidant at rat myenteric neurones was not reversible after washing out, suggesting a covalent modification of channel proteins and/or regulator proteins involved in the modulation of Na^+ channel activity.

However, a fundamental difference to the observations at guinea-pig myenteric plexus consists in the fact that in this species, reactive oxygen metabolites generated e.g. by a hypoxanthine/xanthine oxidase enzymatic system or by direct administration of H_2O_2 were only effective at AH-neurones, which generate tetrodotoxin-resistant action potentials at the neuronal soma mainly by Ca^{2+} currents (Wada-Takahashi and Tamura 2000). In the myenteric plexus of the adult rat, when using whole mount preparation, active AH-neurones with TTX-resistant action potentials have been identified (Browning and Lees 1996). Although action potentials in AH-neurones have been found to be generated by TTX-sensitive Na^+ currents and by N-type high

voltage-activated (HVA) Ca^{2+} channels (Rugiero et al. 2002), it has also been shown by the same author (Rugiero et al. 2002) that this sensitivity to TTX is quite poor as they had to use very high TTX concentrations (ranging from 500 nmol/l up to 2 µmol/l). In addition, tetrodotoxin-resistant Na^+ channels of the type Nav1.9 are expressed by a subpopulation of myenteric neurones, which, however, due to their slow gating properties, are thought to contribute predominantly to the amplification of slow excitatory postsynaptic potentials at the neuronal soma (Padilla et al. 2007).

In contrast, cultured rat myenteric neurones from newborn rats, which I used in my study, generate their action potentials mainly by tetrodotoxin-sensitive voltage-dependent Na^+ channels (Haschke et al. 2002), i.e. would fit to the S-type of neurones. In difference to the observations at guinea-pig (Wada-Takahashi and Tamura 2000, Vogalis and Harvey 2003), all neurones tested responded to the oxidant suggesting species differences in the sensitivity of the myenteric plexus against reactive oxygen species or the equipment with different types of Na^+ channels. The "shoulder" or "hump" during the falling phase of action potentials of type2/AH neurones as mentioned in the Introduction (Figure 1.2C) had not been observed during this study (see for example Figure 3.10.E). Furthermore, these cultured neurones fired trains of action potentials without a visible afterhyperpolarization (Figure 3.10A, C) as shown already in previous studies (see Figure 1.2.B). This further suggests that the dominant neuronal cell type in the culture is the S-type.

4.3 Mediation of H_2O_2 effects, implication of the thiol groups and role of the kinases/ phosphatases system

The hydroxyl radical seems to play a central role in the mediation of the H_2O_2 inhibition of Na^+ currents. Scavenging of this radical by trolox, an antioxidant that protects cells by scavenging the hydroxyl radical and preventing membrane lipid peroxidation (for reference see Boland et al. 2000), and by MPG reduced the inhibitory action of the oxidant on Na^+ currents (Table 3.2). To confirm the presumed

involvement of hydroxyl radicals, the opposite experiment was conducted, i.e providing more hydroxyl radicals in the presence of the oxidant at a lower concentration. A lower concentration of the oxidant was needed because at 5 mM, H_2O_2 induced a maximal inhibition of the inward sodium current so that the presumed involvement of the hydroxyl radical produced in presence of the ferrous iron was masked. The hydroxyl radical was produced via the Fenton reaction. In this reaction (see below), iron sulfate is the iron ferrous (Fe^{2+}) provider and electron donor. Ferrous iron is oxidized by H_2O_2 to ferric iron (Fe^{3+}), a hydroxyl radical (•OH) and a hydroxyl anion (OH^-) as follows (Cohen 1985, Ishii et al. 2006):

$$Fe^{2+} + H_2O_2 \longrightarrow Fe^{3+} + \bullet OH + OH^-$$

The radical produced potentiated the inhibitory effect of H_2O_2 on Na^+ inward currents at rat myenteric neurones (Figure 3.11).

It is assumed that H_2O_2 plays a role in the regulation of enzyme activity via oxidation of cysteine residues (see e.g. Hool and Corry 2007). In accordance with this assumption, the reductant GSH counteracted the inhibition of Na^+ currents by H_2O_2 (Table 3.2) suggesting an interaction of the oxidant with thiol groups. Such an interaction has been studied in detail on the molecular level for the bacterial protein OxyR, which is a model case for a redox-sensitive signaling protein that may be activated either directly by H_2O_2 or by changes in the intracellular glutathione redox state (Slund et al. 1999). In case of direct oxidation by H_2O_2, the Cys199 in this protein is converted to a sulfenic acid derivative which then forms within the molecule a disulfide bond with Cys208 (reviewed in Dröge 2002). This bacterial protein is taken as example for redox-sensitive proteins, i.e. intracellular proteins, which are oxidized in the presence of oxidants such as H_2O_2.

These proteins along with free amino acids amongst which tyrosine, tryptophan, histidine and cysteine neutralize or reduce considerably the oxidative stress induced by H_2O_2 and are therefore referred to as ROS scavengers (Davies et al. 1987a, 1987b). The scavenging function in concert with antioxidative enzymes such as catalase,

glutathione peroxidase, and nonenzymic compounds such as vitamins C and E, β-carotene and glutathione, helps maintaining the redox homeostasis balancing the generation and the clearance of reactive oxygen products.

The shift of the thiol/disulfide bond redox state towards disulfide bonds after oxidation of proteins/amino acids is regulated by glutaredoxin 1 and by thioredoxin (Trx) (Zheng et al. 1998). The 5'-upstream sequence of the human Trx gene contains putative binding sites for the redox-responsive transcription factor AP-1 (Nakamura et al. 1994, 1997). The AP-1 factor up-regulates the expression of many antioxidant genes under oxidative-stress-inducing conditions (Moye-Rowley 2003). Its homologue yAP-1 in Saccharomyces cerevisiae is distributed both in cytoplasm and nucleus. It is found predominantly in cytoplasm under normal conditions (Kuge et al. 1997). This transcription factor has a nuclear export signal sequence in the C terminus, and an exportin that exports yAP-1 from the nucleus to the cytosol under control conditions. In the case of oxidative stress, the interaction between yAP-1 and the exportin is hindered. As consequence, yAP-1 accumulates in the nucleus enhancing the expression of its targets genes (Kuge et al. 1998). A redox sensor made up of three cysteine residues is present in the C terminus and undergoes modifications which likely hinder the interaction of the factor with the exportin due to formation of a disulfide bond between Cys598 and Cys620 after exposure to H_2O_2 (Kuge et al. 2001).

The reducing agent, glutathione, when given alone, did not affect the peak values of Na^+ currents of rat myenteric neurones, but counteracted the inhibition by H_2O_2 (cf. Table 3.2). This is consistent with results obtained at rat sensory and motor axons, where GSH accelerated the inactivation of Na^+ channels, but had no effect on the amplitude of the currents passing across these channels (Mitrovic et al. 1993). In principle, H_2O_2 might act directly at the neuronal Na^+ channels or it might interfere with modulator proteins responsible for the regulation of their activity. Both cases are feasible either separately or synergistically. Evans and Bielefeldt (2000) showed that oxidation of thiol groups within the sodium channel protein reduced sodium currents

and also shifted the voltage dependence to more hyperpolarized potentials without affecting activation.

Although similar results, i.e. hyperpolarization of the neuronal membrane and inhibition of the sodium currents, have been obtained during the present study, the mechanism seems to be more complex. Not only the disulfide bonds or thiol oxidation could be responsible for the hyperpolarization of the cell membrane as mentioned by Evans and Bielefeldt (2000). In the present study, the sensitivity of the membrane potential to the maxi K^+ channel blocker paxilline (Figure 3.5B), i.e the ability of paxilline to prevent the hyperpolarization induced by H_2O_2, reveals the implication of Ca^{2+}, since the increase in the cytosolic concentration of this cation activates the Ca^{2+}-dependent potassium channels that determines the membrane potential. Secondly, neuronal voltage-gated Na^+ channels are known to be regulated by phosphorylation (Scheuer and Catterall 2006); and oxidants have been shown to interact with serine/threonine protein phosphatases (Rao and Clayton 2002) as well as with tyrosine protein phosphatases (Bogeski et al. 2006). Thus, oxidation of thiol groups plays a role in the oxidants-induced effects, but other mechanisms such as Ca^{2+}-activation of potassium channels as well as sodium channels phosphorylation/dephosphorylation had to be considered.

Consequently, different inhibitors of protein phosphatases and protein kinases were tested for their ability to interfere with the action of the oxidant. None of these inhibitors (see for example I_{in}^{max} data in Table 3.2) was able to mimic the inhibition of Na^+ currents by H_2O_2. The inward currents underwent changes only after administration of H_2O_2, i.e. only after oxidation of the channels or regulatory proteins by the oxidant. However, pretreatment of the neurones with different serine/threonine phosphatase inhibitors, especially with the combined PP1/PP2A inhibitor, calyculin A, or the PPA2 inhibitor, endothall, strongly inhibited the action of a subsequent administration of the oxidant. A similar but weaker (not significant) response was observed when pretreating neurones with the tyrosine phosphatase inhibitor vanadate (100 µmol/l). One might concern about the single concentration of vanadate used here

and postulate that perhaps higher concentrations of the inhibitor could have been used to prevent completely or at least significantly (as did calyculin A or endothall) inhibit the oxidant-induced effect. However, vanadate at a concentration of 10 µmol/l already exerts a very potent inhibitory action on tyrosine phosphatases as shown by Swarup et al. 1982. The same authors performed a concentration-dependent study of the inhibitory action of vanadate and the maximal concentration used was 100 µmol/l, the one used in this study. Consequently, a higher concentration of vanadate may not further reduce the effects of the oxidant because the inhibitory property of vanadate is relatively similar at both concentrations 10 µmol/l and 100 µmol/l. This might consequently indicate only a minor participation of tyrosine protein phosphatases in the oxidant-induced effects. Nevertheless, in the presence of the tyrosine kinases inhibitor genistein (50 µmol/l), H_2O_2 failed to inhibit the inward sodium current. Taken together, these observations would be consistent with the ability of H_2O_2 to inhibit phosphatases (Guy et al. 1993, Suzuki et al. 1997, Rao and Clayton 2002) and with the well-known inhibition of neuronal Na^+ channels by phosphorylation at the phosphorylation sites (see Figure 1.4) (Rossie and Catterall 1989, Cantrell et al. 2002, Scheuer and Catterall 2006).

An inhibition of phosphatases will only lead to a hyperphosphorylation of target proteins, when there is an ongoing protein kinase activity. Consequently, blockade of protein kinases with staurosporine would also reduce the action of H_2O_2 as observed here (Table 3.2). However, as none of these blockers alone was able to induce a significant inhibition of Na^+ currents, one would have to postulate that only in the oxidized form, i.e. in the presence of H_2O_2 and therefore after formation of covalent bonds such as disulfide ones, this regulation could take place at the rat myenteric neurones (Figure 10). Application of GSH, breaking down disulfide bonds likely built by the oxidant (Hool and Corry 2007), should then keep the channels in their nonphosphorylated/dephoshorylated open/active form, and thereby suppress the action of H_2O_2 on Na^+ currents (Table 2). The higher the concentration of H_2O_2, the more important is the amount of antioxidative proteins/amino acids targeted and vice-

versa as reported by Nakamura et al. (1993) on protein tyrosine kinase $p56^{lck}$ in T cells.

A further converging action of H_2O_2 might be the activation of PKC via increase in cytosolic Ca^{2+} concentration concomitant e.g. with the transcriptional induction of AP-1 proteins as reviewed by Dröge (2002), which in turn might enhance the phosphorylation of the channel or its regulatory proteins. Although tyrosine kinases may be involved, based on the inhibitory effects of genistein and vanadate, a clear conclusion concerning this signal pathway could not be directly drawn since the inhibitory action of vanadate was quite poor. Furthermore, in the presence of these inhibitors, the Na^+ currents recorded were quite heterogeneous from cell to cell so that more experiments had to be performed to overcome this variability. In fact, while currents in the presence of vanadate were reduced, the amplitude of those measured in the presence of genistein after application of H_2O_2 was varying drastically from higher than control to very tiny values. Taking into consideration these remarks, it is more likely that the protein phosphatases implicated in the oxidant-induced effects are of the type 2A, since calyculin A and endothall (specific inhibitor of the PP2A) showed strong inhibitory actions on the effect of H_2O_2.

4.4 Functional significance of the H_2O_2 effects and pathophysiological consequenses

What is the functional consequence of the decrease in excitability of myenteric neurones by H_2O_2 ? Despite the well known heterogeneity of enteric neurones, which consist of sensoric neurones, interneurones, or excitatory and inhibitory motor neurones expressing different types of transmitter (Wood, 1994), all neurones tested responded with a decrease in their excitability, i.e. a hyperpolarization and an inhibition of the Na^+ current responsible for the generation of action potentials. The overall, predominant action of the enteric nervous system on gastrointestinal motility is an inhibitory one (Wood 1994, Hansen 2003), demonstrated e.g. by the increase in

intestinal motility after blockade of neuronal activity with tetrodotoxin (see e.g. Diener and Gabato 1994).

According to Wood (1994), the intestinal musculature functions like a self-excitable electrical syncytium. This means that action potentials spread from muscle cell to muscle cell throughout the entire muscle. These action potentials trigger the contractile process as they spread. The self-excitable characteristic of the electrical syncytium is assured by a non-neural pacemaker system of electrical slow waves. Based on this conception, all slow wave cycles should induce action potentials in circular muscle and then evoke contractions. In addition, the intestinal musculature being like a syncytium, the action potentials and contractions should spread further throughout the entire length of the intestine each time the slow waves occur. But this is not the case “in vivo”. The reason is that the inhibitory motor neurones prevent the excitation and contractions. The circular muscle can only respond to electrical waves, when the inhibitory motor neurones in a segment of intestine are switched off by input from other neurones (Wood 1994). It appears then that the inhibitory neurones determine, whether the constantly running slow waves initiate a contraction. They also affect the distance and the direction of propagation once the contraction has begun (Wood 1994). The state of activity of inhibitory motor neurones determines the length of a contracting segment in nonsphincteric circular muscle. The contraction can occur in segments where ongoing inhibition has been switched off, while adjacent segments with continuing inhibitory activity can not contract. The same author mentions a continuous neuronal inhibition of the autonomous activity of the small intestine circular muscle in many species such as rabbit, guinea pig, cat, or dog. For instance, in segments of intestine in vitro, when neurones in the myenteric plexus show a spontaneous discharge of action potentials, muscle action potentials and associated contractile activity are absent (Wood 1994). Experimentally, when electrical slow waves are present and when the neuronal discharge is blocked by TTX, every cycle of the electrical slow waves triggers an intense discharge of action potentials in the smooth muscle cells and large-amplitude contractions (Wood 1972). Thus, any treatment or condition that mimics an ablation of the intrinsic inhibitory

neurones (as it is similarly the case in Hirschsprung's disease where there is a congenital absence) results in tonic contracture and achalasia of the intestinal circular muscle (Wood 1994), and an additive simultaneous permanent contracture of the longitudinal muscle, whose activity has been freed from the inhibitory pathway. But where are oxidants coming from and how are they generated in the gastrointestinal tract ?

In fact, lamina propia immune cells undergo a metabolic activation after the binding of a ligand (e.g. bacterial products). This activation also results in the release of large quantities of superoxide anions (O_2^-) and H_2O_2 (Klebanoff 1988). Hydrogen peroxide then oxidizes chloride (Cl^-) in the presence of myeloperoxidase (MPO) released from activated polymorphonuclear leukocytes to form hypochlorous acid (HOCl) as follows (Thomas et al. 1983) :

$$H_2O_2 + Cl^- + H^+ \xrightarrow{MPO} H_2O + HOCl.$$

A further oxidant, monochloramine (NH_2Cl), might be produced from HOCl interacting with ammonia (Thomas et al. 1983):

$$HOCl + NH_3 \longrightarrow H_2O + NH_2Cl.$$

Under physiological conditions, these oxidants are cleared by the aforementioned oxidant scavengers. However, oxidants are produced in great amounts during intestinal inflammation (Pavlick et al. 2002, Cao et al. 2004) and are assumed to play a central role in ischaemia/reperfusion damage (Starkov et al. 2004). The oxidants produced are antimicrobial and therefore supposed to represent a defense line for the hosting organism.

Although the exact concentration of H_2O_2 within the colonic wall is unknown, a production per g tissue of 0.2 – 0.5 mmol/h in inflamed tissue has been estimated (Grisham et al. 1990). The concentration of H_2O_2 can considerably rise since polymorphnuclear neutrophils can continuously generate H_2O_2 for about 3 hours after activation (Nathan 1987). Concentrations of H_2O_2 ranging between 20 - 400 µmol/l

have been shown to enhance proteolysis, while concentration in the millimolar range led to intracellular accumulation of oxidized proteins that buffer the oxidant (Stadtman 1992, Grune et al. 1997).

In case of oxidative bursts or dysregulations of the immune system like allergies, high and/or persistent concentrations of H_2O_2 may be found in the intestinal wall, the oxidant may thereby interfere directly or indirectly (via intermediates such as cytokines, other ROS, histamine, serotonin or prostaglandins) with the enteric nervous system (Hinterleitner and Powel 1991, Amstutz and Diener 1997). In parallel, H_2O_2 at 5 mmol/l has been shown to induce electrolyte secretion in vitro (Schultheiss et al. 2008), which could lead to secretory diarrhea. Although high concentrations of H_2O_2 may be considered to be toxic or proapoptotic (Dumont et al. 1999), cellular apoptotic characteristics in absence of H_2O_2 have been observed (Castedo et al. 1996), indicating the oxidant is not an obligatory trigger or component of the apoptotic process. Furthermore, the reported increase (Banki et al. 1999, Esteve et al. 1999) in cellular ROS production observed in apoptotic processes triggered by some ligands failed in other studies.

In line with the aforementioned effects of oxidants, the inhibition of Na^+ currents by H_2O_2 in the mmolar range as observed in this study may well play a role under in vivo conditions. Consequently, the decrease in the activity of the predominantly inhibitory myenteric motor neurones will result in an increase in gastrointestinal motility and a decreased transit time, which might thereby contribute to the diarrhea frequently observed during inflammatory bowel diseases.

Another perspective of ROS released in the gastrointestinal wall might be an interference with aging, as aging is considered to be associated with a partial loss in SERCA activity (Sharov et al. 2006). Thus it is an interesting implication that ROS are known to inactivate SERCA (Pereira et al. 1996). Furthermore, free radicals such as •OH deriving from hydrogen peroxide could participate as well in the age-related degenerative processes (Harman 1956).

4.5 Conclusion

The aim of this study was to characterize the actions of hydrogen peroxide on cultured rat myenteric neurones. It came out that the oxidant hyperpolarizes myenteric S-neurones by activating Ca^{2+}-dependent K^+ currents, probably from the maxi K^+ type, after increasing the cytosolic Ca^{2+} concentration. This, along with the inhibition of the fast inward sodium currents, reduces the cell excitability. The mechanism of sodium current inhibition seems to implicate thiol groups of the sodium channel or of regulatory proteins of the channel and can be drawn as follows:

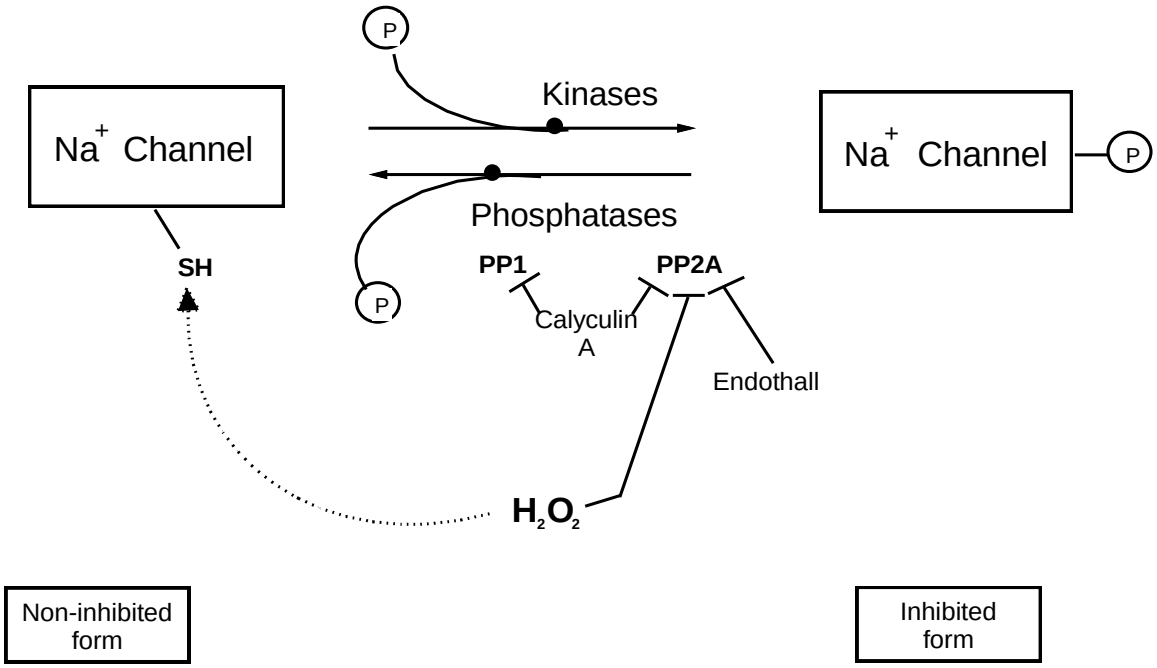

Figure 4.1: Hypothetical mechanism underlying the inhibition of sodium currents by H_2O_2. Hydrogen peroxide likely interacts with the thiol group at the level of the Na^+ channel, enabling the channels to be ready for phosphorylation, inhibits the protein phosphatase type 2A slowing down the phosphatases pathway in favor of the kinases reactions that will phosphorylate the channel; the phosphorylated channel changes into the inhibited form.

Taken all together, an inflammation triggers the release of oxidants from the immune system, and these oxidants in turn modulate the myenteric neurones functions, switching off the neuronal prevalent inhibitory function on the musculature, resulting in an increase in intestinal motility as depicts the following scheme:

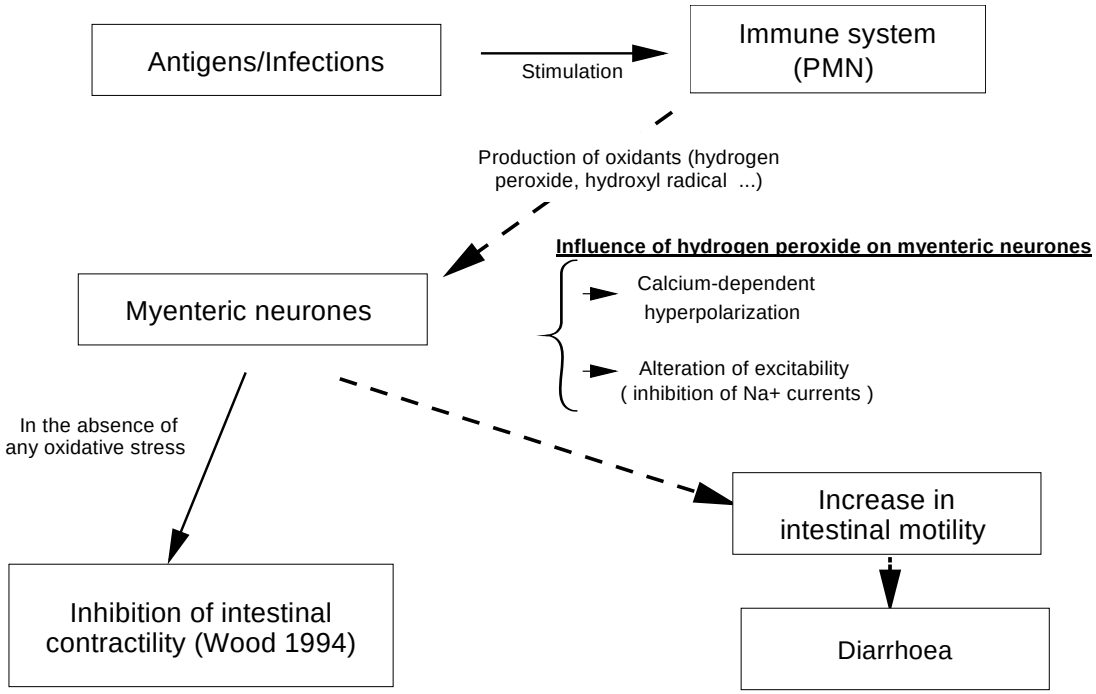

Figure 4.2: The hypothetical "in vivo" pathophysiological consequences of H_2O_2. The oxidant might reduce the "Switch off" of muscle contractions operated normally "in vivo" by the permanent neuronal inhibitory action of the ENS intrinsic neurones. The continuous arrows show direct and/or normal physiological actions, and the interrupted arrows show the actions occurring during oxidative stress.

5 Summary

Oxidants, produced e.g. during inflammation, alter gastrointestinal functions finally leading to diarrhea and/or tissue damage. There is only scarce information about the action of oxidants on enteric neurones, which play a central role in the regulation of many gastrointestinal processes. Therefore, the effect of an oxidant, H_2O_2, on cultured rat myenteric neurones was studied with the whole-cell patch-clamp and imaging (fura-2) techniques.

H_2O_2 (5 mmol/l) induced an increase in the cytosolic Ca^{2+} concentration. Both an intracellular release via IP_3 and ryanodine receptors as well as a Gd^{3+}-sensitive Ca^{2+} influx contributed to this response. Measurement of the membrane potential revealed that the neuronal membrane hyperpolarized by 11.3 ± 0.8 mV (n = 30) in the presence of H_2O_2. Inhibition of Ca^{2+}-dependent K^+ channels by the BK-specific inhibitor paxilline (10 µmol/l) or by 100 µmol/l TPA (a broad inhibitor of Ca^{2+}-dependent K^+ channels) prevented this hyperpolarization. This indicates that the increase in the cytosolic Ca^{2+} concentration likely activates BK channels, which carry an outward K^+ current to hyperpolarize the neuronal membrane.

Voltage-clamp experiments revealed a second action of the oxidant, i.e. a strong inhibition of the fast Na^+ current responsible for the generation of action potentials. This effect seemed to be mediated by the hydroxyl radical (•OH), as Fe^{2+} (100 µmol/l), which leads to the generation of this radical from H_2O_2 via the Fenton reaction, strongly potentiated the action of an ineffective concentration (100 µmol/l) of the oxidant. Inhibition of protein phosphorylation by staurosporine (1 µmol/l), a protein kinase inhibitor, prevented the effect of a subsequent administration of the oxidant. Vice versa, the protein phosphatase (PP) inhibitor calyculin A (100 nmol/l) strongly reduced the inhibition of Na^+ current by H_2O_2. This effect was mimicked by the PP2A specific inhibitor endothall (100 nmol/l), whereas the PP1 blocker tautomycin (3 nmol/l) was less effective.

However, none of the inhibitors used was able to significantly change the basal amplitude of the inward sodium current. Changes appeared only after administration of the oxidant, meaning that a preconditioning of the channels or regulatory proteins, e.g. an oxidation of thiol groups by H_2O_2, is necessary for this action. This was confirmed by the observation that in the presence of the reduced form of GSH (3 mmol/l), H_2O_2 was unable to inhibit inward sodium currents. These results suggest that H_2O_2 might act via a shift of the equilibrium between protein phosphorylation and dephosphorylation involved in the regulation of Na^+ currents in rat myenteric neurones.

The consequence is an inhibition of the sodium currents responsible for the generation of action potentials. Together with the hyperpolarization, H_2O_2 should likely reduce the ongoing inhibitory tone of the ENS on the gastrointestinal muscle, which might result in a hypercontractility leading to diarrhea.

6 Zusammenfassung

Oxidantien, die z.B. während Entzündungsprozessen entstehen, beeinflussen Funktionen des Magen-Darm-Trakts, was im Endeffekt zu Durchfall und/oder Gewebeschäden führt. Es gibt nur wenige Daten über die Wirkung von Oxidantien an enteralen Neuronen, welche eine zentrale Rolle bei der Regulation vieler gastrointestinaler Prozesse spielen. Daher wurde mit der Hilfe von Whole-cell Patch-Clamp- und Imaging (Fura-2)-Techniken die Wirkung des Oxidationsmittels H_2O_2 an kultivierten myenterischen Neuronen aus der Ratte untersucht.

Das Oxidationsmittel H_2O_2 (5 mmol/1) löste einen Anstieg der zytosolischen Ca^{2+} Konzentration aus. Sowohl eine intrazelluläre Freisetzung von Ca^{2+} über IP_3- und Ryanodin-Rezeptoren als auch ein Gd^{3+}-sensitiver Einstrom von Ca^{2+} sind an dieser Antwort beteiligt. Messung des Membranpotentials ergab, dass die Membran der myenterischen Neurone in Gegenwart von H_2O_2 um 11,3 ± 0,8 mV (n = 30) hyperpolarisierte. Die Hemmung von Ca^{2+}-abhängigen K^+-Kanälen durch den BK-spezifischen Inhibitor Paxillin (10 µmol/l) oder durch 100 µmol/l TPA (ein breit wirkender Blocker Ca^{2+}-abhängiger K^+-Kanäle) verhinderte diese Hyperpolarisation. Dies deutet darauf hin, dass der Anstieg der zytosolischen Ca^{2+} Konzentration wahrscheinlich BK-Kanäle aktiviert: diese Kanäle erlauben einen K^+-Auswärtsstrom, der die Hyperpolarization bedingt.

Spannungsklemm-Experimente deckten eine zweite Wirkung des Oxidationsmittels auf: Eine starke Hemmung des schnellen Na^+-Stromes, der für die Erzeugung der Aktionspotentiale zuständig ist. Dieser Effekt scheint von dem Hydroxyl-Radikal (•OH) vermittelt zu sein, denn Fe^{2+} (100 µmol/l), das zur Erzeugung dieses Radikals aus H_2O_2 über die Fenton-Reaktion führt, potenzierte die Wirkung einer unwirksamen Konzentration (100 µmol/l) an H_2O_2. Die Hemmung der Protein-Phosphorylierung durch Staurosporin (1 µmol/l), einen Proteinkinase-Blocker, verhinderte die Wirkung des Oxidationsmittels. Umgekehrt reduzierte auch der Proteinphosphatase (PP)-Blocker Calyculin A (100 nmol/l) stark die von H_2O_2 induzierte Hemmung des Na^+-Stromes. Dieser Effekt wurde durch den PP2A spezifischen Hemmer Endothall (100

nmol/l) nachgeahmt, während der PP1-Blocker Tautomycin (3 nmol/l) weniger wirksam war. Allerdings war keiner der verwendeten Inhibitoren in der Lage, die basale Amplitude des Na^+-Einwärtsstroms zu beeinflussen. Änderungen erschienen erst nach der Zugabe des Oxidationsmittels, was bedeutet, dass eine Vorkonditionierung der Kanäle oder regulatorischer Proteine, wie zum Beispiel eine H_2O_2-bedingte Oxidation von Thiolgruppen, für diese Aktion notwendig ist. Dies wurde durch die Beobachtung, dass in Anwesenheit der reduzierten Form von GSH (3 mmol/l) H_2O_2 nicht in der Lage war, Na^+-Einswärtsströme hemmen, untermauert.

Diese Ergebnisse lassen vermuten, dass Oxidantien durch Veränderungen am enterischen Nervensystem Änderungen der gastrointestinalen Motilität auslösen können.

7 References

1. Amstutz I., Diener M., 1997. Inhibition of antigen-induced muscle contractions by inhibitors of thromboxane pathway in rat small intestine. J. Vet. Med. 44A, 349-359.

2. Angelova P., Müller W., 2006. Oxidative modulation of the transient potassium current I_A by intracellular arachidonic acid in rat CA1 pyramidal neurons. Eur. J. Neurosci. 23, 2375-2384.

3. Auerbach L., 1862. Über einen Plexus myentericus, einen bisher unbekannten ganglionervösen Apparat im Darmkanal der Wirbeltiere. Vorläufige Mitteilung. Breslau : E Morgenstern.

4. Auerbach L., 1864. Fernere vorläufige Mitteilung über den Nervenapparat des Darmes. Arch Pathol Anat Physiol. 30, 457-460.

5. Bae Y.S., Sang S.W., Seo M.S., Baines I.C., Tekle E., Chock P.B., Rhee S.G., 1997. Epidermal growth factor (EGF)-induced generation of hydrogen peroxide. Role in EGF receptor-mediated tyrosine phosphorylation. J. Biol. Chem. 272, 217 – 221.

6. Banki K., Hutter E., Gonchoroff N.J., and Perl A., 1999. Elevation of mitochondrial transmembrane potential and reactive oxygen intermediate levels are early events and occur independently from activation of caspases in Fas signaling. J Immunol .162, 1466-1479.

7. Barford D., Das A.K., Egloff M.P., 1998. The structure and mechanism of protein phosphatases: insights into catalysis and regulation. Ann. Rev. Biophys. Biomol. Struct. 27,133– 164.

8. Bar-Yehuda D., Korngreen A., 2008. Space-clamp problems when voltage clamping neurons expressing voltage-gated conductances. J. Neurophysiol. 99, 1127-1136.

9. Bayliss W.M., Starling E.H., 1899. The movements and innervation of the small intestine. J Physiol (Lond). 24, 99-143.

10. Berridge M. J., Lipp P., Bootman M. D., 2000. The versality and universality of calcium signaling. Nature Reviews, Molecular Cell Biology. 1, 11-21.

11. Birnbaumer L., Zhu X., Jiang M., Boulay G., Peyton M., Vannier B., Brown D., Platano D., Sadeghi H., Stefani E., and Birnbaumer M., 1996. On the molecular basis and regulation of cellular capacitative calcium entry: Roles for Trp proteins. Proc. Nat. Acad. Sci. USA. 93, 15195-15202.

12. Bogeski I., Bozem M., Sternfeld L., Hofer H.W., Schulz I., 2006. Inhibition of protein tyrosine phosphatase 1B by reactive oxygen species leads to maintenance of Ca2+ influx following store depletion in HEK 293 cells. Cell Calcium 40, 1–10.

13. Boland A., Delapierre D., Mossay D., Hans P. Dresse A., 2000. Propofol protects cultured brain cells from iron ion-induced death: comparison with trolox. European Journal of Pharmacology. 404, 21-27.

14. Brehmer A., Schrödl F., Neuhuber W., 1999. Morphological classifications of enteric neurons -100 years after Dogiel. Anat Embryol. 200, 125-135.

15. Broillet M.C., 1999. S-Nitrosylation of proteins. Cell. Mol. Life Sci. 55, 1036-1042.

16. Brookes S.J.H., Meedeniya A.C.B., Jobling P., et al., 1997. Orally projecting interneurones in the guinea- pig small intestine. J. Physiol. 505, 473-91.

17. Browning K.N., Lees G.M., 1996. Myenteric neurons of the rat descending colon: electrophysiological and correlated morphological properties. Neuroscience 73, 1029-1047.

18. Cantrell A.R., Tibbs V.C., Yu F.H., Murphy B.J., Sharp E.M., Qu Y., Catterall W.A., Scheuer T., 2002. Molecular mechanism of convergent regulation of brain Na^+ channels by protein kinase C and protein kinase A anchored to AKAP-15. Mol. Cell. Neurosci. 21, 63-80.

19. Cao W.B., Vrees M.D., Kirber M.T.M., Fiocchi C., Pericolo V.E., 2004. Hydrogen peroxide contributes to motor dysfunction in ulcerative colitis. Am. J. Physiol. Gastrointest. Liver Physiol. 286, G833-G843.

20. Castedo M., Hirsch T., Susin S.A., Zamzami N., Marchetti P., Macho A., and Kroemer G., 1996. Sequential acquisition of mitochondrial and plasma membrane alterations during early lymphocyte apoptosis. J Immunol. 157, 512-521.

21. Catterall W.A., 1980. Neurotoxins that act on voltage-sensitive sodium channels in excitable membranes. Annu. Rev. Pharmacol. Toxicol. 20, 15-43.

22. Catterall W.A., Goldin A.L., Waxman S.G., 2005. International Union of Pharmacology. XLVII. Nomenclature and structure-function relationships of voltage-gated sodium channels. Pharmacol Rev. 57, 397–409.

23. Cohen G., 1985. The Fenton reaction. In: Handbook of methods for oxygen radical research. R.A. Greenwald, editor. CRC Press, Boca Raton. 55-64.

24. Cohen P., Cohen P.T., 1989. Protein phosphatases come of age. J. Biol. Chem. 264, 21435–21438.

25. Cook and Quast, 1990. Potassium channel pharmacology. In: N.S. Cook, Editor, Potassium Channels; Structure, Classification, Function, and Therapeutic Potential, John Wiley and Sons, New York, p.181.

26. Costa M, Brookes S.J.H., Hennig G.W., 2000. Anatomy and physiology of the enteric nervous system. Gut (suppl IV). 47, iv15-iv19.

27. Davies K.J.A., Delsignore M.E., and Lin S.W., 1987. Protein damage and degradation by oxygen radicals . II . Modification of amino acids. J Biol Chem. 262, a9902-9907.

28. Davies K.J.A., Lin S.W., and Pacifici R.E., 1987. Protein damage and degradation by oxygen radicals .IV. Degradation of denatured protein. J Biol Chem. 262, b9914-9920.

29. Derkach V., Surprenant A., North R.A., 1989. 5-HT_3 receptors are membrane ion channels. Nature. 339, 706-709.

30. Diener M., Gabato D., 1994. Thromboxane-like actions of prostaglandin D2 on the contractility of the rat colon in vitro. Acta Physiol. Scand. 150, 95-101.

31. Dogiel A.S., 1899. Über den Bau der Ganglien in den Geflechten des Darmes und der Gallenblase des Menschen und der Säugetiere. Arch Anat Physiol Anat Abt. 130-158.

32. Dröge Wulf, 2002. Free radicals in the physiological control of cell function. Phyiol Rev. 82, 47-95.

33. Dumont A. Hehner S.P., Hofmann T.G., Ueffing M., Dröge W., and Schmitz M.L., 1999. Hydrogen peroxide-induced apoptosis is CD95-independent , requires the release of mitochondria-derived reactive oxygen species and the activation of NF-kB. Oncogene. 8, 747-757.

34. Emptage N.J., Reid C.A., Fine A., 2001. Calcium stores in hippocampal synaptic boutons mediate short-term plasticity, store-operated Ca^{2+} entry, and spontaneous transmitter release. Neuron. 29, 197-208.

35. Esteve J.M., Mompo J., De la Asuncion J.G., Sastre J. Asensi M., Boix J., Vina J.R., Vina J., and Pallardó F.V., 1999. Oxidative damage to mitochondrial DNA and glutathion oxidation in apoptosis: studies in vivo and in vitro. FASEB J .13, 1055-1064.

36. Evans J.R and Bielefeldt K., 2000. Regulation of sodium currents through oxidation and reduction of thiol residues. Neuroscience .101, 229-236.

37. Faber E.S., Sah P., 2007. Functions of SK channels in central neurons. Clin. Exp. Pharmacol. Physiol. 34, 1077-83.

38. Fajardo O., Meseguer V., Belmonte C., Viana F., 2008. TRPA1 channels mediate cold temperature sensing in mammalian Vagal sensory neurons: Pharmacological and genetic evidence. J. Neurosci. 28, 7863-7875.

39. Friel D.D., Tsien R.W., 1992. A caffeine- and ryanodine-sensitive Ca^{2+} store in bullfrog sympathetic neurones modulates effects of Ca^{2+} entry on $[Ca^{2+}]_i$. J. Physiol. 450, 217-246.

40. Furness J.B, Costa M., 1987. The enteric nervous system. Edinburgh: Churchill Livingstone.

41. Furness J.B. and Costa M., 1980. Types of nerves in the enteric nervous system. Neuroscience. 5, 1-20.

42. Furness J.B., 2006. The enteric nervous system. Blackwell Publishing. 288p.

43. Gerasimenko O.V., Gerasimenko J.V., Tepikin A.V., and Petersen O.H., 1996. Calcium transport pathways in the nucleus. Pflugers Arch. 432, 1-6.

44. Gershon M.D., 1981. The enteric nervous system. Ann. Rev. Neurosci. 227-72.

45. Gershon M.D., 1999. The enteric nervous system: A second brain. Hosp. Pract. 34, 31-32.

46. Gershon M.D., Erde S.M., 1981. The nervous system of the gut. Gastroenterology. 80, 1571-1594.

47. Gershon M.D., Kirchgessner A.L., and Wade P.R., 1994. Functional anatomy of the enteric nervous system. In: L.R. Johnson (ed.), Physiology of the gastrointestinal tract, 3. edition, pp. 381-422, Raven Press, New York.

48. Goeger D.E. and Riley R.T., 1989. Interaction of cyclopiazonic acid with rat skeletal muscle sarcoplasmic reticulum vesicles. Effect on Ca^{2+} binding and Ca^{2+} permeability. Biochem. Pharmacol. 38, 3995-4003.

49. Gordon J.A., 1991. Use of vanadate as protein-phosphotyrosine phosphatase inhibitor. Meth. Enzymol. 201, 477-482.

50. Grisham M.B., Gaginella T.S., von Ritter C., Tamai H., Be R.M., Granger D.N., 1990. Effects of neutrophil-derived oxidants on intestinal permeability, electrolyte transport, and epithelial cell viability. Inflammation 14, 531-542.

51. Grune T., Reinheckel T., and Davies K.J.A, 1997. Degradation of oxidized proteins in mammalian cells. FASEB J. 11, 526-534.

52. Gupta V., Ogawa A.K., Du X., Houk K.N., Armstrong R.W., 1997. A model for binding of structurally diverse natural product inhibitors of protein phosphatases PP1 and PP2A. J. Med. Chem. 40, 3199-3206.

53. Guy G.R., Cairns J., Ngu S.B., Tan Y.H., 1993. Inactivation of a redox-sensitive protein phosphatase during the early events of tumor necrosis factor/interleukin-1 signal transduction. J. Biol. Chem. 268, 2141-2148.

54. Halliwell B., Whiteman M., 2004. Measuring reactive species and oxidative damage in vivo and in cell culture: how should you do it and what do the results mean? Brit. J. Pharmacol. 142, 231–255.

55. Hamodeh S.A., Rehn M., Haschke G., Diener M., 2004. Mechanism of butyrate-induced hyperpolarization of cultured rat myenteric neurons. Neurogastroenterol. Motil. 16, 597-604.

56. Hansen M.B., 2003. Neurohumoral control of gastrointestinal motility. Physiol. Res. 52, 1-30.

57. Harman D., 1956. Aging: theory based on free radical and radiation chemistry. J Gerontol. 11, 298-300.

58. Haschke G., Schäfer K.H., Diener M., 2002. Effect of butyrate on membrane potential, ionic currents and intracellular Ca^{2+} concentration in cultured rat myenteric neurons. Neurogastroenterol. Motil. 14, 133-142.

59. Hinterleitner T.A. and Powell D.W., 1991. Immune system control of intestinal ion transport. Immune System and intestinal transport. 249-257.

60. Hirst G.D.S., Holman M.E, Spence I., 1974. Two types of neurones in the myenteric plexus of duodenum in the guinea-pig. J physiol (Lond). 236, 303-326.

61. Holman M.E., Hirst G.D.S., Spence I., 1972. Preliminary studies of the neurones of Auerbach's plexus using intracellular microelectrodes . Aust J Exp Biol Med Sci. 550, 795-801.

62. Hool L.C., Corry B., 2007. Redox control of calcium channels: from mechanisms to therapeutic opportunities. Antiox. Redox Signal. 9, 409-435.

63. International Union of Pharmacology. Potassium Channels, 2002. 59-63.

64. Ishii M., Shimizu S., Hara Y., Hagiwara T., Miyazaki A., Mori Y., Kiuchi Y., 2006. Intracellular-produced hydroxyl radical mediates H2O2-induced Ca^{2+} influx and cell death in rat beta-cell line RIN-5F. Cell Calcium 39, 487-494.

65. Jiang Y., Pico, A., Cadene M., Chait B.T., MacKinnon R., 2001. Structure of the RCK domain from the E.Coli K^{+} channel and demonstration of its presence on the human BK channel. Neuron. 29, 593-601.

66. Johnson S.M., North R.A., 1980. Slow synaptic potentials in neurones of the myenteric plexus. J Physiol (Lond). 301, 505-516.

67. Kaplin A.I., Ferris C.D., Voglmaier S.M., Snyder S.H., 1994. Purified reconstituted inositol 1,4,5-trisphosphate receptors. Thiol reagents act directly on receptor protein. J. Biol. Chem. 269, 28972-28978.

68. Kerst G., Fischer K.G., Normann C., Kramer A., Leipziger J., Greger R., 1995. Ca^{2+} influx induced by store release and cytosolic Ca^{2+} chelation in HT29 colonic carcinoma cells. Pflügers Arch. Eur. J. Physiol. 430, 653-665.

69. Kirichok Y., Krapivinsky G., and Clapham D.E., 2004. The mitochondrial calcium uniporter is a highly selective ion channel. Nature. 427, 360-364.

70. Klebanoff S.J., 1988. Phagocytic cells : Products of oxygen metabolism. In Inflammation, Basic Principles and Clinical Correlates. J.I. Gallin, I. M. Goldstein, and R. Snyderman editors. Raven Press, New York. 391-444.

71. Kuge S., Arita M., Murayama A., Maeta K., Izawa S., Inoue Y., and Nomoto A., 2001. Regulation of the yeast Yap1 nuclear export signal is mediated by

redox signal-induced reversible disulfide bond formation. Mol.Cell.Biol. 21, 6139-6150.

72. Kuge S., Jones N., and Nomoto A., 1997. Regulation of yAP-1 nuclear localization in response to oxidative stress. EMBO J. 16, 1710-1720.

73. Kuge S., Toda T., Lizuka N., and Nomoto A., 1998. Crm1(Xpol) dependent nuclear export of the budding yeast transcription factor yAP-1 is sensitive to oxidative stress. Genes cells. 3, 521-532.

74. Lambeth D.J., 2004. NOX enzymes and the biology of reactive oxygen. Nature Rev. Immunol. 4, 181-189.

75. Langley J.N., 1921. The autonomic nervous system , part 1. W. Heffer and sons , Cambridge.

76. Llinas R., Sugimori M, Lin J.W., and Cherksey B., 1989. Blocking and isolation of a calcium channel from neurons in mammals and cephalopods utilizing a toxin fraction (FTX) from funnel-web spider poison. Proc Natl Acad Sci USA. 86, 1689-1693.

77. Lupu-Meiri M., Lipinsky D., Ozaki S., Watanabe Y., Oron Y., 1994. Independent external calcium entry and cellular calcium mobilization in Xenopus oocytes. Cell Calcium. 16, 20-28.

78. MacKintosh C., Klumpp S., 1990. Tautomycin from the bacterium Streptomyces verticillatus. Another potent and specific inhibitor of protein phosphatases 1 and 2A. FEBS Letters 277, 137-140.

79. Maguire D., MacNamara B., Cuffe J.E., Winter D., Doolan C.M., Urbach V., O' Sullivan G.C., Harvey B.J., 1999. Rapid responses to aldosterone in human distal colon. Steroids 64, 51-63.

80. Martinez-Azorin F., 2004. Cyclopiazonic acid reduces the coupling factor of the Ca^{2+}-ATPase acting on Ca^{2+} binding. FEBS Letters. 576, 73-76.

81. Maruyama T., Kanaji T., Nakade S., Kanno T., Mikoshiba M., 1997. 2-APB, 2-aminoethoxydiphenyl borate, a membrane-penetrable modulator of Ins(1,4,5)P_3-induced Ca^{2+} release. J. Biochem. 122, 498-505.

82. Meissner G., 1857. Über die Nerven der Darmwand. Z Ration Med N F. 8, 364-366.

83. Mitrovic N., Quasthoff S., Grafe P., 1993. Sodium channel inactivation kinetic of rat sensory and motor nerve fibres and their modulation by glutathione. Pflügers Arch. Eur. J. Physiol. 425, 453-461.

84. Moye-Rowley W.S., 2003. Regulation of the transcriptional response to oxidative stress in fungi: similarities and differences. Eukaryot. Cell. 2, 381-389.

85. Nakamura H., Nakamura K., and Yodoi J., 1997. Redox regulation of cellular activation. Annu Rev Immunol.15, 351-369.

86. Nakamura H., Matsuda M., Furuke K., Kitaoka Y., Iwata S., Toda K., Inamoto T., Yamaoka Y., Ozawa K., and Yodoi J., 1994. Adult T cell leukemia-derived factor/human thioredoxin protects endothelial F-2 cell injury caused by activated neutrophils or hydrogen peroxide. Immunol lett. 42, 75-80.

87. Nakamura K., Hori T., Sato N., Sugie K., Kawakami T., and Yodoi J., 1993. Redox regulation of a Src family protein tyrosine kinase $p56^{lck}$ in T cells. Oncogene. 8, 3133-3139.

88. Nathan C.F., 1987. Neutrophil activation on biological surfaces: massive secretion of hydrogen peroxide in response to products of macrophages and lymphocytes. J. Clin. Invest. 80, 1550-1560.

89. Nemeth P.R., Ort C.A., Wood J.D., 1984. Intracellular study of effects of histamine on electrical behavior of myenteric neurons in guinea-pig small intestine. J Phyiol. 355, 411-425.

90. Nishi S., North R.A., 1973. Intracellular recording from the myenteric plexus of the guinea-pig. J Physiol. 231, 471-491.

91. Nowycky M.C. Fox A.P., and Tsien R.W., 1985. Three types of neuronal calcium channel with different calcium agonist sensitivity. Nature. 316, 440-443.

92. Olsson C., Holmgren S., 2001. The control of gut motility. Comp Biochem Physiol A. 128, 481-503.

93. Padilla F., Couble M.L., Coste B., Maingret F., Clerc N., Crest M., Ritter A.M., Magloire H., Delmas P., 2007. Expression and localization of the Nav1.9 sodium channel in enteric neurons and in trigeminal sensory endings: Implication for intestinal reflex function and orofacial pain. Mol. Cell. Neurosci. 35, 138-152.

94. Parekh A.B. , and Putney Jr. J.W., 2005. Store-operated calcium channels. Physiol. Rev. 85, 757-810.

95. Pavlick K.P., Laroux F.S., Fuseler J., Wolf R.E., Gray L., Hoffman J., Grisham M.B., 2002. Role of reactive metabolites of oxygen and nitrogen in inflammatory bowel disease. Free Radic. Biol. Med. 33, 311-322.

96. Pereira C., Ferreira C., Carvalho C., Oliveira C., 1996. Contribution of plasma membrane and endoplasmic reticulum $Ca2^{+}$-ATPases to the synaptosomal $[Ca2+]_i$ increase during oxidative stress. Brain Res. 713, 269–277.

97. Pouokam E., Rehn M., Diener M., 2009. Effects of H_2O_2 at rat myenteric neurones in culture. Eur. J. Pharmacol. 615, 40-49.

98. Putney Jr. J.W., 1986. A model for receptor-regulated calcium entry . Cell Calcium. 7, 1-12.

99. Putney Jr. J.W., 2003. Capacitative calcium entry in the nervous system. Cell Calcium 34, 339-344.

100. Randall A.D., and Tsien R.M., 1995. Pharmacological dissection of multiple types of Ca^{2+} channel currents in rat cerebellar granule neurons. J. Neurosci. 15, 2995-3012.

101. Randall A.D., and Tsien R.M., 1997. Contrasting biophysical and pharmacological properties of T-type and R-type calcium channels. Neuropharmacology. 36, 879-893.

102. Rao R.K., Clayton L.W., 2002. Regulation of protein phosphatase 2A by hydrogen peroxide and glutathionylation. Biochem. Biophys. Res. Commun. 293, 610-616.

103. Rehn M., Diener M., 2006. Effect of the stable thromboxane derivative, carbocyclic thromboxane A2, on membrane potential of rat myenteric neurons in culture. Neurogastroenterol. Motil. 18, 1084-1092.

104. Rehn M., Hübschle T., Diener M., 2004. TNF-a hyperpolarises membrane potential and potentiates the response to nicotinic receptor stimulation in cultured rat myenteric neurons. Acta Physiol. Scand. 181, 13-22.

105. Rossie S., Catterall W.A., 1989. Phosphorylation of the alpha subunit of rat brain sodium channels by cAMP-dependent protein kinase at a new site containing Ser686 and Ser687. J.Biol. Chem. 264, 14220-14224.

106. Rugiero F., Gola M., Kunze W. A.A., Reynaud J-C., Furness J.B. and Clerc N., 2002. Analysis of whole-cell currents by patch clamp of guinea-pig myenteric neurones in intact ganglia. J. Physiol. 538, 447-463.

107. Sanchez and McManus, 1996. Paxilline inhibition of the alpha-subunit of the high-conductance calcium-activated potassium channel. Neuropharmacology. 35, 963-968.

108. Sawada Y., Hosokawa H., Matsumura K. and Kobayashi S., 2008. Activation of transient receptor potential ankyrin 1 by hydrogen peroxide. European Journal of Neuroscience. 27, 1131-1142.

109. Schäfer K.H., Saffrey M.J., Burnstock G., Mestres-Ventura P. A., 1997. New method for the isolation of myenteric plexus from the newborn rat gastrointestinal tract. Brain Res. Prot. 1, 109-113.

110. Schemann M., 2000. Enterisches Nervensystem und Innervation des Magen-Darm-Tracktes. In: Physiologie der Haustiere, Hrsg.: von Engelhardt W., Breves G., Enke Verlag, Stuttgart: 308-317.

111. Schemann M., Wood J.D., 1989. Synaptic behavior of myenteric neurones in the gastric corpus of the guinea-pig. J physiol (Lond). 417, 519-535.

112. Scheuer T., Catterall W.A., 2006. Control of neuronal excitability by phosphorylation and dephosphorylation of sodium channels. Biochem. Soc. Transact. 34, 1299–1302.

113. Schreiber M. and Salkoff L., 1997. A novel calcium-sensing domain in the BK channel. Biophysical Journal. 73, 1355-1363.

114. Schultheiss G., Hennig B., and Diener M., 2008. Sites of action of hydrogen peroxide on ion transport across rat distal colon. British Journal of Pharmacology. 154, 991-1000.

115. Schultheiss G., Kocks S.L., Diener M., 2005. Stimulation of colonic anion secretion by monochloramine: action sites. Pflügers Arch. Eur. J. Physiol. 449, 553-563.

116. Shah M.M., Miscony Z., Javadzadeh-Tabatabaie M., Ganellin C.R. and Haylett D.G, 2001. Clotrimazole analogues: effective blockers of the slow afterhyperpolarization in cultured rat hippocampal pyramidal neurones. Br. J. Pharmacol. 132, 889-898.

117. Sharov V.S., Dremina E.S, Galeva N.A., Williams T.D., and Schoneich C., 2006. Quantitative mapping of oxidation-sensitive cysteine residues in SERCA in vivo and in vitro by HPLC-electrospray-tandem MS: selective protein oxidation during biological aging. Biochem J. 394, 605-615.

118. Slund F. Zheng M., Beckwith J., and Storz G., 1999. Regulation of the OxyR transcription factor by hydrogen peroxide and the cellular thiol –disulfide status. Proc Natl Acad Sci USA. 6161-6165.

119. Stadtman E.R., 1992. Protein oxidation and aging . Science . 257, 1220-1224.

120. Starkov A.A., Chinopoulos C., Fiskum G., 2004. Mitochondrial calcium and oxidative stress as mediators of ischemic brain injury. Cell Calcium 36, 257-264.

121. Strobaek D., Christophersen P., Holm N.R., Moldt P., Ahring P.K., Johansen T.E., Olesen S.P., 1996. Modulation of Ca(2+)-dependent K+ channel, hslo, by the substituted diphenylurea NS 1608, paxilline and internal Ca2+. Neuropharmacology. 35, 903-14.

122. Sugi K., Musch M.W., Di A., Nelson D.J., Chang E.B., 2001. Oxidants potentiate Ca^{2+}- and cAMP -stimulated Cl^{-} secretion in intestinal epithelial T84 cells. Gastroenterology 120, 89-98.

123. Surprenant A., 1984. Slow excitatory synaptic potentials recorded from neurones of guinea-pig submucous plexus. J. Physiol. 351, 343-361.

124. Surprenant A., 1994. Control of the gastrointestinal tract by enteric neurons. Annu. Rev. Physiol. 56, 117-140.

125. Surprenant A., North R.A., 1988. Mechanism of synaptic inhibition by noradrenaline acting at alpha 2-adrenoceptors. Proc R Soc (Lond). 234, 85-114.

126. Suzuki Y.J., Forman H.J., Sevanian A., 1997. Oxidants as stimulators of signal transduction. Free Radic. Biol. Med. 22, 269-285.

127. Swarup G., Cohen S., and Garbers D.L., 1982. Inhibition of membrane phosphotyrosyl-protein phosphatase activity by vanadate. Biochemical and biophysical research communications. 107, 1104-1109.

128. Tamai H., Kachur J.F., Baron D.A., Matthew B.G., Gaginella T.S., 1991. Monochloramine, a neutrophil-derived oxidant, stimulates rat colonic secretion. J. Pharmacol. Exp. Ther. 257, 887-894.

129. Tamaoki T., Nomoto H., Takahashi I., Kato Y., Morimoto M., Tomita P., 1986. Staurosporine, a potent inhibitor of phospholipid/Ca^{++} dependent protein kinase. Biochem. Biophys. Res. Commun. 135, 397-402.

130. Thièry J.P., Blazsek I., Legras S., Marion S., Reynes M., Anjo A., Adam R., Misset J.L., 1999. Hepatocellular carcinoma cell lines from diethylnitrosamine pheobarbital-treated rats. Characterization and sensitivity to endothall, a protein serine/threonine phosphatase-2A inhibitor. Hepatology 29, 1406-1417.

131. Thomas E.L., Grisham M.B., and Jefferson M.M, 1983. Myeloperoxidase dependent effects of amines on functions of isolated neutrophils. J. Clin. Invest. 72, 441-454.

132. Togashi K., Inada H., Tominaga M., 2008. Inhibition of the transient receptor potential cation channel TRPM2 by 2-aminoethoxydiphenyl borate (2-APB). Brit. J. Pharmacol. 153, 1324-1330.

133. Trendelenburg P., 1917. Physiologische und pharmakologische Versuche über die Dünndarm Peristaltik. Naunyn Schmiedebergs Arch Exp Pathol Pharmakol. 81, 55-129.

134. Tsien R.W., Lipscombe D., Madison D.V., Bley K.R., and Fox A.P., 1988. Multiple types of neuronal calcium channels and their selective modulation. Trends Neurosci.; 11, 431-438.

135. Usachev Y.M., Thayer S.A., 1999. Ca^{2+} influx in resting rat sensory neurones that regulates and is regulated by ryanodine-sensitive Ca^{2+} stores. J. Physiol. (Lond.). 519, 115-130.

136. VanDerWinden J.M., 1999. Role of intestinal cells of Cajal and their relationship with the enteric nervous system .Eur J Morphol. 37, 250-256.

137. Vogalis F., Harvey J.R., 2003. Altered excitability of intestinal neurons in primary culture caused by acute oxidative stress. J. Neurophysiol. 89, 3039-3050.

138. Vogalis Fivos, Furness J.B., and Kunze W.A.A., 2001. Afterhyperpolarization current in myenteric neurons of the guinea pig duodenum. The American Physiological Society. 1941-1951.

139. Wada-Takahashi S., Tamura K., 2000. Actions of reactive oxygen species on AH/type 2 myenteric neurons in guinea pig distal colon. Am. J. Physiol. Gastrointest. Liver Physiol. 279, G893-G902.

140. Wang Y., Deng X., Hewavitharana T., Soboloff J., and Gill D.L., 2008. STIM, Orai and TRPC channels in the control of calcium entry signals in the smooth muscle. Clinical and experimental pharmacology and physiology. 35, 1127-1133.

141. Wei A., Gutman G. A., Aldrich R., Chandy G. K., Grissmer S. and Wulf H., 2005. International union of Pharmacology. LII. Nomenclature and molecular relationships of calcium-activated potassium channels. Pharmacol. Rev. 57, 463-472.

142. Wood J.D., 1972. Excitation of intestinal muscle by atropine, tetrodotoxin and xylocaine. Am J Physiol. 222, 118-125.

143. Wood J.D., 1994. Physiology of the enteric nervous system. In: L.R. Johnson (ed.), Physiology of the gastrointestinal tract, 3. edition, pp. 423–482, Raven Press, New York.

144. Wood J.D., Mayer C.J., 1979. Slow synaptic excitation mediated by serotonin in Auerbach's plexus. Nature. 276, 836-837.

145. Xu L., Tripathy A., Pasek D.A., Meissner G., 1999. Ruthenium red modifies the cardiac and skeletal muscle Ca2+ release channels (ryanodine receptors) by multiple mechanisms. J. Biol. Chem. 274, 32680-32691.

146. Yoo A. S., Cheng I., Chung S., Grenfell T. Z., Lee H., Pack-Chung E., Handler M., Shen J., Xia W., Tesco G., Saunders A.J., Ding K., Frosch M. P., Tanzi R. E., Kim T., 2000. Presenilin-mediated modulation of capacitative calcium entry. Neuron 27, 561-572.

147. Yu B.P., 1994. Cellular defenses against damage from reactive oxygen species. Physiol. Rev. 74, 139–162.

148. Zheng M., Alsung F., and Storz G., 1998. Activation of the OxyR transcription factor by reversible disulfide bond formation. Science. 279, 1718-1721.

149. Zima A.V. Copello J.A., Blatter L.A., 2004. Effects of cytosolic NADH/NAD^+ levels on sarcoplasmic reticulum Ca^{2+} release in permeabilized rat ventriclular myocytes. J. Physiol. 555, 227-74.

8 Declaration

I declare that the present thesis is my original work and that it has not been previously presented in this or any other university for any degree. I have also abided by the principles of good scientific conduct laid down in the charter of the Justus Liebig University of Giessen in carrying out the investigations described in the dissertation.

9 Aknowledgements

My sincere gratitude goes to my supervisors Prof. Dr. Martin Diener and Prof. Dr. Wolfgang Kummer. I would like to especially thank Prof. Dr. Martin Diener for hosting me in his research group, giving me the opportunity to learn science and train to become a good scientist, his unflinching encouragement and invaluable guidance during my whole Ph.D period, sharing with me his wide experience. He was always there with the right support when it came to professional and personal concerns, not only concerning mine, but also at all times keeping that harmony among people who need to work together in a group, which helped me continue forward. I extend my heartfelt and sincere thanks for his excellent supervision, inspiring ideas and valuable advice. His care makes me really realize why a supervisor in Germany is called "Doktorvater", Doctorate's father, father being more family, he took on his role of "Father" beyond that of supervisor.

I am also indebted to all distinguished members of Prof. Dr. Diener's research group, both past and present members (2006-2009), who assisted me technically and with invaluable counsel. Especially, many thanks go to Prof. Dr. Gerhard Schultheiss for his fruitful ideas and counsel, Dr. Matthias Rehn who was my main collaborator in all the studies and who patiently explained the techniques, Dr. Guido Haschke for initiating some techniques and his permanent collaboration, Dr. Kirsten Brockmeier, Dr. Gundula Prinz and Dr. Britta Hennig for their helpful and challenging questions. Karl-Herrmann Maurer, Gerd Herber, Alexander Heinrich our engineers whose readiness and technical skills helped getting hardware and instruments fixed or newly made for specific works, my fellow doctorate and Ph.D colleagues Janine Avemary, Julia Steidle, Kaoru Onodera, Ann Gabriella Wolf, Danielle Kohr, Pratiba Singh for their discussions, critics and correcting this thesis, our technical assistants Eva Haas, Alice Stockinger, Brigitta Brück, Barbara Schmidt, Michael for their technical assistance obviously but also for the family ambiance they manage to keep at work.

My gratitude also goes to the Deutscher Akademischer Austausch Dienst (DAAD) for financing my language course in Frankfurt, my stay in Germany and my study/research.

I am also grateful to the Streitenberger family in Frankfurt/M, for hosting me during my first six months in Germany.

Publications

--***Ervice Pouokam***, *Matthias Rehn, Martin Diener*

Effects of H_2O_2 at rat myenteric neurones in culture. *Eur.J.Pharmacol***. 2009**; 615, 40-49.

-- ***Pouokam E.***, *Rehn M., Diener M.*

Effects of H_2O_2 on Na^+ currents at rat myenteric neurones. *J Physiol Biochem.* **2008**; 64 (4), 300. (Abstract).

-- ***Pouokam E.***, *Rehn M., Diener M.*

Actions of oxidants on myenteric neurones. *J Physiol Biochem*. **2007;** 63 (1), 69. (Abstract).

-- *Rene* Kamgang , *Hortense* Gonsu Kamga , *Pascal* Wafo , *Jean Alexis* Mbungni N , ***Vidal*** **Pouokam Ervice** , *Michel Archange* Fokam Tagne , *Christine* Fonkoua Marie

Activity of aqueous ethanol extract of Euphorbia prostrata ait on Shigella dysenteriae type 1 induced diarrhea in rats . *I.J.P*. **2007**; 39(5) , 240-244.

-- *Kamgang R,* ***Vidal Pouokam Kamgne E****., Fonkoua MC, Penlap N Beng V, Biwole Sida M.*

Activities of aqueous extracts of Mallotus oppositifolium on Shigella dysente riae1 induced diarrhoea in rats. *Clin Exp Pharmacol Physiol*. **2006** Jan-Feb; 33 (1-2): 89-94.

-- *Kamgang R,* ***Pouokam KE****, Fonkoua MC, Penlap NB, Biwole SM.*

Shigella dysenteriae type 1-induced diarrhea in rats. *Jpn J Infect Dis*. **2005** Dec; 58(6): 335-7.